学位申請論文

岩嶋樹也

論文内容の要旨

報告番号	甲才　号	氏名	岩嶋樹也
	主査　山元龍三郎 中島暢太郎・国司秀明		

（論文題目）

Studies on the atmospheric ultra-long waves

（大気超長波の研究）

（論文内容の要旨）

大気の超長波の観測的研究は，気象観測網が充実した約50年代から始められ，複数のモードがあることが明らかにされて来た。大山脈や海陸の温度差のため生じた停滞性の大振幅の波動の上に，長波との非線型相互作用のために生じた移動性波動が重なっているのである。在来の研究では，時間平均パターンで示されるものを準停滞部分，それからのずれを移動部分と定義されて来たが，申請者は在来の研究結果において準停滞部分の振幅の変化が示唆されている事に着目し，超長波の日日の変動を明らかにしようとした。

主論文が1部において，申請者は，準停滞性波動の振幅の日日の変化を抽出する新しい方

法を示している。8個のバンドパスフィルターおよび1個のローパスフィルターを作り，それらを，超長波の日日の資料の時系列に適用する。ローパスフィルターを通ったものの位相を，準停滞部分の位相とし，バンドパスフィルターを通ったものに若干の数学的操作を施こして準停滞性波動の日日の振幅変化を求めるのである。さらに，申請者は，気象観測資料に不可避な誤差を考慮して，解析結果の有意性に関する判定則を導いている。

この解析方法を用いて，申請者は1967年から1968年にかけての成層圏突然昇温時の超長波の日日の振舞を詳細に研究した。その結果，準停滞性波動の振幅変化が著しく，特に波数2の準停滞部分の振幅が時々，在来用いられていた時間平均波の振幅の2倍以上になる事を明らかにした。

主論文第2部で，申請者は，まず，波数空間におけるエネルギー過程について準停滞部分と移動部分の役割を区別し，またそれらの間のエネルギー交換をも含めて，エネルギー方程式を導いた。

この方程式を用いて，申請者は1967年から1968年にかけての成層圏突然昇温時のエネルギ

一過程を解析した。各波数の準停滞部分や移動部分の，運動エネルギーや有効位置エネルギーの日々の変動を明らかにすると共に，それらの間の交換についても詳細に研究した。これらの結果を，突然昇温の前と後の二つの時期に分けエネルギーの流れの図にまとめて，成層圏の突然昇温という現象における超長波の準停滞部分と移動部分の役割を明らかにしている。

参考論文その1およびその2は，主論文に示された研究の先駆的なものであり，その3，その4およびその5は，種々の時間尺度での超長波の変動に関する研究である。

主論文目録

Studies on the Atmospheric Ultra-Long Waves

題目　大気超長波の研究

第1部　Observational studies of the ultra-long waves in the atmosphere (I). Part 1. Daily behaviour of the quasi-stationary and travelling ultra-long waves during the stratospheric sudden warming.

(大気中における超長波の解析的研究(I). 第1部 成層圏突然昇温前後の準停滞性・移動性超長波の振舞について)

第2部　Observational studies of the ultra-long waves in the atmosphere (II). Part 2. Ultra-long-wave energy processes during the stratospheric sudden warming.

(大気中における超長波の解析的研究(II). 第2部 成層圏突然昇温前後の超長波エネルギー過程)

Observational Studies of the Ultra-Long Waves in the Atmosphere (I)

Part 1. Daily Behaviour of the Quasi-Stationary and Travelling Ultra-Long Waves during the Stratospheric Sudden Warming

By Tatsuya Iwashima

Geophysical Institute, Kyoto University, Kyoto
(Manuscript received 4 December 1972, in revised form 15 June 1973)

Abstract

Analytical studies of day-to-day behaviour of the travelling and quasi-stationary ultra-long waves in the 1967/68 winter stratosphere are made by means of the time-filter method [Iwashima and Yamamoto (1971)].

A brief description of the method of analysis and a criterion of numerical reliability for treating erroneous data are provided in the first place.

Daily variations of zonal mean temperature and zonal mean wind which characterize the sudden warming are firstly depicted. Secondly from the analysis of the total ultra-long waves with wavenumbers one, two and three, such a few characteristic features as amplitude-decay of the wavenumber one and simultaneous amplification of the wavenumber two at the sudden warming, which has been suggested by Teweles (1963), etc., are confirmed again. Thirdly, in order to show the process of applying the time-filter method, the wavenumber two is analyzed somewhat in detail, because of its predominance during the period of sudden warming. It is found out that the amplification of several fluctuating components of the quasi-stationary part is accompanied with the sudden warming. The travelling part is classified into the westsward and eastward-moving modes.

Finally, the travelling and quasi-stationary parts of the ultra-long waves with the wavenumbers one, two and three are described in meridional- and vertical-time sections. The travelling part of wavenumber one predominates during the warming stage and rapidly decays at the mature stage of the warming. The former stage may correspond to the "third stage of the sudden warming" by Miyakoda (1963) or the "migratory-stage" termed by Hirota (1967). While the quasi-stationary parts of wavenumber one and both parts of wavenumber two amplify with the warming and decay afterward. Taking account of the results of the former observational and theoretical studies [Hirota (1968), Matsuno (1971), etc.], we may infer the following close relations:

i) the non-linear interaction between the travelling part of wavenumber one and that of wavenumber two, and

ii) the interaction between the quasi-stationary part and the travelling one of the respective wavenumber, as Murakami (1960) showed the energetical relation between the stationary disturbance and the transient eddy.

1. Introduction

Observational studies of the ultra-long waves have been made by many authors [e.g., Kubota and Iida (1954), Eliasen (1958), Haney (1961), Deland (1964, 1965, 1972), Eliasen and Machenhauer (1965, 1969), Benwell (1968), Deland and Lin (1967), Deland and Johnson (1668), Bradley and Wiin-Nielsen (1968)]. According to their results, it may be considered that the ultra-long wave consists of the travelling and quasi-stationary parts, and that the superposition of the former part with a small amplitude upon the latter with a large amplitude leads to its apparent fluctuation in position and amplitude. Hitherto, in most observational studies of the

ultra-long waves, much attention have been given to its transient [strictly speaking, fluctuating] part. Then, in most of their analyses, the transeint part was defined by the deviation from the quasi-stationary part or mean over the whole period of the analysis. While, by means of a few time-filters, Bradley (1968), Bradley and Wiin-Nielsen (1968) and Eliasen and Machenhauer (1969) divided the ultra-long wave into the fast, slow-moving and standing parts. However, it should be considered that the fluctuating part defined by the deviation and the moving part defined by the time-filter may include not only the travelling part but also the fluctuating part of the amplitude of the quasi-stationary part. For the behaviour of the ultra-long waves averaged throughout the sampling period, Kao (1968, 1970) and his collaborators [Kao and Wendell (1976), Kao, Jenne and Sagendorf (1970)] have performed the power spectral analysis by the aid of Fourier analysis in both wavenumber and frequency domains. In their results, there is such a fact suggesting that the amplitude of the quasi-stationary part may remarkably changes with various periods. On the other hand, Hayashi (1971) has proposed a method for separating all waves into progressive and retrogressive parts by space Fourier and time-cross spectral analyses. Deland (1972) proposed a method of spectral analysis of travelling waves based on space- and time-Fourier analyses. These methods are, at any rate, available for discussing mean behaviour of the ultra-long waves averaged throughout sampling duration.

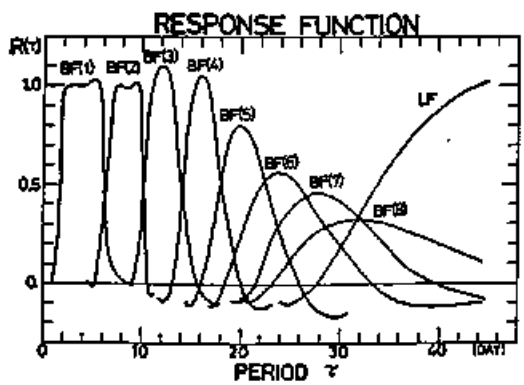

Fig. 1. Response functions $R(\tau)$ for band-pass filters [$BF(1)$, $BF(2)$, $BF(3)$, $BF(4)$, $BF(5)$, $BF(6)$, $BF(7)$ and $BF(8)$] and a low-pass filter [LF]. τ is the period. Unit in day.

For the purpose of investigating the day-to-day behaviour of the ultra-long waves, we have proposed a time-filter method, which makes it possible to separate the ultra-long waves into the quasi-stationary and travelling parts [Iwashima and Yamamoto (1971)]. By means of this method, variation of the amplitude of the quasi-stationary part can be separately obtained on a daily basis.

In the present paper a brief description of the time-filter method with a modification will be given, and then the significance (or numerical reliability) for treating the erroneous data will be discussed. Applying this method to the stratosphere in the 1967/68 winter, we will describe a behaviour of the quasi-stationary and travelling ultra-long waves.

2. Method of analysis

Separation of the ultra-long waves into the travelling and quasi-stationary parts is performed by the time-filter method, whose filters consist of a low-pass filter and several band-pass filters (see Fig. 1). The main procedure of the analysis has been already proposed by us [Iwashima and Yamamoto (1971)]. However, in the subsequent paper, an alteration has been added to the decision of phase-angle of the quasi-stationary part, as noted, by our recent paper [Iwashima and Yamamoto (1973)]. Therefore, the method of analysis is described again in the Appendix A. Also, the relationship of the time-filter method to the Fourier method, which is adopted by Deland (1972), etc., is referred to in the Appendix B.

3. Criterion for significance of the results

The actual raw data should be considered to contain observational and/or any other errors. In treatment of the results obtained from those erroneous data, any criterion for numerical reliability or significance is desired.

Discussion of reliability will be made for each stage of the analysis. The procedure consists of two stages, *i.e.* the first one where the Fourier harmonic analysis of geopotential height along a latitude is made, and the second where some filters are applied to the time series data obtained at the first stage, and the quasi-stationary and travelling parts are separately calculated.

At the first stage of Fourier harmonic analysis, the criterion can be given after Brooks and Carruthers (1953). The probability df that any

amplitude A of Fourier harmonic analysis of N random values with standard deviation σ_1 falls between A and $A+dA$ is

$$df=\frac{NA}{2\sigma_1^2}\exp(-NA^2/4\sigma_1^2)dA \tag{3-1}$$

Therefore, if the probability which any amplitude exceeds A_{01} is assumed to be equal to or less than 1%, the following relation will be held;

$$\int_{A_{01}}^{\infty}\frac{NA}{2\sigma_1^2}\exp(-NA^2/4\sigma_1^2)dA \leqq 0.01 \tag{3-2}$$

i.e.

$$A_{01} \geqslant 2\sigma_1\sqrt{\ln 100/N} \tag{3-3}$$

The numerical value of A_{01} is given as follows;

$$\begin{aligned} A_{01} &\geqslant 0.51\,\sigma_1 \quad \text{for } N=72, \\ A_{01} &\geqslant 0.72\,\sigma_1 \quad \text{for } N=36. \end{aligned} \tag{3-4}$$

The standard deviation of the height of isobaric surfaces may probably vary with location (height, latitude or longitude) or time. No definite data of numerical value of the standard deviation in the lower stratosphere is at the present author's hand. However, we will employ the standard deviation $\sigma_1=400$ gpm throughtout this work, taking into consideration the fact that its value around the tropopause is about 150 gpm, and that it increases as altitude [Sawyer (1962), Johnson and Gelman (1968)], but seldom exceeds 500 gpm. In this case, we have

$$\begin{aligned} A_{01} &\geqslant 204 \text{ gpm for } N=72, \\ A_{01} &\geqslant 286 \text{ gpm for } N=36. \end{aligned} \tag{3-5}$$

We should, further, discuss the significance of filtered time-series data at the second stage of the analysis. Operation of the filter is equivalent to weighted-running mean of data X_k, such as

$$\bar{X}=\sum_k W_k X_k \tag{3-6}$$

where W_k is the weight. Therefore, the standard deviation σ_2 of $\bar{X}$ is obtained by the use of the following relation,

$$\sigma_2^2=\sum_k W_k^2\sigma_k^2 \tag{3-7}$$

[e.g. see p. 138 in Shchigolev (1965)].

Table I

BF	1	2	3	4	5	6	7	8
$\sqrt{\sum_k W_k^2}$	0.815	0.359	0.228	0.167	0.121	0.087	0.068	0.060

The value of $\sqrt{\sum W_k^2}$ for each filter $BF(j)$ is given in Table 1.

The travelling part of the wave is obtained by such a computational manipulation as summation of all the parts that pass the band-pass filters, and the quasi-stationary one by subtraction of the former part from the original data. From the relation (3-7) and the condition that all the standard deviation for $BF(j)$ are equal to σ_1, the total standard deviation can be easily obtained. Thus, from summation of the above values in Table 1, we obtain the following standard deviation, σ_2 for the travelling and quasi-stationary parts;

$$\sigma_2=0.95\,\sigma_1 \tag{3-8}$$

And the criterion for 99% significance of the amplitude A_{02} of both parts becomes

$$\begin{aligned} A_{02} &\geqslant 210 \text{ gpm for } N=72, \\ \text{or} \\ A_{02} &\geqslant 294 \text{ gpm for } N=36. \end{aligned} \tag{3-9}$$

From the above consideration, a travelling part and quasi-stationary one whose amplitude exceeds 200 gpm may be considered to be significant, and that of smaller amplitude does not deserve further treatment.

Employing the above-mentioned for $N=36$ and the standard deviation $\sigma_1'=50$ gpm [referring to Sawyer (1962)], we can obtain the following critical amplitude A_{01}' for the total ultra-long waves and A_{02}' for the travelling and quasi-stationary ultra-long waves in the middle or lower troposphere;

$$A_{01}' \geqslant 36 \text{ gpm}, \quad A_{02}' \geqslant 37 \text{ gpm} \tag{3-10}$$

A_{01}' seems to be reasonable, compared with the empirical value of Arai (1970), such as 20 gpm for the middle latitudes and 30 gpm for the higher latitudes.

4. Data and synoptic condition

Data

The method described in the previous section 2 will be applied to the daily geopotential field

Table 2. Period of data, levels and grid points

Period	Nov. 1, 1967–Feb. 29, 1968 (121 days)
Pressure levels	10, 30, 50, 100 mb
Grid points	30, 35, 40, 45, 50, 55, 60, 65, 70, 75, 80, 85°N each 10° long.

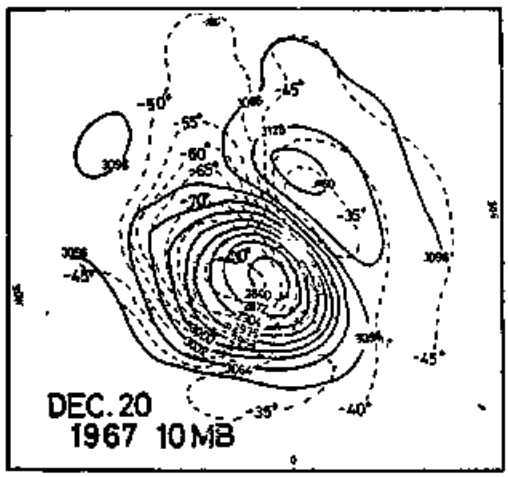

Fig. 2. Northern Hemisphere 10 mb chart for Dec. 26, 1967 (after Free University of Berlin: 1968).

in the 1967/68 winter stratosphere. The original data have been read off from the stratospheric maps issued by Free University of Berlin (1968, 69). The details of the data are given in Table 2.

Synoptic condition

In this period of the analysis, a remarkable stratospheric sudden warming appeared. Detailed description of the warming has been already given by Johnson (1969). He divided the warming period into three stages, *i.e.* initial stage of the warming (Dec. 15-27, 1967), circulation breakdown (Dec. 28, 1967-Jan. 10, 1968) and circulation restoration (Jan. 11, 1968-). The synoptic situations during the period are shown in Figs. 2, 3 and 4. At the first stage can be seen an elongated polar vortex which has been a center of low geopotential height near the North Pole (Fig. 2). At the second stage, the polar vortex splits into the bipolar circulation pattern (Fig. 3). At the third stage it gradually returns to the usual winter circulation pattern (Fig. 4). In this work the period corresponding to the former two stages is selected.

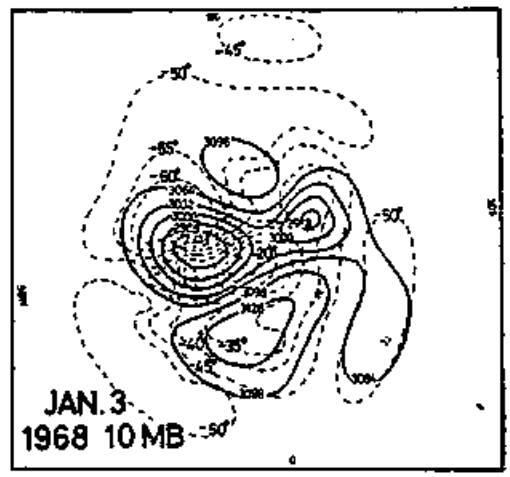

Fig. 3. 10 mb chart for Jan. 3, 1968 (after Free University of Berlin 1969).

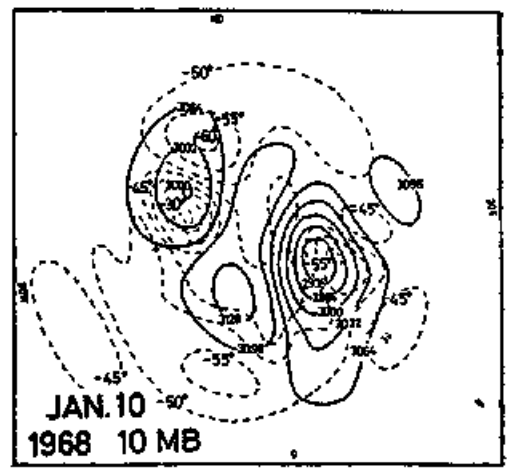

Fig. 4. 10 mb chart for Jan. 16, 1968, as in Fig. 3.

5. Analytical results

The results of analysis by the time-filter method will be presented in this section, with brief descriptions of day-to-day variations of the zonal mean wind and temperature fields. Daily behaviour of the apparent ultra-long waves (or "total ultra-long waves") will be outlined prior to separating them. Finally the results for the quasi-stationary and travelling parts of the waves will be illustrated.

5.1. *Zonal mean temperature and zonal mean wind*

The daily variations of zonal mean fields are illustrated. The zonal mean temperature ($\bar{T}$) and wind ($\bar{U}$) are computed at every 5 degrees of latitude from 30(35)°N to 85(80)°N, at 10, 30, 50 and 100 mb levels.

A meridional-time section of the zonal mean temperature $\bar{T}$ at 10 mb, and a vertical-time section of $\bar{T}$ at 80°N are shown in Figs. 5 and 6, respectively. A region warmer than −30°C can be found at 10 mb and all latitudes higher than 75°N about Jan. 2, 1968. The date of the highest temperature at each latitude is shown by thick line in Fig. 5.

The peak moved from 30°N at Dec. 23, 1967 to 80°N at Jan. 3, 1968 with a speed of about 5° lat/day. This sudden warming is illustrated more remarkably in Fig. 7, where day-to-day variations of $\bar{T}$ at 10 mb are given at every 10° latitudes from 30°N to 80°N.

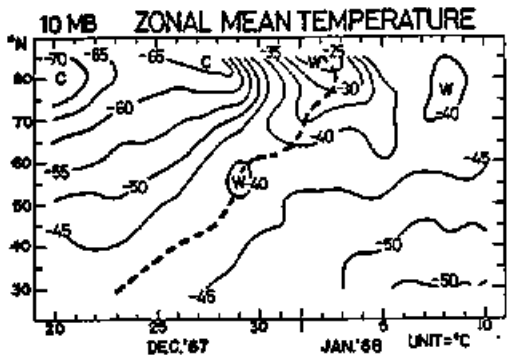

Fig. 5. Meridional-time section of zonal mean temperatures $\bar{T}$ at 10 mb in degree Celcius, 30°-85°N for Dec. 20, 1967-Jan. 10, 1968. Isotherms at 5°C intervals.

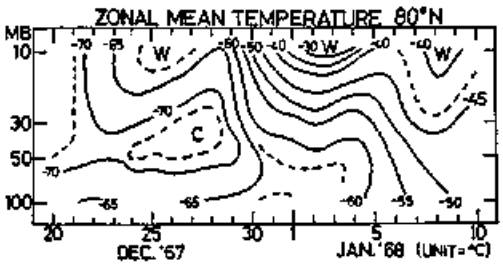

Fig. 6. Vertical-time section of zonal mean temperatures $\bar{T}$ at 80°N and 10-100 mb levels.

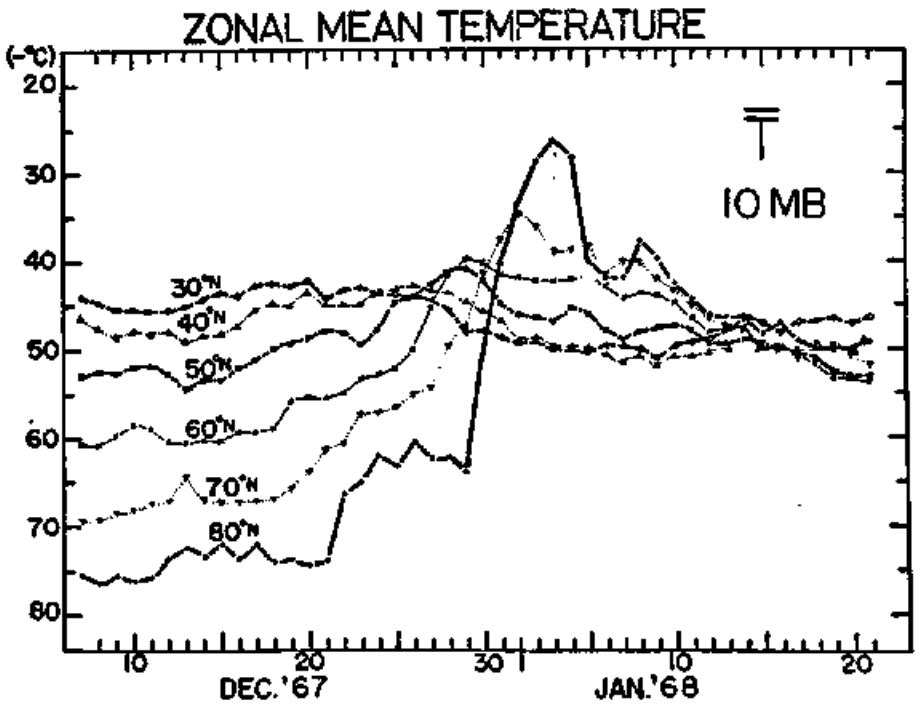

Fig. 7. Zonal mean temperatures at 10 mb for each latitudes from 30°N to 80°N every 10° lat. intervals.

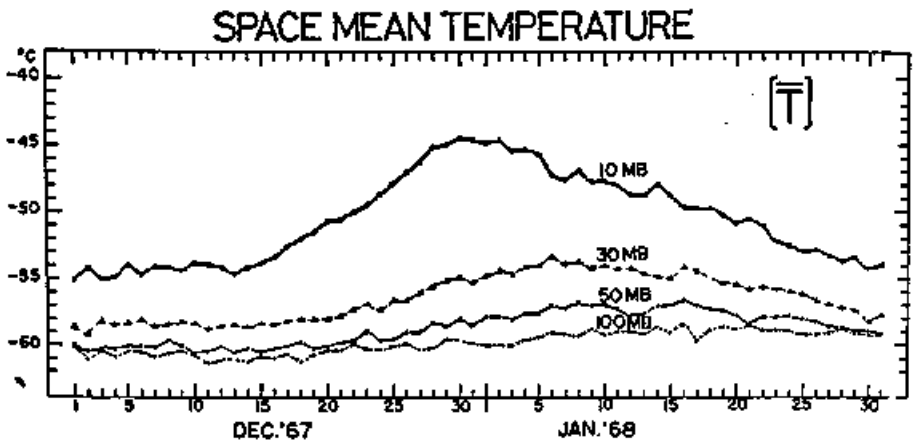

Fig. 8. Zonal and meridional (30°-85°N) averaged temperature $[\overline{T}]$ at 10, 30, 50 and 100 mb levels.

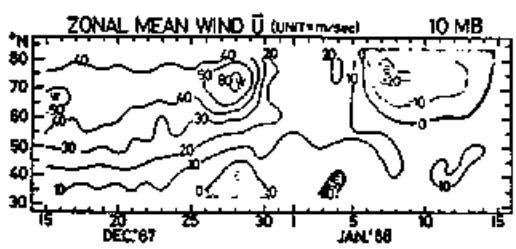

Fig. 9. Meridional-time section of zonal mean wind $\overline{U}$ at 10 mb. Unit in m/sec.

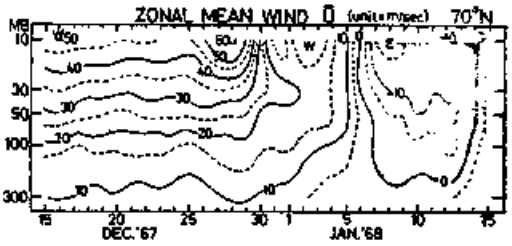

Fig. 10. Vertical-time section of zonal mean wind $\overline{U}$ at 70°N.

Quite conspicuous increase of $\overline{T}$ started at 80°N on Dec. 30, 1967, and the maximum appeared on Jan. 3, 1968. While an appreciable decreasing of $\overline{T}$ can be noticed at 30°N about Dec. 28, 1967, by about 3°C. A similar feature can be also detected for $\overline{T}$ at 40°N and 50°N. This cooling at low latitudes may perhaps play some role of compensating the sudden warming at high latitudes suggested by Matsuno's numerical model of the sudden warming [Matsuno (1971)] and Julian and Labitzke (1965). Fig. 6 illustrates the vertical-time section of the zonal mean temperature $\overline{T}$ at 80°N. It is noted that a little temperature decreasing occurred at the middle level preceding the major warming at higher levels. The temperature averaged over the area north of 30°N $[\overline{T}]$ is given in Fig. 8. The warming still remains appreciably, with a peak in $[\overline{T}]$ at 10 mb about Dec. 30, 1967. At 30 mb level, the warming of $[\overline{T}]$ is delayed by about 10 days with less magnitude. These may throw a light on the mechanism of the sudden warming.

While, the zonal mean wind $\overline{U}$ in meridional- and vertical-time sections are given in Figs. 9 and 10, respectively. Maximum westerlies appeared about 70°N just before the start of sudden warming at high latitudes, simultaneously with intensification of meridional temperature gradient (Fig. 5). Then, almost simultaneously the easterlies appeared in the southern region of 40°N. It seems that the rapid decreasing of westerlies corresponds to the warming. At higher latitudes, the zonal mean wind $\overline{U}$ became easterly, when the warming finished, and meridional gradient of the zonal mean temperature $\overline{T}$ changed its sign. Fig. 10 shows that such a change of the zonal mean wind $\overline{U}$ north of 60°N almost simultaneously occurred at the lower levels, without a few days delay. If we compare Fig. 9 with the theoretical result of Matsuno (1971) [*i.e.*, for the numerical model C 2 of the wavenumber two], a few similar and/or different point are found out in their gross pattern. A similar point is the above-mentioned time-change of $\overline{U}$ from westerly to easterly. Two maxima of westerlies appear at high latitudes, although

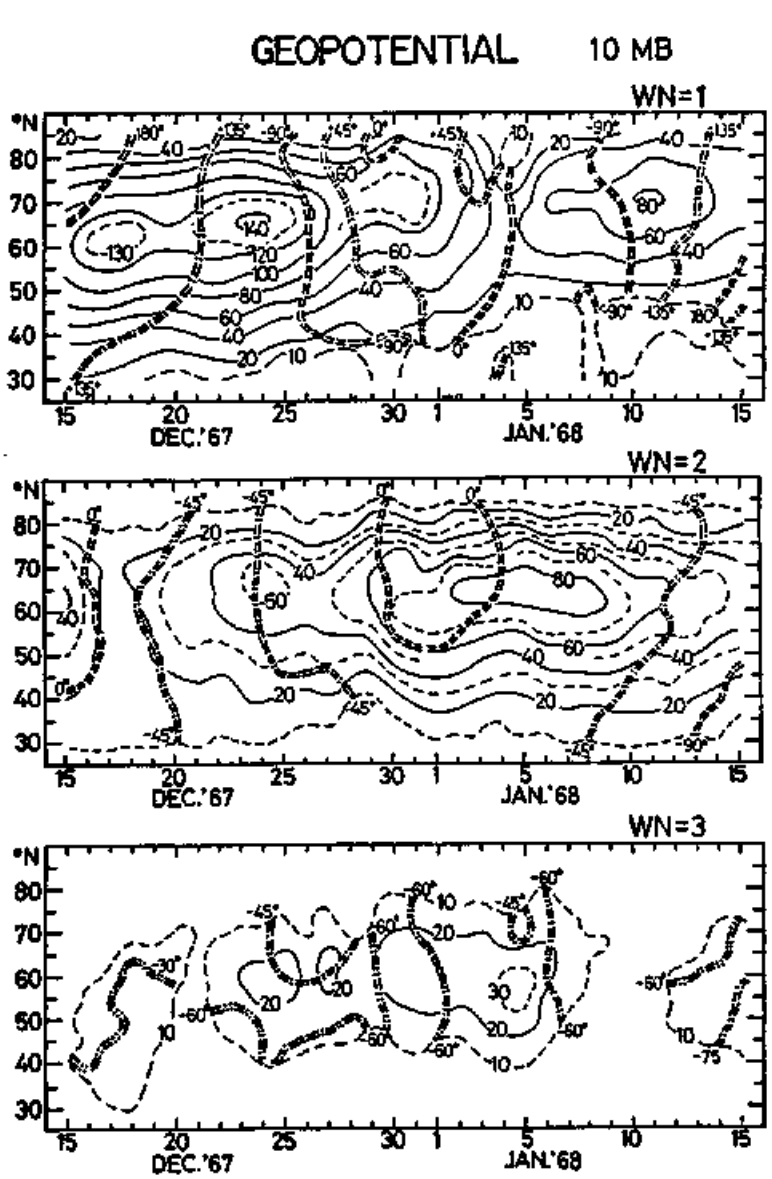

Fig. 11. Meridional-time section of amplitudes and phase-angles of the ultra-long waves with wavenumbers one (top), two (mid) and three (bottom) at 10 mb. Unit of the amplitude is 10 gpm, and that of the phase-angle east (+) or west (−)° longitude.

their magnitudes are different from each other. It is a different point that in his theoretical case the sudden warming occurred with decreasing of the second maximum, while in our result the warming occurred at the decreasing of the first maximum. In the observational results [*e.g.*, Webb (1966)] corresponding to the Matsuno's numerical experiment, the sudden warming occurred at the time of the earlier weakening of the first maximum westerly. However, we cannot answer whether these agreement and disagreement points are an essential one for the warming or not.

5.2. Day-to-day behaviour of the total ultra-long waves

In this section, day-to-day behaviour of the total ultra-long waves to which the time-filters are not yet applied, will be described. The amplitude and phase-angle of the ultra-long waves of

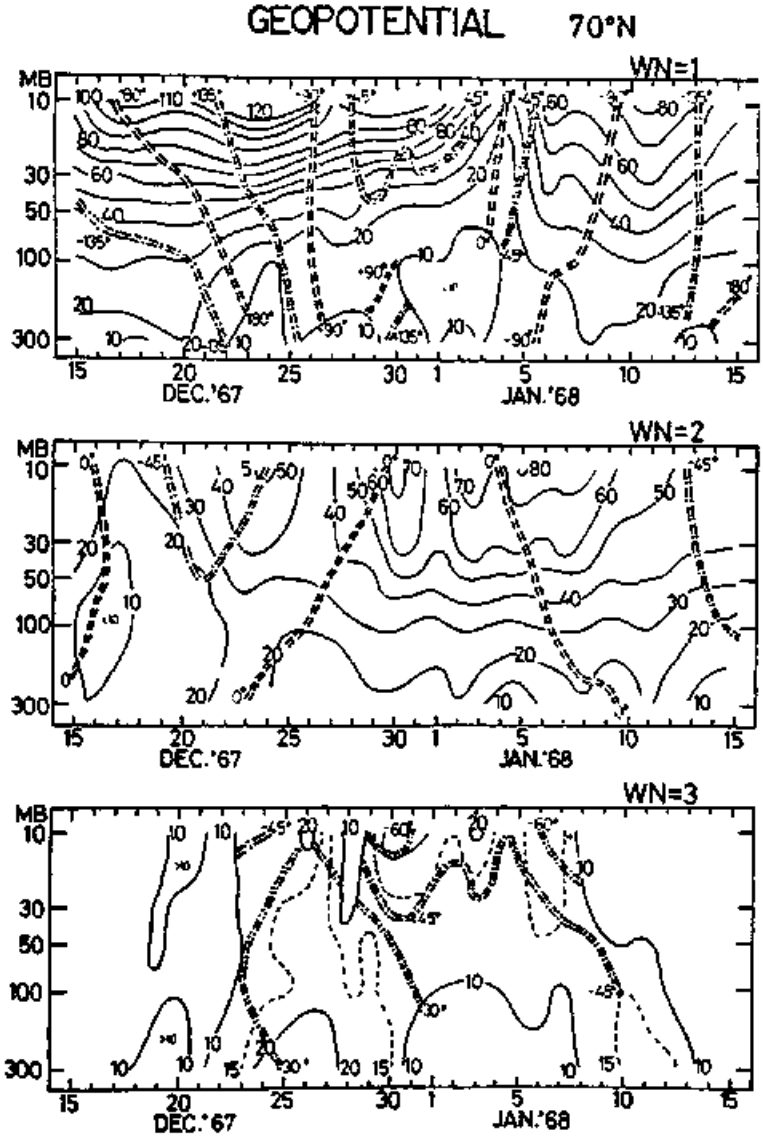

Fig. 12. Vertical-time section of amplitudes and phase-angles of the ultra-long waves with wavenumbers one (top), two (mid) and three (bottom) at 70°N from 300 mb to 10 mb. Units are the same as Fig. 11.

wavenumbers one, two and three at 10 mb are shown in meridional-time section (Fig. 11). The amplitude of wavenumber one had a maximum from 60°N to 70°N throughout the whole period. While that of wavenumber two has a maximum at 60-65°N, as well as that of wavenumber one, the amplitude reached a maximum about Jan. 5, 1968. The amplitude of wavenumber one began to decrease just after the sudden warming peak all over the most latitudes. Time-change of the phase-angle is shown by the double dashed lines in Fig. 11. Although the isopleths have rather complicated features, they show a general tendency of westward travelling with a speed about 10°long/day. It is noted that the maximum amplitude of wavenumber two and the minimum of wavenumber one appeared nearly simultaneously. Until Dec. 22, 1967, the former wave moved westwards, thereafter turned to eastward. After the time of sudden warming peak, this

wave travelled westward again. From Figs. 9 and 11, it is noted that the zonal wind and the amplitude of wavenumber one show a periodic day-to-day variation with about two weeks and with negative correlation. Such a characteristic change is found out during the other periods of the sudden warming [Hirota and Sato (1969)].

The amplitude of wavenumber three is much smaller than those of the wavenumbers one and two. Maximum amplitude appeared in the narrow region from 55°N to 65°N during the period from Dec. 23, 1967 to Jan. 6, 1968. In day-to-day variation of the phase-angle, no clear feature such as systematic travelling can be found out.

Fig. 12 shows amplitudes and phase-angles in vertical-time section at 70°N from 300 mb to 10 mb. The amplitudes of wavenumbers one and two clearly decrease downwards, and that of wavenumber three does not so. The characteristic features of time change of wavenumbers one and two at 10 mb can be also found out in the lower levels, and maximum or minimum at the lower layer somewhat precedes those at the upper layer. It suggests that the cause of time change of the amplitude may be probably in the lower layer. The ridge (or trough) axis of wavenumber one tilts westward with increasing of altitude before the sudden warming, while it does eastward after appearance of the maximum temperature. Those of wavenumbers two and three are mostly westward throughout the period, though their magnitudes are small. The magnitude of westward-tilt of wavenumber two in our result seems to be considerably small, as compared with that of Muench (1965).

5.3. *Day-to-day behaviour of the travelling and quasi-stationary ultra-long waves*

By means of the time-filter method mentioned in the foregoing section, the total ultra-long waves can be separated into the travelling and quasi-stationary parts. Day-to-day behaviour of both parts will be depicted in this section.

Before presentation of the results of separation, a few results obtained through only application of the time-filter will be provided for better understanding of the method of analysis. For its purpose, we will choose the wavenumber two, taking into consideration that it dominated during the warming period as shown Figs. 11 and 12. Applying the eight band-pass filters and one low-pass filter to the time-series of cosine and sine coefficients of wavenumber two at 10 mb, 65°N, we obtain the amplitude and phase-angle for each filter illustrated in Fig. 13. It is easily seen that the amplitude of low-pass-filtered part (LF) is the most significant, and that those of the other band-pass-filtered parts [$BF(j)$, $j=1, 2, 3, 4, 5, 6, 7$ & 8] nearly periodically fluctuate around some mean value. Time variation of the phase-angle of $BF(5)$, $BF(6)$, $BF(7)$ and $BF(8)$ are rather slower than those expected from the central frequency of the filter, except abrupt shift found when the amplitude is quite small. This fact and conspicuous periodic time-change of their amplitudes suggest that they contain not only the travelling mode but also a fluctuating component of the quasi-stationary part as expected from the relation (A-4) and (A-5). Such a mode with an amplitude less than the corresponding critical value given in the section 3 may be worthless to be treated furthermore, and therefore it is excluded here. From the results for 36 terms Fourier harmonic analysis in the section 3, the significanse levels are about 260 gpm for $BF(1)$, 90 gpm for $BF(2)$, 60 gpm for $BF(3)$, 45 gpm for $BF(4)$ and 40 gpm for $BF(5)$, $BF(6)$, $BF(7)$ and $BF(8)$, respectively. Thus, all modes, except $BF(1)$ and $BF(2)$, are separated into two parts, *i.e.* the travelling part and fluctuating component of the quasi-stationary one. Such results are illustrated in Fig. 14. Hereafter, for convenience, we express each travelling mode with T_3, T_4,…, T_8 referring to each band-pass filter. The fluctuating components of quasi-stationary part which pass each band-pass filter are also represented by $Q_3, Q_4, \cdots, Q_8$.

As expected, the amplitudes of $Q_3, Q_4, \cdots, Q_8$ vary periodically with the central period of the band-pass filter. The amplitudes of the travelling modes T_3, T_4,…, T_8 are approximately constant, compared with those shown in Fig. 13. Phase-angles of T_5, T_6, T_7 and T_8 show their westward travelling and their phase speeds fall in the range from 5° long/day to 10°long/day. Phase change of T_4 implies eastward travelling with a value nearly equal to 11°long/day.

Although the travelling direction of T_3 shows an abrupt change at Jan. 2 from westward to eastward, its change may not be significant because of the small amplitude during the last half of the days.

In the discussion of filtering in the Appendix

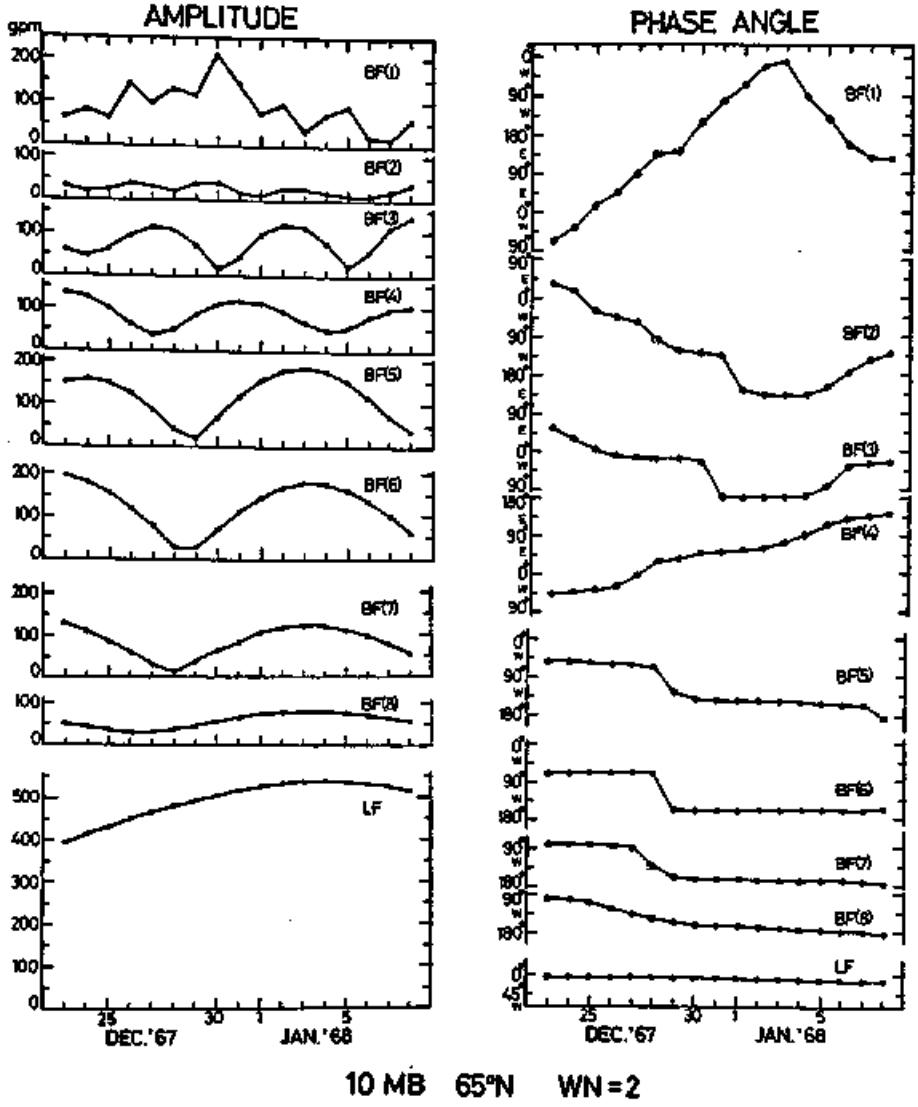

Fig. 13. Amplitudes and phase-angles of the travelling modes and fluctuating-components of the quasi-stationary part with wavenumber two at 10 mb, 65°N after passing through the band-pass filters [$BF(1)$, $BF(2)$, $BF(3)$, $BF(4)$, $BF(5)$, $BF(6)$, $BF(7)$ and $BF(8)$] and low-pass filter [LF]. Unit of the amplitude is gpm, and that of the phase-angle east (+) or west (−)° longitude.

A, the amplitude of travelling part is treated to be constant. If it changes with several periods, one travelling wave may simultaneously pass through a few band-pass filters. Moreover, taking account of overlap of the range of pass-band of $BF(6)$, $BF(7)$ and $BF(8)$ shown in Fig. 1, it is permissible to infer that T_5, T_6, T_7 and T_8 come from one travelling mode. Therefore, all travelling modes passing through the filter of $BF(3)$, $BF(4)$, $BF(5)$, $BF(6)$, $BF(7)$ and $BF(8)$ will be temporarily classified into the two groups, *i.e.* eastward-travelling mode and westward-travelling one. Then the amplitudes and phase-angles of such two modes are respectively shown in meridional-(Fig. 15) and vertical-(Fig. 16) time sections.

Fig. 15 shows the meridional-time section of amplitudes and phase-angles of westward-(upper

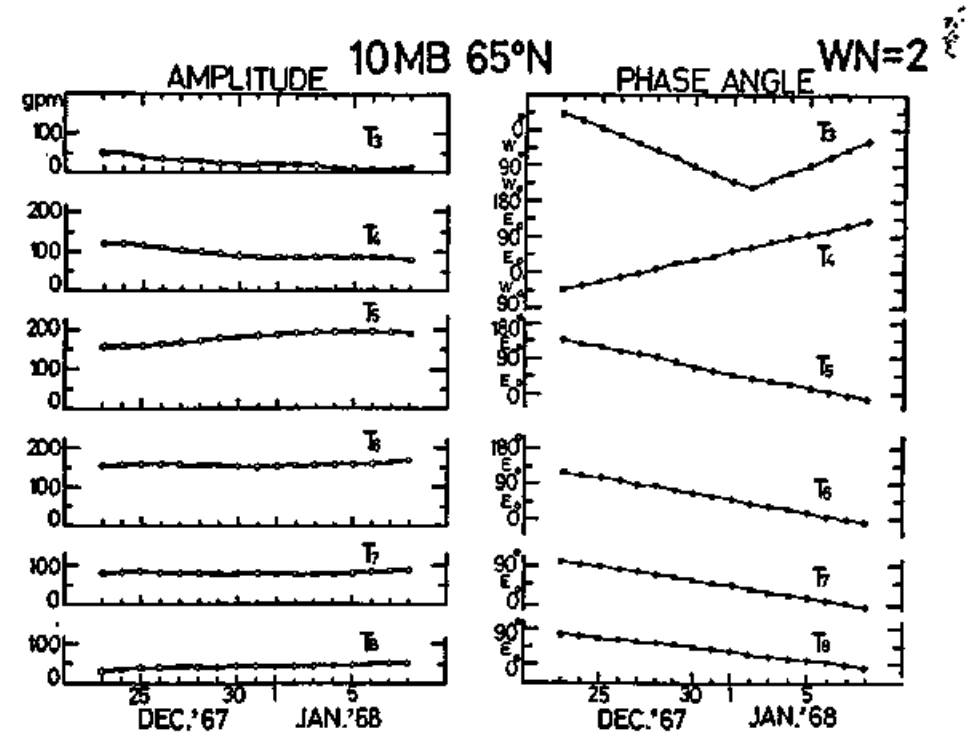

Fig. 14a.

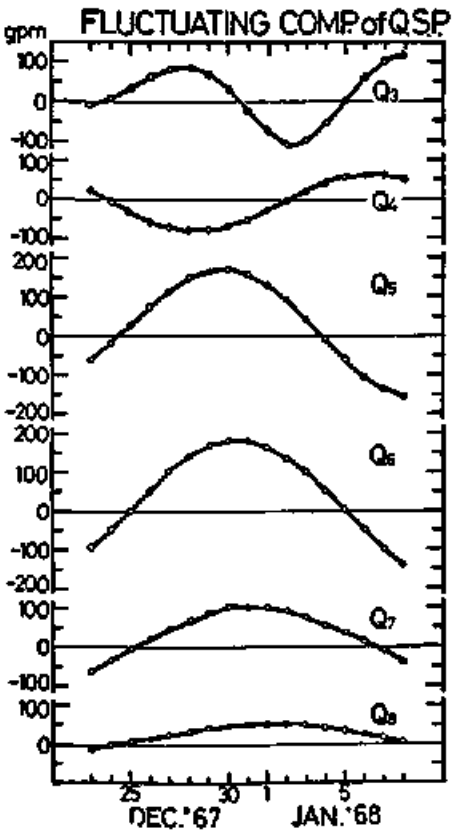

Fig. 14b.

Fig. 14. Amplitudes and phase-angles of the travelling modes (T_3, T_4, T_5, T_6, T_7 and T_8) (Fig. 14a) and fluctuating components of the quasi-stationary part (Q_3, Q_4, Q_5, Q_6, Q_7 and Q_8) (Fig. 14b) of wave-number two at 10 mb and 65°N. Their units are gpm and east (+) or west (−)° longitude, respectively.

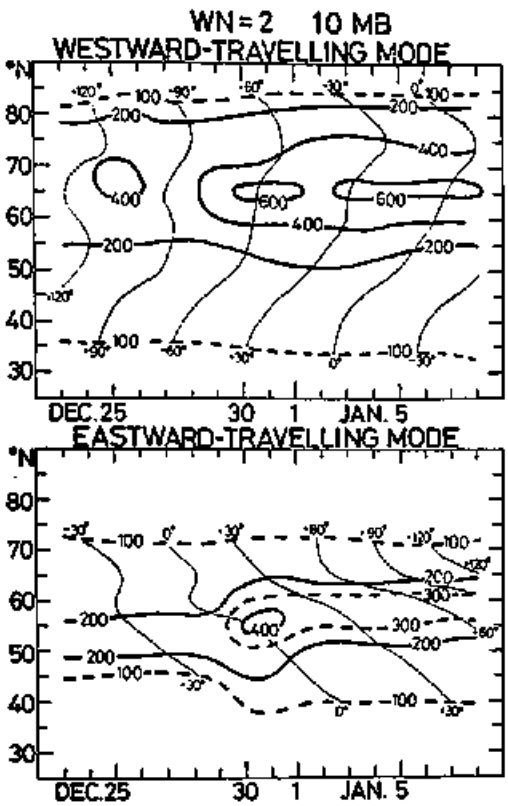

Fig. 15. Meridional-time section of amplitude and phase-angle of the westward (upper) and eastward (lower) travelling modes of wavenumber two at 10 mb. Units are the same as Fig. 14.

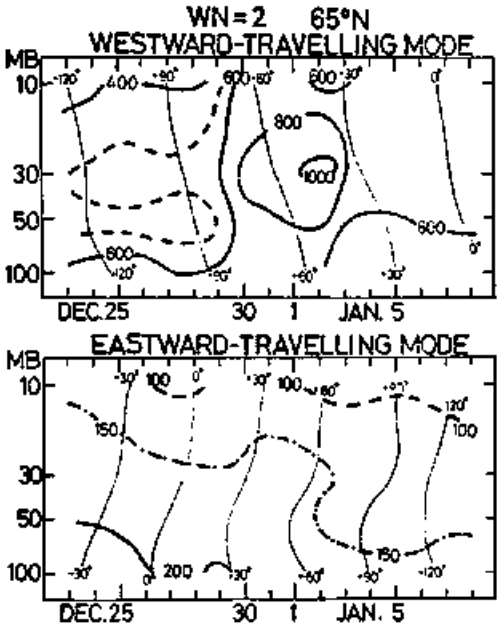

Fig. 16. Vertical-time section of amplitude and phase-angle of the westward (upper) and eastward (lower) travelling modes of wavenumber two at 65°N. Units are the same as Fig. 14.

part) and eastward-(lower one) travelling modes at 10 mb level. From this figure the following facts are found out:

(i) The maximum amplitudes of westward-travelling mode are about twice those of eastward-travelling one. During the period from Dec. 31, 1967 through Jan. 8, 1968, the former amplitude is about 600 gpm and the latter about 300 gpm.

(ii) Both the amplitudes conspicuously increased about Dec. 30, 1967.

(iii) The meridional scale of westward-travelling mode is rather larger than that of eastward-travelling one.

(iv) The phase speed of the eastward-travelling mode is about 10°long/day, and that of the westward-travelling one is equal to or a little less than the value.

(v) Their trough-ridge axes generally tilt eastward with increasing of latitude.

(vi) The eastward-tilt of eastward-travelling mode is mostly larger than that of westward-travelling one.

Fig. 16 illustrates the amplitudes and phase-angles in the vertical-time section at 65°N lat., where we have multiplied the amplitude at a pressure level p below 30 mb by a factor of $\sqrt{p/10\,\mathrm{mb}}$, considering the influence of density distribution [Matsuno (1971)]. A few features are found out in their vertical structure as follows;

(vii) The westward-travelling mode has a maximum at 30 mb about Dec. 30 to Jan. 2. Except this period, the amplitude is nearly uniform in vertical direction.

(viii) The amplitude of eastward-travelling mode decreases with increasing of altitude, and it is smaller than that of westward-travelling one.

(ix) Trough-ridge axes of both the modes tilt westward with almost equal magnitude.

Classification of travelling mode has been made by Bradley and Wiin-Nielsen (1968). Taking account of the phase speed and vertical structure, we may consider that both the eastward- and

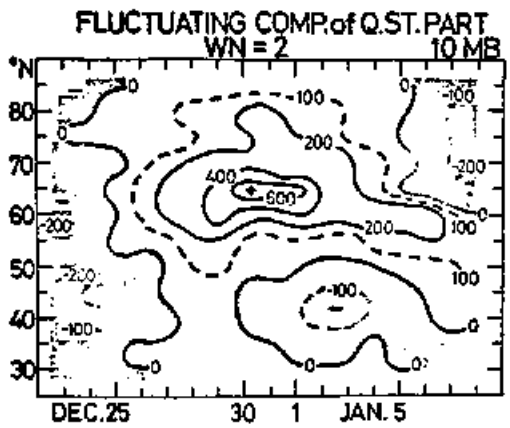

Fig. 17a. Meridional-time section of the fluctuating component of the quasi-stationary part corresponding to $BF(3)$, $BF(4)$, $BF(5)$, $BF(6)$, $BF(7)$ and $BF(8)$ of wavenumber two at 10 mb. Units are the same as Fig. 14.

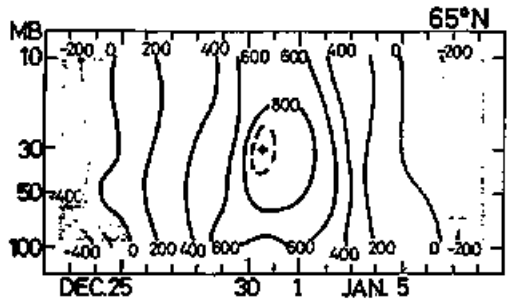

Fig. 17b: The same as Fig. 17a, except vertical-time section at 65°N from 100 mb to 10 mb.

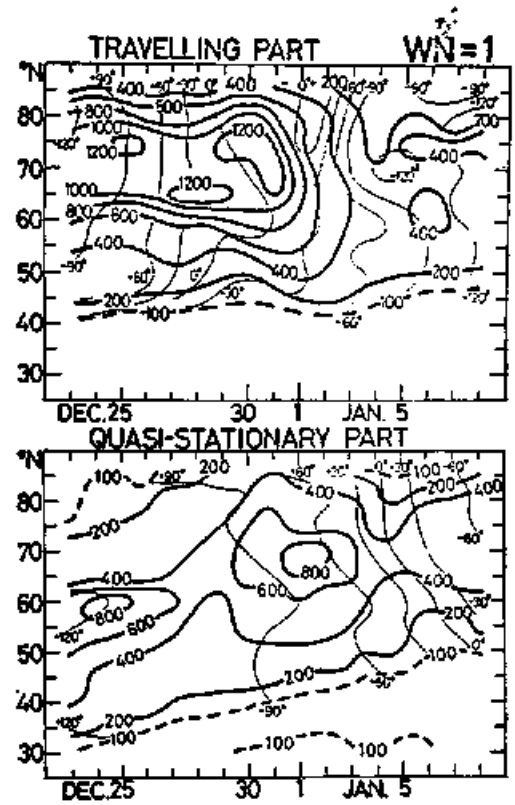

Fig. 18. Meridional-time section of amplitude and phase-angle of the travelling and quasi-stationary ultra-long waves with wavenumber one at 10 mb. Units are the same as Fig. 14.

westward-travelling modes correspond to the "forced mode" of Bradley and Wiin-Nielsen (1968), although their analyses were limitted at the levels below 200 mb. They also indicated existence of the "free mode". Its phase speed corresponds to that in the range of $BF(2)$. However, such a mode filtered through $BF(2)$ is excluded here, because of its quite small amplitude as mentioned above. Comparing our results of analysis with the observational results of Bradley and Wiin-Nielsen (1968), we may infer that their first- and second-vertical modes correspond to the westward- and eastward-travelling modes, respectively.

Fig. 17a and Fig. 17b show the meridional- and vertical-time sections of the fluctuating component of the quasi-stationary part corresponding to $BF(3)$, $BF(4)$, $BF(5)$, $BF(6)$, $BF(7)$ and $BF(8)$. It is noted that quite a large amplification is found out around 65°N during the warming period from Dec. 27 to Jan. 3. Before and after that time, the amplitude contrarily decreased. Comparing this result with Fig. 15, we can find out that the magnitude of the fluctuating component is comparable with the amplitude of the westward-travelling mode. In the vertical section, the amplitudes at all the levels vary almost simultaneously, except the time when the maximum range of the amplitude-change is found at 30 mb, as well as the westward-travelling mode. Henceforth, besides the result of wavenumber two, those of wavenumbers one and three are also illustrated in meridional- and vertical-time sections, where the total ultra-long waves are separated into the fluctuating quasi-stationary part and one travelling part without discriminating between eastward-travelling mode and westward-travelling one. This

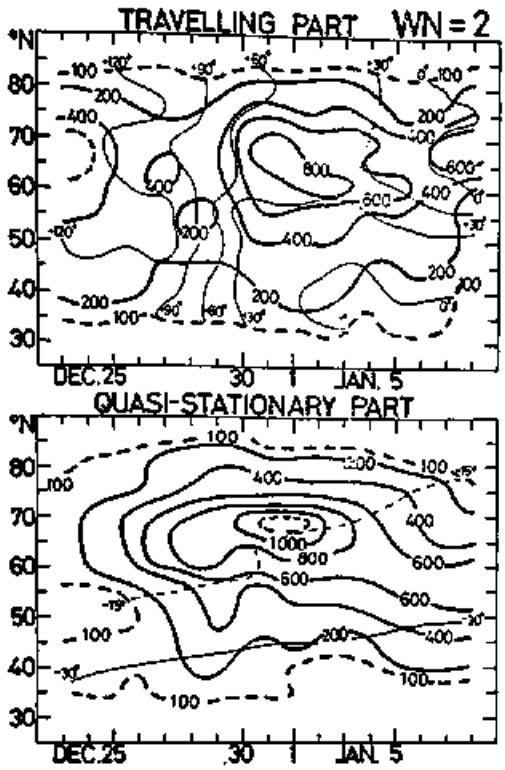

Fig. 19. The same as Fig. 18 except wavenumber two.

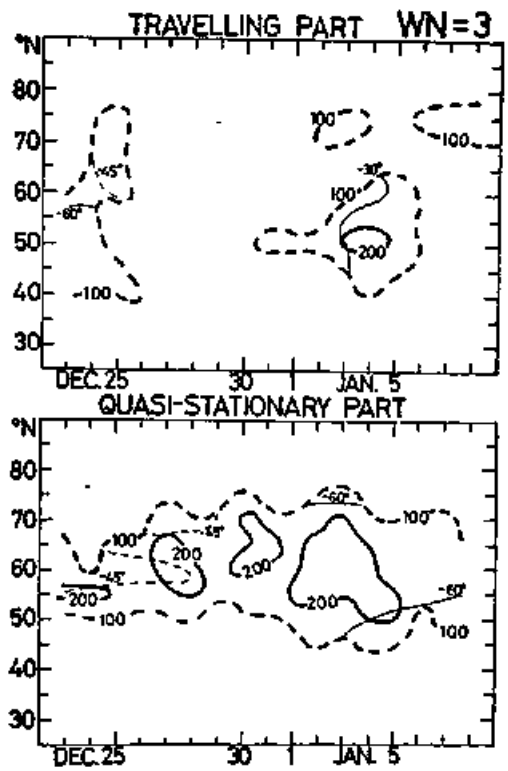

Fig. 20. The same as Fig. 18 except wavenumber three.

is because our major interest is directed to variation of the quasi-stationary part rather than the travelling one.

Fig. 18 is the results of wavenumber one in meridional-time section at 10 mb. The amplitude of the travelling part between 65°N and 70°N is larger than 1000 gpm before the sudden warming. It abruptly decreased about Dec. 31, and remained to be small afterwards. While the amplitude of the quasi-stationary part gradually increased, and reached a maximum at 70°N about Jan. 1. Afterwards it decreased till Jan. 5. Such a characteristic amplitude-change of both parts permits us to speculate some close energetical relation between them, as Murakami (1960) showed the energy flow from the stationary disturbance to the transient eddy. The phase-angles are illustrated only in the region where the amplitude is greater than 100 gpm. The travelling part moved westward with the speed of 15–20°long/day. Time-change of phase-angle of the quasi-stationary part is mostly less than 5°long/day for the first half period. While for the last half it reached 30°long/day or so. Strictly speaking, the low-pass filter LF is not ideal, in such a sense that its response for the short period is not completely zero. Therefore, it is very difficult to exclude such a mixing of travelling mode with a conspicuously large amplitude and short period completely. Since at the last several days the amplitude of the travelling part was not so large, the large phase change seems to have been induced by combined effects of nearly periodic amplitude-change and travelling of the travelling part, as well as by the abrupt shift of phase of the quasi-stationary part.

Fig. 19 shows the meridional-time section of wavenumber two. Maximum amplitude of the quasi-stationary part is nearly equal to that of the travelling one. Both parts have a maximum amplitude about Jan. 1 at 65°N. The date of this maximum corresponds to the time of the mature stage of the sudden warming. The quasi-stationary part moved westward with the speed about 15°long/day, while phase-angle of the quasi-stationary one is almost constant.

The amplitude of wavenumber three is very

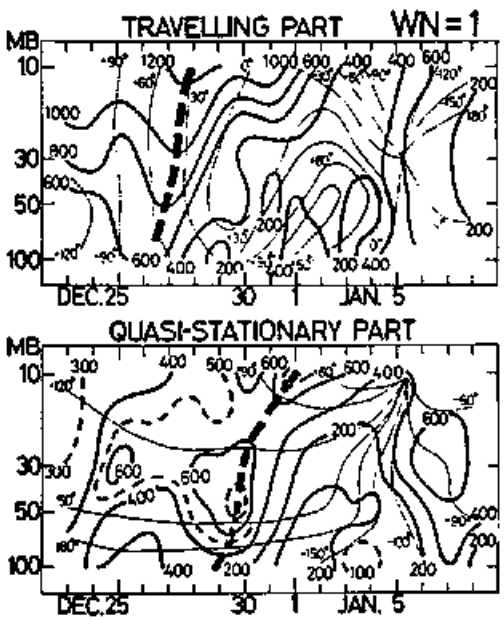

Fig. 21. Vertical-time section of amplitude and phase-angle of the travelling and quasi-stationary ultra-long waves with wavenumber one at 65°N from 100 mb to 10 mb. Units are the same as Fig. 14.

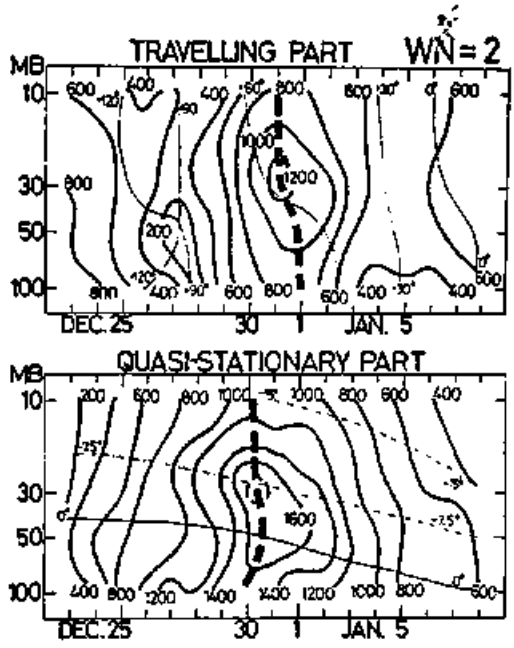

Fig. 22. The same as Fig. 21 except wavenumber two.

small, as compared with the wavenumbers one and two all over the latitudes and days as shown in Fig. 20. That of the quasi-stationary part has a region larger than 100 gpm from 50°N to 70°N, including several maxima greater than 200 gpm.

Similar results will be described in vertical-time section, where the amplitude below 30 mb level is multiplied by a square-root density factor as well as in Fig. 16.

Fig. 21 is the result of wavenumber one. The amplitudes of both parts generally increase with altitude except a few maxima at 30 mb level.

Furthermore, it is noted that both parts have an indication of the vertical propagation of amplification before the warming stage, as illustrated with a thick-dashed line. That of the travelling part occurred at the first half stage of the sudden warming, preceding that of the quasi-stationary one. The latter almost coincides with the time of sudden warming at 65°N. Their speeds of vertical propagation are about 10 km/day or so. The ridge (or trough) axes of the quasi-stationary part considerably tilt westward all over the days. Their phase difference between 10 mb and 100 mb is greater than 100°long. While the ridge axes of the travelling part are nearly in vertical during the first half of the warming stage, and tilted westward afterwards.

The vertical section for wavenumber two is illustrated in Fig. 22. The amplitudes of both parts have a maximum at 30 mb level about Dec. 30 or 31, and their amplification almost simultaneously occurred at all the levels from 100 mb to 10 mb. The ridge (or trough) axes of both modes are nearly vertical, different from the westward-tilt of wavenumber one. No pronounced delay of amplification is found out. An evidence of slant propagation of amplification from lower level and lower latitude to higher level and higher latitude will be shown in another paper [Yamamoto and Iwashima (1972)]. The travelling parts moved westward with the speed of about 10°long/day at all levels.

The quasi-stationary part of wavenumber three in Fig. 23 is considerably dominant at lower levels, in contrast with insignificant amplitude at 10 mb (Fig. 20). There is an indication of westward-tilting of the quasi-stationary part. Amplitude of the travelling part is too small to be discussed further. No pronounced features are found out in this vertical structure.

Further investigations are required to answer a question whether the above-mentioned

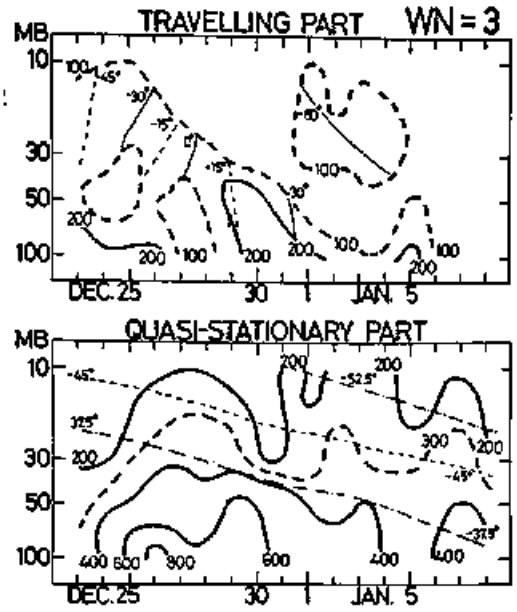

Fig. 23. The same as Fig. 21 except wavenumber three.

characteristics of the ultra-long waves are common to the stratospheric sudden warming or particular for the 1967/68 sudden warming. The present author expects that similar analyses will be performed on the other seasons and situations.

6. Summary and concluding remarks

A method of separating the total ultra-long waves into the travelling and quasi-stationary parts on a daily basis, was outlined together with a criterion for reliability of the results.

This method was applied to the geopotential data in the 1967/68 winter stratosphere. In the first stage the total ultra-long waves of wavenumbers one, two and three were obtained by the Fourier harmonic analysis along a latitudinal circle. Secondly the eight band-pass and one low-pass time filters were operated to the time series of cosine and sine coefficients obtained at the first stage. Thirdly, after some manipulation, a travelling mode and a fluctuating component of the quasi-stationary part were obtained from such a part that had passed each band-pass filter. Finally one travelling part and a quasi-stationary one were given.

The main results at each stage are summarized as follows;

(i) In the field concerned with the total ultra-long waves, wavenumbers one and two show a periodical change with negative correlation and the period of about two weeks during the warming as shown by Teweles (1963), Hirota and Sato (1969), etc.. At the abrupt warming stage the former wave decayed and the latter amplified. While, after the warming peak, the former gradually recovered and the latter decayed.

(ii) Both the westward- and eastward-travelling modes of wavenumber two have different vertical and meridional structures.

(iii) The travelling part of wavenumber one, which was obtained without descriminating the travelling direction, abruptly decayed at the warming stage just before its maximum peak, when the quasi-stationary part reached a maximum. As compared with this result, the total ultra-long wave with the same wavenumber decayed somewhat gradually.

(iv) Just at the warming peak, both the parts of wavenumber two became most predominant.

(v) Roughly speaking, the ridge (or trough) axes of the quasi-stationary part with wavenumbers one and two tilted westward with increasing of altitude, and the tilting of wavenumber one was much larger than that of wavenumber two.

(vi) Westward vertical-tilting of the ridge axes was found out in the travelling parts of wavenumbers one and two. However, their magnitudes were smaller than the magnitude of the quasi-stationary part.

(vii) From the amplitude-change of the travelling part of wavenumbers one and two, they seem to correlate non-linearly each other.

(viii) In the amplitude-change of (iii) and (iv), we can find out such a feature that makes us infer the energetical relation between the quasi-stationary part and travelling one with the same wavenumber.

The above-mentioned results urge us into the next study of the energy processes of the quasi-stationary and travelling ultra-long waves. Such a further investigation will disclose a qualitative relationship between both the waves, which are, from many former studies, speculated to have different origins. Also, some interesting features

of the travelling part obtained here require us to analyze them in detail. The results of those studies will be published in the near future.

Acknowledgements

The author wishes to express his hearty thanks to Professor Ryozaburo Yamamoto of the Faculty of Science, Kyoto University for his warm-hearted encouragement, guidance and discussions throughout this work.

All the computations in this study were made by the use of KDC-II (HITAC 5020) at the Computation Center (Job No. E 5000) of Kyoto University and the FACOM 230-60 computer at the Data Processing Center (Job Nos. 5001PD 003 and 5001DF 751) of Kyoto University.

References

Arai, Y., 1970: Harmonic analysis and seasonal variation of the ultra-long waves. *Gurosubetta*, **9**, No. 1 (in Japanese).

Benwell, G.R.R., 1966: The behaviour of the first six zonal wave numbers at 50 and 500 millibars during some winter months in 1958 and 1959. *Meteor. Mag.*, 95, 33–47.

Bradley, J.H.S., 1968: The transient parts of the atmospheric planetary waves. *AMRG Publication in Meteorology*, 90, 61–70.

———— and A. Wiin-Nielsen, 1968: On the transient part of the atmospheric planetary waves. *Tellus*, **20**, 535–543.

Brooks, C.E.P. and N. Carruthers, 1953: *Handbook of Statistical Methods in Meteorology*. Her Majesty's Stationary Offices, London, 412 pp.

Conrad, V. and L.W. Pollack, 1970; *Methods in climatology*. Harvard Univ. Press, Cambridge, Mass., 459 pp.

Deland, R.J., 1964: Traveling planetary waves. *Tellus*, **16**, 271–273.

———— 1965: Some observations of the behaviour of spherical harmonic waves. *Mon. Wea. Rev.*, **93**, 307–312.

———— 1972: On the spectral analysis of traveling waves. *J. meteor. Soc. Japan*. **50**, 104–109.

———— and Y.-J. Lin, 1967: On the movement and prediction of traveling planetary scale waves. *Mon. Wea. Rev.*, 95, 21–31.

———— and K.W. Johnson, 1968: A statistical study of the vertical structure of traveling planetary scale waves. *Mon. Wea. Rev.*, 69, 12–22.

Eliasen, E., 1958: A study of the long atmospheric waves on the basis of zonal harmonic analyses. *Tellus*, **10**, 206–215.

———— and B. Machenhauer, 1965: A study of the fluctuation of the atmospheric planetary flow patterns represented by spherical harmonics. *Tellus*, **17**, 220–238.

———— and ————, 1969: On observed large-scale atmospheric wave motions. *Tellus*, **21**, 149–166.

Free University of Berlin, 1968: Daily and monthly northern hemisphere 100-, 50-, 30- and 10-millibar synoptic weather maps of the year 1967. Part IV, October-December. *Meteor. Abhand., Freien Univ. Berlin*, Band LXXX, LXXXI LXXXII, Heft 4.

————, 1969: Daily and monthly northern hemisphere 100-, 50-, 30-, and 10-millibar-synoptic weather maps of the year 1968. Part I, January-March. *Meteor. Abhand., Freien Univ. Berlin*, Band XCV, XCVI, XCVII, Heft 1.

Haney, R.L., 1961: Harmonics of selected 5-day mean 500 mb charts. *Mon. Wea. Rev.*, 89, 391–396.

Hayashi, Y., 1971: A generalized method of resolving disturbances into progressive and retrogressive waves by space Fourier and time cross-spectral analyses. *J. meteor. Soc. Japan*, 49, 125–128.

Hirota, I., 1967: The vertical structure of the stratospheric sudden warming. *J. meteor. Soc. Japan*, 45, 422–435.

————, 1968: Planetary waves in the upper stratosphere in early 1966. *J. meteor. Soc. Japan*, 46, 418–430.

———— and Y. Sato, 1969: Periodic variation of the winter stratospheric circulation and intermittent vertical propagation of planetary waves. *J. meteor. Soc. Japan*, 47, 396–402.

Iwashima, T. and R. Yamamoto, 1971: A method for separation of the ultra-long waves in the atmosphere into the quai-stationary and transient parts by the time-filters. *J. meteor. Soc. Japan*, 49, 158–162.

———— and ————, 1973: Remarks on the analysis of the quasi-stationary and travelling ultra-long waves in the atmosphere. *J. meteor. Soc. Japan*, 51, 151–154.

Johnson, K.W., 1969: A preliminary study of the stratospheric warming of December 1967-January 1968. *Mon. Wea. Rev.*, 97, 553–564.

———— and M.E. Gelman, 1968: Temperature and height variability in the middle and upper stratosphere during 1964-1966 as determined from constant pressure charts. *Mon. Wea. Rev.*, 96, 371–382.

Julian, P.R. and K.B. Labitzke, 1965: A study of atmospheric energetics during the January-February 1963 stratospheric warming. *J. atmos. Sci.*, 22, 597–616.

Kao, S.-H., 1968: Governing equations and spectra for atmospheric motion and transports in frequency-wavenumber space. *J. atmos. Sci.*, 25,

32-38.

————, 1970: Wavenumber-frequency spectra of temperature in the free atmosphere. *J. atmos. Sci.*, 27, 1000-1007.

————, R.L. Jenne and J.F. Sagendorf, 1970: The kinetic energy of the large-scale atmospheric motion in the wavenumber-frequency space, II. *J. atmos. Sci.*, 27, 1008-1020.

———— and L.L. Wendell, 1970: The kinetic energy of the large-scale atmospheric motion in the wavenumber-frequency space, I. *J. atmos. Sci.*, 27, 359-375.

Kubota, S. and M. Iida, 1954: Statistical characteristics of the atmospheric disturbances. *Pap. Meteor. Geophys.*, 5, 22-34.

Matsuno, T., 1971: A dynamical model of the stratospheric sudden warming. *J. atmos. Sci.*, 28, 1479-1494.

Miyakoda, K., 1963: Some characteristic features of winter circulation in the troposphere and lower stratosphere. Tech. Rept., 14, Dept. Geophys. Sci., University of Chicago, 93 pp.

Muench, H.S., 1965: On the dynamics of the winter-time stratospheric circulation. *J. atmos. Sci.*, 22, 349-360.

Murakami, T., 1960: On the maintenance of kinetic energy of the large-scale stationary disturbances in the atmosphere. *Sci. Rept.* No. 2, M.I.T. Plan. Circ. Proj., AF 19 (664)-6108.

Sawyer, J.S., 1962: Performance requirements of aerological instruments. *WMO Technical Notes* No. 45, 29 pp.

Shchigolev, B.M., 1965: *Mathematical Analysis of Observations*. Publishing Company Inc., New York, 350 pp.

Teweles, S., 1963: A spectral study of the warming epoch of January-February 1958. *Mon. Wea. Rev.*, 91, 565-519.

Webb, W.L., 1966: Structure of the Stratosphere and Mesosphere. *International Geophysical Series* Vol. 9, Academic Press, New York and London, 382 pp.

Yamamoto, R. and T. Iwashima, 1972: An analysis of the ultra-long waves (The 4 th report). Presented at the Autumn 1972 Meetings of the Meteorological Society of Japan at Niigata (to be published).

Appendix A.

Procedure

The method of analysis is divided into two parts;

(I) the first part where the ultra-long waves are taken out from the data in space domain by means of the Fourier harmonic analysis, and

(II) the second one where the ultra-long waves are further separated into the travelling and quasi-stationary parts by the time-filter method.

At the first part of the procedure (I), the ultra-long waves are extracted from such data geopotential height by means of the Fourier harmonic analysis along a latitude as usual. Since the ultra-long waves can be considered to consist of the quasi-stationary and travelling parts, the cosine and sine coefficients of the n-th harmonic, $C_n(t)$ and $S_n(t)$ may be expressed as follows;

$$C_n(t) = T_n(t) \cos\{n(\lambda_{1,n} + V_n t)\} + Q_n(t) \cos(n\lambda_{0,n}) \quad \text{(A-1)}$$

$$S_n(t) = T_n(t) \sin\{n(\lambda_{1,n} + V_n t)\} + Q_n(t) \sin(n\lambda_{0,n}) \quad \text{(A-2)}$$

where t is the time. The first term in the right-hand side of the above equations is concerned with the travelling part, and $T_n(t)$ is the amplitude, V_n the phase speed and $\lambda_{1,n}$ the initial phase, respectively. The second term is the quasi-stationary part, and $Q_n(t)$ is the amplitude, and $\lambda_{0,n}$ the ridge position. This Fourier harmonic analysis is performed for daily data throughout the period of analysis longer than 100 days, and thus time series of $C_n(t)$ and $S_n(t)$ are obtained.

The second part of procedure (II) is subdivided into three steps as follows;

(II-1) Applying the low-pass filter LF [$LF(6)$ in the previous paper] to the time series of $C_n(t)$ and $S_n(t)$ respectively, we obtain $\bar{C}_n(t)$ and $\bar{S}_n(t)$. The phase-angle $n\lambda_{0,n}$ and the amplitude $\bar{Q}_n(t)$ of low-frequency component of the quasi-stationary part are defined as follows;

$$\bar{Q}_n(t) = \{\bar{C}_n(t)^2 + \bar{S}_n(t)^2\}^{1/2},$$

$$n\lambda_{0,n} = \tan^{-1}\{\bar{S}_n(t)/\bar{C}_n(t)\} \quad \text{(A-3)}$$

where the bar ($\bar{}$) is referred to application of LF. The low-pass filter should be selected so that its cut-off period is large enough to exclude the travelling part.

(II-2) High-frequency component of amplitude change of the quasi-stationary part together with travelling one may remain in the quantities obtained by subtracting the low-frequency part [$\bar{Q}_n(t) \cos(n\lambda_{0,n})$ and $\bar{Q}_n(t) \sin(n\lambda_{0,n})$] from the original quantities $C_n(t)$ and $S_n(t)$. At the next step, such a high frequency component of $C_n(t)$

and $S_n(t)$ are divided into several frequency ranges, using eight band-pass time filters [$BF(j)$ $j=1, 2, 3, 4, 5, 6, 7$ & 8], which cover almost all frequencies higher than the cutoff frequency of the low-pass filter. This is convenient for separating the travelling part from the quasi-stationary part in the later step, as well as picking up the travelling modes with various phase speeds.

Applying a band-pass filter $BF(j)$ to the time series $C_n(t)$ and $S_n(t)$, we obtain the $C_{n,j}(t)$ and $S_{n,j}(t)$. It is reasonable to consider that these quantities consist of the travelling part and a component of amplitude-change of the quasi-stationary one with the period of which is within the range of the band-pass filter. Thus, we obtain

$$C_{n,j}(t)=T_{n,j}(t)\cos\{n(\lambda_{1,n,j}+V_{n,j}t)\}+Q_{n,j}(t)\cos(n\lambda_{0,n}) \quad \text{(A-4)}$$

$$S_{n,j}(t)=T_{n,j}(t)\sin\{n(\lambda_{1,n,j}+V_{n,j}t)\}+Q_{n,j}(t)\sin(n\lambda_{0,n}) \quad \text{(A-5)}$$

where the first term in the right-hand side of (A-4) and (A-5) belongs to the travelling part with the phase speed $V_{n,j}$, and the second one to the quasi-stationary part whose amplitude $Q_{n,j}(t)$ varies with a frequency nearly equal to $n|V_{n,j}|$. Subscript j is referred to application of $BF(j)$. This band-pass filtering is made for all frequency range by the use of $BF(1)$, $BF(2)$, $BF(3)$, $BF(4)$, $BF(5)$, $BF(6)$, $BF(7)$ and $BF(8)$.

At this step, equalization for these quantities must be made, referring to each response-function (Fig. 1), because their magnitude may be reduced by operation of the filter.

(II-3) In the next place, the travelling and quasi-stationary parts in $C_{n,j}(t)$ and $S_{n,j}(t)$ are separated. For its purpose, the following quantity is defined by $n\lambda_{0,n}$ obtained at the preceding step (II-1), and $C_{n,j}(t)$ and $S_{n,j}(t)$ at (II-2);

$$A_{n,j}(t)\equiv C_{n,j}(t)\sin(n\lambda_{0,n})-S_{n,j}(t)\cos(n\lambda_{0,n}) \quad \text{(A-6)}$$

From the relations (A-4) and (A-5), this is reduced to

$$A_{n,j}(t)=T_{n,j}(t)\sin\{n(\lambda_{0,n}-\lambda_{1,n,j}-V_{n,j}t)\} \quad \text{(A-7)}$$

The time series of $A_{n,j}(t)$ is shifted by a quarter of the period of the band-pass filter. It is nearly equal to $\pi/2\,n|V_{n,j}|$. It brings about the relation;

$$A_{n,j}(t\pm\Delta t)=\mp\frac{V_{n,j}}{|V_{n,j}|}T_{n,j}(t\pm\Delta t)\cos\{n(\lambda_{0,n}-\lambda_{1,n,j}-V_{n,j}t)\} \quad \text{(A-8)}$$

where $\Delta t=\pi/2\,n|V_{n,j}|$ and the double signs ($\pm$) should be selected in the same order. Under such an approximation

$$T_{n,j}(t)\fallingdotseq(T_{n,j}(t+\Delta t)+T_{n,j}(t-\Delta t))/2 \quad \text{(A-9)}$$

the relations (A-7) and (A-8) provide a relation which gives a value of $T_{n,j}(t)$;

$$T_{n,j}(t)=\left[A_{n,j}(t)^2+\left\{\frac{A_{n,j}(t-\Delta t)-A_{n,j}(t+\Delta t)}{2}\right\}^2\right]^{1/2} \quad \text{(A-10)}$$

The phase-angle $[n(\lambda_{0,n}-\lambda_{1,n,j}-V_{n,j}t)]$ is determined by the relations (A-7) and (A-8). The phase of travelling part θ is given by subtraction of this phase from $n\lambda_{0,n}$.

Substituion of the phase-angle and the amplitude of travelling part (A-10) into (A-4) and (A-5) gives the high-frequency component of the quasi-stationary part $Q_{n,j}(t)$. Separation of travelling part and high-frequency component of the quasi-stationary one is made in this way for a frequency range ($=n|V_{n,j}|$). The initial guess of the sign of $V_{n,j}$ is equivalent to that of $d\theta/dt$. $d\theta/dt$ is expressed by (A-4), (A-5) and (A-9) as follows;

$$\frac{d\theta}{dt}=\frac{T_{n,j}(t)\cdot nV_{n,j}[T_{n,j}(t)+Q_{n,j}(t)\cos\{n(\lambda_{0,n}-\lambda_{1,n,j}-sgn(V_{n,j})t)\}]}{T_{n,j}(t)^2+Q_{n,j}(t)^2+2\,T_{n,j}(t)Q_{n,j}(t)\cos\{n(\lambda_{0,n}-\lambda_{1,n,j}-V_{n,j}(t)\}} \quad \text{(A-11)}$$

Using some quantities $T_{n,j}$, $Q_{n,j}$, $\cdots$ on the right-hand side of (A-11) obtained by the initial guess of sign of $V_{n,j}$, we can ascertain whether its guess is right or wrong. If the initially guessed sign of $d\theta/dt$ coincides with that of the right-hand side of (A-11), either of the double signs in (A-8) should be selected approximately. The another sign should be selected, when the initially guessed sign of $d\theta/dt$ does not coincide with that of (A-11).

Appendix B

The time-filter expressed by spectral function

In order to extract the travelling and quasi-stationary parts from the ultra-long waves, we have employed the time-filter method. While other investigators [e.g. Kao (1968), Deland (1972)] did Fourier harmonic analyses in time- and space-domain. In this appendix the relationship of the time-filter method to the Fourier method is described.

A band-pass time filter in this paper is constructed by weighted-running-mean with the weighting function $w(t)$. Its operation to a function $f(t)$ is expressed as follows;

$$BF(f(t))=\int_{-T_m}^{T_m} w(\tau)f(t+\tau)d\tau$$

or

$$=\sum_{k=-I}^{I} w(k\Delta t)f(t+k\Delta t) \qquad \text{(B-1)}$$

where the former expression is used for continuous data, and the latter for discrete case. And T_m is a half of the running mean range, Δt time interval of two adjacent data and "I" is the number of data during the period T_m, so that $T_m=I\cdot\Delta t$. Integral or summation of $w(t)$ is set to be unity;

$$\int_{-T_m}^{T_m} w(t)dt=\sum_{k=-I}^{I} w(k\Delta t)=1 \qquad \text{(B-2)}$$

The larger T_m or "I" will be employed, the sharper the cutoff of the filter will become.

$w(t)$ is derived from the response function $R(n)$ as follows;

$$w(t)=\frac{1}{2\pi}\int_{-\infty}^{\infty} R(m)\exp(-imt)dm \qquad \text{(B-3)}$$

where m is the frequency. Let us consider an ideal band-pass filter such that the response function $R(m)$ is given by

$$\begin{aligned} R(m)&=1 \text{ for } n-\frac{\Delta n}{2}<m<n+\frac{\Delta n}{2} \\ &\quad \text{or } -n-\frac{\Delta n}{2}<m<-n+\frac{\Delta n}{2} \\ &=0 \text{ for } m<-n-\frac{\Delta n}{2} \text{ or } m>n+\frac{\Delta n}{2} \end{aligned} \qquad \text{(B-4)}$$

where the frequency n is chosen to be positive. Then, the weighting function for this ideal filter is obtained by

$$\begin{aligned} w(t)&=\frac{1}{2\pi}\int_{-n-\Delta n/2}^{-n+\Delta n/2}\exp(-imt)dm \\ &\quad+\frac{1}{2\pi}\int_{n-\Delta n/2}^{n+\Delta n/2}\exp(-imt)dm \\ &=\frac{1}{\pi}\int_{n-\Delta n/2}^{n+\Delta n/2}\cos(mt)dm \\ &=\frac{2}{\pi t}\cos(nt)\cdot\sin\left(\frac{\Delta n}{2}t\right) \end{aligned} \qquad \text{(B-5)}$$

Therefore, from the relations (B-2) and (B-5), the operation of the band-pass filter $BF\{\ \}$ for the discrete time-series data $f(t)$ can be approximately expressed as follows;

$$\begin{aligned} BF(f(t))&=\sum_{k=-I}^{I}\frac{2\cos(nk\Delta t)}{\pi k\Delta t}\sin\left(\frac{\Delta n}{2}k\Delta t\right)f(t+k\Delta t) \\ &=\sum_{k=-I}^{I}f(t+k\Delta t)\int_{n-\Delta n/2}^{n+\Delta n/2}\left[\frac{1}{2\pi}\left\{\exp(imk\Delta t)\right.\right. \\ &\quad\left.\left.+\exp(-imk\Delta t)\right\}\right]dm \\ &=\frac{1}{2\pi}\int_{n-\Delta n/2}^{n+\Delta n/2}\sum_{k=-I}^{I}[f(t+k\Delta t)\{\exp(imk\Delta t) \\ &\quad+\exp(-imk\Delta t)\}]dm \end{aligned} \qquad \text{(B-6)}$$

where $I\Delta t$ should be selected so as to be sufficiently large. Introducing the complex Fourier transform of $f(t)$,

$$F(m,t)=\frac{1}{2I}\sum_{k=-I}^{I}f(t+k\Delta t)\exp(-imk\Delta t) \qquad \text{(B-7)}$$

and using the mean value theorem, we can rewritten the above $BF\{f(t)\}$ as follows;

$$\begin{aligned} BF(f(t))&=\frac{I}{\pi}\int_{n-\Delta n/2}^{n+\Delta n/2}\{F(m,t)+F^*(m,t)\}dm \\ &=\frac{I}{\pi}\{F(n,t)+F^*(n,t)\}\Delta n \end{aligned} \qquad \text{(B-8)}$$

where $F^*(n,t)$ and $F^*(m,t)$ are the complex conjugates of $F(n,t)$ and $F(m,t)$, respectively. This relationship (B-8) implies that operation of the band-pass filter is equivalent to an integral or summation of the Fourier-transform for the frequency band in which the response of function $R(n)$ is unity.

大気中における超長波の解析的研究（I）
第1部　成層圏突然昇温前後の準停滞性・移動性超長波の振舞について

岩　嶋　樹　也
京都大学理学部地球物理学教室

1967/68年冬季成層圏における準停滞性・移動性超長波に関する解析的研究を，先に提案した時間フィルター法 [Iwashima and Yamamoto (1971)] により，daily basis で行なった．

最初に，解析方法について簡単に述べ（付録Aで，変更点などについて詳述），続いて error を含むデータの信頼性に対する基準を求めた．

従来知られている，帯状平均気温および帯状平均風速の突然昇温時における特徴的な時間変動が再確認された．この帯状平均場の変動に対応して，Teweles (1963) などにより示された，波数2の波動擾乱の顕著な振幅増大，波数1の振幅減衰が見られた．これらの等圧面高度場のフーリエ解析結果を，さらに時間フィルター法により，準停滞・移動性両部分に分離した．この過程が，卓越波数2の最も詳細な結果によって示される．

最終的結果として，波数 1, 2, 3 それぞれの準停滞性・移動性両部分の解析結果が，meridional-time section と vertical-time section で示される．突然昇温に伴って，以下のことが見られた．すなわち，

i）波数1の移動部分は昇温前に卓越し，その後急速に減衰する．

ii）波数1の準停滞部分，波数2の準停滞，移動両部分は昇温に伴って増幅し，昇温末期には徐々に減衰する．

なお，上記（i）は，Miyakoda (1963) の解析における，「突然昇温第3段階」に，あるいは，Hirota (1967) の "migratory stage" に相当すると思われる．

以上と従来の解析 [Hirota (1968), etc.] や理論 [Matsuno (1971)] の結果を合わせ考えると，波数 1, 2 の準停滞，移動の両部分それぞれの非線型相互作用とともに，Murakami (1960) の示した stationary, transient eddy 間のエネルギー的関係に類似の，各波数毎の準停滞性・移動性両部分間の密接な関係が予想される．

Observational Studies of the Ultra-Long Waves in the Atmosphere (II)

Part 2. Ultra-Long-Wave Energy Processes during the Stratospheric Sudden Warming

by

Tatsuya Iwashima

Geophysical Institute, Kyoto University, Kyoto

CONTENTS

Abstract

In the previous paper [Iwashima(1973)], it has been shown that, by means of the time-filter method, the ultra-long wave in the atmosphere is generally separated into the two parts, i.e. travelling and quasi-stationary parts, and that the latter part of the ultra-long wave is usually associated with an amplitude-change.

In the present paper the energy equations for both parts of the wave are derived, and applied to an energetical study on the 1967/68 stratospheric sudden warming.

From an analysis before separating the wave into the travelling and quasi-stationary parts, it is shown that the energy processes are similar to the results obtained by Reed et al.(1963), Julian and Labitzke(1963), etc.

Separating the each ultra-long wave into the quasi-stationary part and the travelling one, we can obtain the respective energy processes. Some of the results are summarized as follows:

i) At the warming stage, the kinetic energies of the quasi-stationary and travelling ultra-long waves of wavenumber two [KS(2) and KT(2)] increase, and especially the increment of the former part is remarkable.

ii) The increase (or decrease) of KS(2) is mainly due to

that of the energy transfer from the troposphere through the so-called pressure-interaction term of the quasi-stationary part of wavenumber two BGS(2).

iii) Increasing of KS(2) during the warming stage is also controlled by the energy transfer from the travelling waves of the various wavenumbers.

iv) The available potential energies of both parts of wavenumber one increase during the warming stage. these are mainly converted from the zonal available potential energy.

I. Introduction

Dramatic temperature rising occurs usually at high latitudes a few times in the winter stratosphere, associated with a remarkable change of the large-scale circulation pattern. Since such a sudden warming was documented by Scherhag(1952), a number of observational and theoretical studies have been made with development of the hemispheric aerological network. Many synoptic analyses indicate that the pattern of circulation in the winter stratosphere is mainly composed of the ultra-long waves superposed upon the zonal circulation. The fact that the ultra-long wave of wavenumber two does usually intensify in accompany with the sudden warming suggests a close connection between the development of ultra-long waves and the occurrence of sudden warming [Teweles(1963)].

Energetical studies of the sudden warming have been made by many investigators [e.g. Miyakoda(1963), Muench(1965a,b), Murakami(1965), Julian and Labitzke (1965)]. According to their results it is shown that the vertical energy flux from the troposphere into the stratosphere increases during the sudden warming. Reed et al.(1963), Teweles(1963), Perry(1966,67), Paulin(1968,70) and Miller and Johnson(1970) investigated the spectral energy processes in wavenumber domain. They showed that the ultra-long waves play an important role

in the energy processes of the stratospheric sudden warming, especially in the energy transfer from the troposphere. These authors have not taken into consideration such a fact that the ultra-long wave consists of two parts, the quasi-stationary and travelling [Deland(1965), etc.]. Murakami(1960), Newell and Richards(1969) and Holopainen(1970) have studied the energetics of the stationary disturbances, which were defined by the departure of the time-averaged flow from the zonal- and time-mean flow.

In the previous paper [Iwashima(1973)], the present author showed that the transient part of the ultra-long wave is composed of the travelling part and quasi-stationary part with amplitude-changes. Taking account of these characteristics, we will perform an analysis of energetical processes of the ultra-long waves during the stratospheric sudden warming in the 1967/68 winter in the present paper.

II. Basic spectral equations for the energetics

In this section, the spectral energy equations for the quasi-stationary and travelling parts are separately derived. Their derivation and description of the symbols will be given in the Appendices A and B.

The spectral energy equations for each part of the ultra-long waves integrated over the chosen volume (i.e. 30°N-85°N; 10mb-100mb) are symbolically expressed as follows. Here, the eddy kinetic and available potential energies are respectively separated into the travelling and quasi-stationary parts.

The equation for the zonal kinetic energy, KZ:

$$\frac{\partial}{\partial t}KZ = BKZ - \sum_{n=1}^{\infty}\{CKT(n) + CKS(n)\} + BGZ + CAKZ - DZ \qquad (1)$$

The time change of the eddy kinetic energy of wavenumber n, K(n) is separated into the travelling part KT(n) and the quasi-stationary one KS(n);

$$\frac{\partial}{\partial t}K(n) = \frac{\partial}{\partial t}KT(n) + \frac{\partial}{\partial t}KS(n) \qquad (2)$$

The equation for the eddy kinetic energy of travelling part, KT(n):

$$\frac{\partial}{\partial t}KT(n) = BKT(n) + LKT(n) + CKT(n) + BGT(n) + CAKT(n) - DT(n) + \sum_{\substack{m=-\infty \\ \neq 0}}^{\infty} CKTS(n,m) \qquad (3)$$

The equation for the quasi-stationary eddy kinetic energy of wavenumber n, KS(n):

$$\frac{\partial}{\partial t}KS(n) = BKS(n) + LKS(n) + CKS(n) + BGS(n) + CAKS(n) - DS(n) - \sum_{\substack{m=-\infty \\ \neq 0}}^{\infty} C\,KTS(m,n) \tag{4}$$

The equation for the zonal available potential energy, AZ:

$$\frac{\partial}{\partial t}AZ = BAZ - \sum_{n=1}^{\infty}\{CAT(n) + CAS(n)\} - CAKZ + GZ \tag{5}$$

The eddy available potential energy of wavenumber n, A(n) is separated into the travelling part AT(n) and the quasi-stationary part AS(n);

$$\frac{\partial}{\partial t}A(n) = \frac{\partial}{\partial t}AT(n) + \frac{\partial}{\partial t}AS(n) \tag{6}$$

The equation for the eddy available potential energy of wavenumber n of the travelling part, AT(n):

$$\frac{\partial}{\partial t}AT(n) = BAT(n) + LAT(n) + CAT(n) - CAKT(n) + GT(n) + \sum_{\substack{m=-\infty \\ \neq 0}}^{\infty} CATS(n,m) \tag{7}$$

The equation for the quasi-stationary eddy available potential energy of wavenumber n, AS(n):

$$\frac{\partial}{\partial t}AS(n) = BAS(n) + LAS(n) + CAS(n) - CAKS(n) + GS(n) - \sum_{\substack{m=-\infty \\ \neq 0}}^{\infty} CATS(m,n) \tag{8}$$

Here, the designation of the individual terms on the right-hand side of equations (1) - (8) are given in the Appendix A.

Comparing the above equations with the spectral energy equations of Perry(1966,67) and Paulin(1968, 70), we can find the energy transfer or exchange terms between the quasi-stationary and travelling parts, such as CKTS(n,m) and CATS(n,m) have been newly introduced. The introduction and estimation of these new terms are one of the important points in this work.

relative vorticity, $V(n-1)$ the horizontal velocity vector and $V(n)$ the meridional component of $V(n)$. By using this equation, $\frac{\partial}{\partial p}\Omega(n)$ is evaluated at each level. Then, by fitting a third-degree least square polynomial to $\frac{\partial}{\partial p}\Omega(n)$ together with a boundary condition $\Omega(n) = 0$ at $p = 0$, we can obtain the $\Omega(n)$ at each level.

In order to estimate the non-adiabatic heating rate or the generation term of available potential energy, the adiabatic omega $\Omega^{ad}(n)$ is calculated by means of the so-called adiabatic method. These vertical p-velocities $\Omega(n)$ and $\Omega^{ad}(n)$ are also separated into the quasi-stationary part [$\Omega_S(n)$ and $\Omega_S^{ad}(n)$] and the travelling one [$\Omega_T(n)$ and $\Omega_T^{ad}(n)$] by the time-filter method.

Finally, using the quantities $W_T(n)$, $W_S(n)$, $\Omega_T(n)$, $\Omega_S(n)$, $\Theta_T(n)$ and $\Theta_S(n)$, we can easily estimate the various kinds of energy and their conversion or transfer terms. The procedure of such a computation is described in the flow-chart in Fig. 1.

The geopotential and temperature data used in this work were read from the stratospheric maps for the same period and region as employed in the previous paper[Iwashima(1973)], i.e. Nov. 1, 1967 - Feb. 29, 1968 and 10mb-100mb; 30°N-85°N, issued by Free University of Berlin (1967/68, 1968a,b, 1968/69, 1969a,b).

IV. Mean meridional circulation

The zonal mean vertical p-velocity $\Omega(0)$ is computed by the procedure mentioned in the previous section. Using the value of the horizontal divergence $\frac{\partial}{\partial p}\Omega(0)$ and the zonal mean continuity equation;

$$\frac{1}{a\cos\varphi}\frac{\partial}{\partial\varphi}\left\{V(0)\cos\varphi\right\} + \frac{\partial}{\partial p}\Omega(0) = 0 , \quad (10)$$

we can obtain the zonal mean meridional velocity V(0), with a boundary condition V(0) = 0 at 80°N. This procedure is similar to that employed by Perry(1966).

Figs. 2a and 2b illustrate the results during the first half period from Dec. 23 to 31 and during the latter half from Jan. 1 to 8, respectively. Throughout the period, they show ascending motion at high latitudes and descending motion at mid-latitudes. The southerly current around 40°N for the latter half period at 10 mb suggests a two-cell pattern, although the ascending motion at low-latitudes cannot be found out because of lack of data. These features are similar to the results of Julian and Labitzke(1965) and Perry(1966,67). The northern cell seems to have intensified from the first half period to the latter one. For example, at 70°N of 10 mb, horizontal and vertical motions respectively change from -36 cm/sec to -81 cm/sec, and from 0.2 cm/sec to 1.2 cm /sec. The magnitudes of horizontal and vertical velocities are roughly equal to those of Julian and Labitzke

(1965) and Perry(1966,67), although the velocities at some latitudes of 10 mb are somewhat greater than the latter.

Fig. 3 illustrates the meridional-time section of $\bar{\theta}^*$, which means the deviation of the zonal mean potential temperature from the zonal-meridional mean one $[\bar{\theta}]$ at 10 mb and 100 mb. At 10 mb the meridional gradient of $\bar{\theta}^*$ abruptly changed ints sign just before the temperature peak day. At 100 mb, the warm belt can be found at mid-latitudes throughout the period in question here, and furthermore, for a few days after the temperature peak day at 10 mb the zonal mean temperature higher than the spatial mean temperature appeared at highest latitudes. Taking account of these temperature distribution, the northern cell is an indirect circulation at the former half period, and a direct one at the latter one. The indirect circulation at the warming time has been discussed by Mahlman(1969), etc., while no literature concerning the direct cell during the several days after the sudden warming is at the present author's hand. Energy conversion between the zonal kinetic energy and zonal available potential energy also shows the change of meridional circulation from indirect to direct as described in the following section.

V. Energetics

V-1. Changes of zonal and eddy energies

The change of energies in zonal and eddy forms will be depicted, before giving the results concerning the quasi-stationary and travelling ultra-long waves. Then, it will be examined whether several apparent characteristic features described by Reed et al.(1963), Julian and Labitzke(1965) and Perry(1966) would be found out.

Fig. 4 illustrates the time-change of various energies. Here, KZ, KE, AZ and AE denote the zonal kinetic energy, the eddy kinetic energy, the zonal available potential energy and the eddy available potential energy, respectively. We may notice the following features:

i) KE increases during the warming period, and decreases afterwards except from Jan. 4 to 5. AE has a similar tendency, although its change is not so remarkable. The maximum of KE appears two days after AE peak.

ii) KZ and AZ show a decreasing trend throughout the period, although AZ recovers somewhat for several days around the warming peak. Relatively rapid decline of these energies are seen during the last few days of December. The mag-

nitude of KZ during the latter half period is about a half of that of the first period.

These features are quite similar to the results of 1963 warming by Perry(1966). Furthermore, the values of KE, AE, KZ and AZ are of the same order of magnitude as Perry's values.

Fig. 5 illustrates the energy conversions and transfers. Here, the notations of CK, CA, CAKZ and CAKE are the transfer or conversion terms; KZ to KE, AZ to AE, AZ to KZ and AE to KE, respectively. The BGE represents the net transfer of KE across the upper (10 mb) and lower (100 mb) boundaries through the pressure-work term. These values are of the same order of magnitude as those of the previous studies [e.g. Julian and Labitzke(1965)]. For the first half period a large value of CA is seen, and CAKE is noticiable for the latter half period.

Comparing these features with 5-day mean results computed by Julian and Labitzke(1965), we can find out a gross similarity around the sudden warming, in spite of differences of the year and the computed interval.

It is noticed that the gross feature of time-change of BGE corresponds with that of KE in Fig. 4 quite well, and this fact suggests that a change of KE may be largely contributed by BGE.

Taking account of time-change of the zonal mean temperature $\bar{T}$ at the higher latitudes of 10 mb [see Fig. 7 in the author's previous paper , Iwashima (1973)], the period of analysis may be temporarily divided into two stages, i.e. the warming stage of the first half period (before Jan.2 or 3) and the mature stage of the latter half period (after then). In this paper "the warming period", "the warming stage" and "the warming time" are used in a similar meaning, although there is a little difference of nuance among them.

The mean energy-flow diagrams are represented in Fig. 6a for the period from Dec. 23 to 31, and Fig. 6b for the period from Jan. 1 to 8, respectively. GZ and GE are evaluated from the non-adiabatic heating rate and temperature by using the [illegible] procedure as given in Appendix B. The kinetic energy flux through the vertical and horizontal boundaries BKZ and BKE are calculated from the wind structure along the boundaries. BAZ^*, BAE^*, DZ^* and DE^* terms contain the energy fluxes required for balance.*)

During the first period the energy transfers CA and CK predominate. CAKZ and CAKE are one order of magnitude less than CA and CK. Decreasing of AZ corresponds to the large value of C_A and the small value of CAKZ. While, in spite of relatively large value of CK and small CAKE value, KE increases by a

large BGE. The direction of mean energy cycle in the type of four kinds of energies is AZ → AE → KE → KZ → AZ.

For the second half period, absolute values of CAKZ and CAKE become large, and especially CAKE is one order of magnitude larger than CA and CK. BGE becomes somewhat larger than that during the first period. Therefore, KE shows a decreasing tendency. The mean energy flow is KE → AE → AZ → KZ ← KE. These directions of mean energy flow during the first and second half periods agree with the results of other studies (e.g. Julian and Labitzke(1965)). The agreement in magnitudes is not so satisfactory, especially the CAKZ and CAKE conversion terms for the first period, and BGE for the second period. However it must be kept in mind that Julian and Labitzke(1965) have taken the 1963 warming and 25-30 days as an averaging period.

Non-adiabatic energy generation GE is negative throughout the period, and the magnitude during the latter half period is one order of magnitude greater than that of the first period. While, GZ of the first half period is negligibly small. During the second half period, GZ and GE values are of the same order of magnitude as compared with Perry(1966,67)'s result.

*)

The terms of BAZ^*, BAE^*, DZ^* and DE^* computed from balance requirement seem to be rather larger than the other directly computed terms, although the values are not shown in Figs. 6a and 6b. There remains a question whether their large values are due to the truncation of the part with wavenumber larger than 5.

Such a similar problem as mentioned above may be found in the results of previous works, e.g. Perry (1966), Paulin(1968), etc.. To our deep regret, we have also left exact estimation and discussion of the above terms as a problem for further studies.

V-2. Energetics in the wavenumber domain

The eddy energies AL and AE will be described in the wavenumber domain in this section. Figs. 7 and 8 illustrate the change of spectral kinetic energy K(n) and spectral available potential energy A(n) (n= 1, 2, 3), where n is the wavenumber. It is evident that K(2) has a remarkable peak and A(1) has a maximum about the temperature peak day. It is seen that the increase of K(2) during the sudden warming mostly contribute to that of KE, and that the change of A(1) is similar to that of AE, as shown in Fig. 4. K(2) evidently exceeds A(2), but K(1) is less than A(1) before and around the temperature maximum day.

Figs. 9, 10 and 11 illustrate the energy processes for the ultra-long waves of wavenumber one, two and three, respectively. They show that the non-linear energy transfer term (LK) and baroclinic energy conversion (CAKE) largely contribute to the energy-change of wavenumber one, and that LK and BG mainly govern the energy-change of wavenumber two. For the wavenumber three, K(3) is mostly controlled by LK and CAKE.

The LK terms of wavenumbers one and three are positive throughout the period. That of wavenumber two is positive during the several days about the temperature peak day, and negative for the remaining periods. Roughly speaking, the magnitude of LK(2) is

nearly equal to that of LK(1) during a few days before and after the temperature maximum day. During these periods LK(3) is relatively smaller than LK(2) and LK(1). These results suggest a close interaction between the wavenumbers one and two during the several days before and after the temperature peak. In Perry(1967)'s case, the direction of non-linear energy transfer is from the wavenumbers one and two to the wavenumber three.

At the temperature peak and thereafter, the baroclinic process CALA prevails for the wavenumber one. Its sign is negative, i.e., the energy flow is from K(1) to A(1).

The pressure-interaction term BG(2) is positive, and its magnitude is larger than that of BG(1), which is negative throughout the period. Such a difference of magnitude between BG(2) and BG(1) can be found in Perry's result, although BG(1) has shown a negative sign during a few days only. The former has a maximum at the time of temperature peak, similar to Perry's result. BG(3) is positive around the temperature peak day, and negative during the remaining periods. The magnitude of BG(3) is generally smaller than that of BG(2) by one order of magnitude. Such changes of BG(3) are different from Perry's case, where its term has large negative values with the same order of magnitude as BG(2).

The time-change of the respective kinetic energies K(1), K(2) and K(3) are controlled by a few conversion and/or transfer terms as mentioned above.

V-3. Energies of the quasi-stationary and travelling ultra-long waves

The spectral kinetic and available potential energies will be further separated into the quasi-stationary and travelling parts.

Figs. 12 and 13 illustrate the features of KT(1), KS(1), KT(2), KS(2), AT(1), AS(1), AT(2) and AS(2). Here, the results concerning the wavenumber three are not presented, because KT(3), KS(3), AT(3) and AS(3) are relatively smaller than the energies of wavenumbers one and two, and no appreciable change for the sudden warming is seen. In these figures, the following facts are noticed:

i) Each component of kinetic energies exceeds the corresponding component of the available potential energies, except KS(1).

ii) KS(2) and KT(2) prominently increase associated with the sudden warming, and decrease after Dec. 30 or 31. KS(2) is one and a half times of or twice KT(2) except the initial few days of the period. On the other hand, KT(1) is greater than KS(1) at the warming time.

iii) Both AT(1) and AS(1) reach a maximum at the end of December, when AZ is minimum. The change of AT(1) is more remarkable rather than that of AS(1). AT(2) has no appreciable change, and AS(2) has a

maximum, preceding the maximum of AT(1) by a few days.

iv) The magnitude of the energy of the quasi-stationary part is larger than the corresponding energy of the travelling one for the same wavenumber, except KS(1).

Of the energies mentioned above, four energies KT(2), KS(2), AT(1) and AS(1) which have remarkable changes are taken, and the vertical distributions are given in Figs. 14 and 15. KT(2) and KS(2) reach a maximum at all levels without a time lag greater than a day or so. At 10 mb, KT(2) becomes larger rather than KS(2), while the vertically integrated KT(2) is smaller than the corresponding KS(2) as mentioned above. Fig. 15 shows the horizontally averaged AT(1) and AS(1). About Dec. 30 the maximum of the former appears above 30 mb level, and that of the latter at 10 mb. At 10 mb AT(1) changes more remarkably rather than AS(1). The relatively large values of the above four energies are restricted in the uppermost levels, except KS(2).

V-4. Energetics of the quasi-stationary and travelling ultra-long waves

In this section it will be examined how the quasi-stationary and travelling parts of the waves contribute to the energy processes during the stratospheric sudden warming.

The main results for the kinetic energies of the travelling and quasi-stationary parts of wavenumbers one and two are illustrated in Figs. 16 and 17. Here, the terms CKT, CKS, CAKT, CAKS, BKT, BKS, BGT, LKT, LKS and CKTS are taken. The quantities less than 1.0×10^{-3} J/m^2/mb/sec throughout the period are not shown except the respective time-change of energy, for avoiding the complication of curves. The dissipation term also has not been given in the figures. It seems that such an unbalance of energy budget as seen in the case of KT(2) of Fig. 17 suggests need of taking account of the dissipation term.

The following facts are noticed:

i) The non-linear energy transfer between different wavenumbers LKT and LKS, and the exchange term CKTS between the quasi-stationary part and the travelling one largely contribute to the energy-change throughout the period, especially at the sudden warming time.

ii) Roughly speaking the direction of energy-transfer

by CKTS concerning the wavenumber two is from the travelling part to the quasi-stationary one during the first half period, and from the latter to the former during the latter half period. For the travelling part of the wavenumber one, the direction of energy-flow through CKTS for the first half period is from the travelling part of wavenumber one to the quasi-stationary waves with various wavenumbers. For the latter half period the direction is from the latter to the former one.

The CKTS terms for both parts of the same wavenumber do not always cancel each other. It implies that the energy exchange through the CKTS term is performed between the travelling part and the quasi-stationary one of the same wavenumber as well as between those of the different wavenumbers.

iii) An opposite time-change is found between LKS(1) and LKS(2), as well as between LKT(1) and LKT(2). That is, LKS(1) has a minus sign from Dec. 31 to Jan. 2, and LKS(2) has the opposite sign during the corresponding period except last two days. LKT(1) and LKT(2) have a similar relationship, although they vary with a short period after the sudden warming.

iv) The other important terms to be noticed are CAKS and BGS(2). The former term has a larger

magnitude in the latter period rather than the first half period. The major part of the upward flux of geopotential is due to the BGS(2) term. It contributes to a large amount of the energy increase of wavenumber two.

The time sequences of conversion and transfer terms for AT(1), AS(1), AT(2) and AS(2) are illustrated in Figs. 18 and 19, respectively. Here, the terms CAT, CAS, LAT, LAS, CAKS and CATS are taken, but the terms with such a value less than 1.0×10^{-3} $J/m^2/mb/sec$ throughout the period are not illustrated. From these figures, the follwoing facts are found:

i) For the time-change of AT(1), it is noticed that CAT(1) has a relatively large value which contributes to the maximum of $\frac{\partial}{\partial t}$AT(1) during the warming time.

ii) CAKS(1) keeps a large negative value after the temperature peak. The other terms are relatively small in spite of negative value of $\frac{\partial}{\partial t}$AS(1).

iii) Concerning the time-change of AT(2), there are no prominent terms.

iv) For the time-change of AS(2), CAS(2) shows a maximum corresponding to that of AS(2).

Dividing the period into two parts, we may depict the above results in the mean energy-flow diagrams of Figs. 20a and 20b. Fig. 20a illustrates the first part from Dec. 23 to 31, 1967, and Fig. 20b from Jan. 1 to 8, 1968. The prominent terms indicated by thick lines are the geopotential upward flux term BGS(2), the non-linear energy transfer terms among the waves LKT(1), LKS(1), LKT(2) and LKS(2), and the energy exchange terms between the quasi-stationary part and the travelling one CKTS(1,m), CKTS(m,1), CKTS(2,m) and CKTS(m,2). Rough pictures of the energy-flow will be depicted as follows:

During the first half period, the kinetic energy KS(2), which is supplied from the troposphere through BGS(2), is transfered to KS(1) by LKS(2) and/or LKS(1). Thereafter, the kinetic energy KS(1) is carried to the travelling waves (except to that of wavenumber one) through CKTS(m,1). While the CKTS terms for KT(1) and KT(2) have minus and plus signs, respectively. The increase of KT(2) may depend on the energy transfer from the quasi-stationary waves by CKTS(2,m). For the same period the energy transfer from AZ to AT(1) prevails.

For the latter half period, BGS(2) also mainly gives the kinetic energy to KS(2). Furthermore, the energy KS(2) is transfered to the travelling waves through CKTS(m,2), and simultaneously to KS(1) by the non-linear interaction terms LKS(2) and LKS(1). KS(1) is convered

into AS(1), and the energies AS(1) and AS(2) are exchanged through LAS(1) and LAS(2). Finally, AS(2) is transfered to AS. The decreasing of KT(2) as shown in Fig. 12 may correspond to that of the CKT term (and increase of absolute value).

VI. Discussion

As was mentioned by Perry(1967), it is risky to draw conclusions about detailed behaviour of the ultra-long waves from an only case. The present results have not enough accuracy to discuss their absolute values of magnitude, and partly contain unbalance of energy budget. However, we can find out several characteristic features similar to the previous studies by the other authors. Therefore the present work should contribute to an understanding not only the energy processes of the 1967/68 stratospheric warming in question here, but also those of the other years.

The eddy energies KE and AE increase during the warming period and reach a maximum, while the zonal kinetic and available potential energies relatively suddenly decrease. These tendencies of KE, AE and AZ reversed accompanies with the reversal of zonal mean temperature gradient. The decrease of KZ and AZ is not enough for the increase of KE (or the barotropic and baroclinic instability). Such a deficiency is compensated by the energy from the troposphere through the BG term. It is consistent with the previous studies [e.g. Reed et al.(1963)].

Such a pressure-interaction term BG is mostly contributed by the wavenumber two, as was indicated

by Miller and Johnson(1970). From the present study we have obtained such an important conclusion that the energy inflow from the troposphere mostly depends on the quasi-stationary part of wavenumber two. The non-linear energy exchange terms between the different wavenumbers LK(1) and LK(2) are important for the time-change of K(1) and K(2), respectively. The corresponding terms LKT(1), LKS(1), LKT(2) and LKS(2) are also important for the time-change of KT(1), KS(1), KT(2) and KS(2), respectively. This important role of the non-linear interaction between the different wavenumbers for the sudden warming is inferred also in a few theoretical studies [Rutherford(1969) and Matsuno(1971)].

VII. Summary and concluding remarks

Energy processes of the quasi-stationary and travelling ultra-long waves during the 1967/68 stratospheric sudden warming were analyzed, using the time-filter method [Iwashima and Yamamoto(1971,73) and Iwashima(1973)]. Various energy transfer and conversion terms are derived for the quasi-stationary and travelling parts of the waves. The vertical velocity was estimated mainly by the use of the "vorticity equation method". Estimating the diabatic heating rate, we obtain the term of generation of available potential energy.

From the results of the vertical motion, the zonal-mean meridional circulation was computed. The mean circulation was a two-cell pattern throughout the period. During about ten days before the sudden warming, the northern cell was a indirect one. After the mature stage of the sudden warming, its cell became a direct one and strengthened.

During the sudden warming a few characteristic features of the zonal energy and eddy energy, and the energies of the ultra-long waves of wavenumbers one and two were described. The follwoing conclusions were drawn:

i) The eddy kinetic energy, to which the energy of wavenumber two mostly contributed, increased at

the warming time. Furthermore, as was concluded by Perry(1965,67), the growth of the wavenumber two at the last stage of the warming was due to convergence of geopotential flux. However, the effect of the "baroclinic processes" was not so prominent as those of Perry(1966).

ii) Also, non-linear interaction of wavenumbers one and two was dominant throughout the period.

These general and qualitative agreement with the former studies may permit our further discussion of the energetics.

From the results concerned with the energy processes of the travelling and quasi-stationary parts of the ultra-long waves, the following facts are concluded:

iii) It is concluded that the sudden warming is mainly due to time-change of the kientic energies of the quasi-stationary and travelling ultra-long waves with wavenumber two, the zonal available potential energy and the available potential energy of quasi-stationary part of wavenumber one.

iv) Concerning the convergence of eddy-geopotential upward-flux term, the quasi-stationary part of the wave plays an important role for the wavenumber two.

v) The non-linear interaction terms between wave-

numbers one and two are important for both parts of the ultra-long wave, respectively.

vi) For both wavenumbers one and two, the interaction terms between the quasi-stationary part and the travelling one is important throughout the period, as was expected from the former study by the present author (1973), especially at the rapid warming time.

vii) The energy transfer through the CATS term from (or to) the various travelling waves contributed to the increase (or decrease) of the kinetic energy of the quasi-stationary part of wavenumber two before (or after) the temperature peak day.

In the present work it was disclosed that the energy transfer from the troposphere mainly by the quasi-stationary ultra-long wave of wavenumber two was important for the stratospheric sudden warming. For the theoretical study or construction of numerical model based upon the above results for the quasi-stationary and travelling ultra-long waves, it is need to confirm the above conclusion by a further similar investigation. In order to understand a close relation between the sudden warming and the tropospheric blocking phenomenon suggested by Miyakoda(1963),

Julian and Labitzke(1965), etc., the present author intends to study of the quasi-stationary and travelling ultra-long waves in the troposphere.

Acknowledgements

The author expresses his hearty thanks to Professor Ryozaburo Yamamoto for giving a lot of facility to this work and for stimulative discussions and guidance throughout the present study.

The extensive computations in this work were carried out with the use of the FACOM 230-60 Computer (Job Nos. 5001PD003, 5001DF751 and 5001EA692) at the Data Processing Center of Kyoto University.

Last but not least, the author's sincere gratitudes are extended to Prof. R.Yamamoto, Prof. Tomio Asai* of the Faculty of Science and Prof. Yasushi Mitsuta of the Disaster Prevention Research Institute, Kyoto University, for their kind offering of financial support to the present author's lavish expenditure of computation time.

---

*) Present affiliation: Ocean Research Institute, Tokyo University.

References

Craig,R.A. and W.S.Hering,1959: The stratospheric warming of January-February 1957. J.Meteor.,16,91-107.

Deland,R.J.,1965: Some observations of the behaviour of spherical harmonic waves. Mon.Wea.Rev.,93,307-312.

Free University of Berlin,1967/68: Täglicher Höhenkarten der 100-mb-Fläche und der 50-mb-Fläche sowie monatliche Mittelkarten für das Jahr 1967. Teil IV. Meteor.Abhandl., Band LXXX, Heft 4.

———,1968a: Daily and monthly northern hemisphere 30-millibar-synoptic weather maps of the year 1967. Part IV. October-December. Meteor.Abhandl., Band LXXXI, Heft 4.

———,1968b: Daily and mothly northern hemisphere 10-millibar-synoptic weather maps of the year 1967. Part IV. October-December. Meteor.Abhandl., Band LXXXII, Heft 4.

———,1968/69: Täglicher Höhenkarten der 100-mb-Fläche und der 50-mb-Fläche sowie monatlicher Mittelkarten für das Jahr 1968. Teil I. Meteor.Abhandl., Band XCIV, Heft 1.

———,1969a: Daily and monthly northern hemisphere

30-millibar-synoptic weather maps of the year 1968. Part I. January-March. Meteor.Abhandl., Band XC, Heft 1.

———,1969b: Daily and monthly northern hemisphere 10-millibar-synoptic weather maps of the year 1968. Part I. January-March. Meteor.Abhandl., Band XCVI, Heft 1.

Iwashima,T.,1973: Observational studies of the ultra-long waves in the atmosphere (I). J.meteor.Soc.Japan,51,209-229.

——— and R.Yamamoto,1971: A method for separation of the ultra-long waves in the atmosphere into the quasi-stationary and transient parts by the time filters. J.meteor.Soc.Japan,49,158-162.

———————,1973: Remarks on the analysis of the quasi-stationary and travelling ultra-long waves in the atmosphere. J.meteor.Soc.Japan,51,151-154.

Johnson,K.W.,1969: A preliminary study of the stratospheric warming of December 1967 - January 1968. Mon.Wea.Rev.,97,553-364.

Julian,P.R. and K.Labitzke,1965: A study of atmospheric energetics during the January-February 1963 stratospheric warming. J.atmos.Sci.,22,597-610.

Mahlman,J.D.,1969: Heat balance and mean meridional circulation in polar stratosphere during sudden warming of January 1958. Mon.Wea.Rev.,97,534-540.

Matsuno,T.,1971: A dynamical model of the stratospheric sudden warming. J.atmos.Sci.,28,1479-1494.

Miller,A.J. and K.W.Johnson,1970: On the interaction between the stratosphere and troposphere during the warming of December 1967 - January 1968. Quart.J.Roy.Met.Soc.,96,24-31.

Miyakoda,K.,1963: Some characteristic features of winter circulation in the troposphere and lower stratosphere. Tech.Rept. 14, Dept. Geophys. Sci., University of Chicago., 93pp.

Muench,H.S.,1965a: Stratospheric energy processes and associated atmospheric long-wave structure in winter. Environmental Research Papers No.95, AFCRC-65-236, 120pp.

_____,1965b: On the dynamics of the wintertime stratospheric circulation. J.atmos.Sci.,22,349-360.

Murakami,T.,1960: On the maintenance of kinetic energy of the large-scale stationary

disturbances in the atmosphere. Scientific Report No.2, Massachusetts Institute of Technology, Cambridge, Massachusetts, 42pp.

———,1965: Energy cycle of the stratospheric warming in early 1958. J.meteor.Soc.Japan,43,262-283.

Newell,R.E. and M.E.Richards,1969: Energy flux and convergence pattern in the lower and middle stratosphere during the IQSY. Quart.J.R.Met.Soc.,95,310-328.

Paulin,G.,1968: Spectral atmospheric energetics during January 1959. Pub.Met., No.91, A.M.R.G., McGill Univ., Montreal, Quebec, 328pp.

———,1970: A study of the energetics of January 1959. Mon.Wea.Rev.,98,759-809.

Perry,J.S.,1966: The energy balance during a sudden stratospheric warming. Ph.D.thesis, Univ. Washington, Seattle,185pp.

———,1967: Long-wave energy processes in the 1963 sudden stratospheric warming. J.atmos.Sci.,24,539-550.

Reed,R.J., J.L.Wolf and H.Nishimoto,1963: A spectral analysis of the energetics of the stratospheric sudden warming of early 1957. J.atmos.Sci.,20,256-275.

Rutherford,I.D.,1969: The vertical propagation of geostrophic waves in a low-order spectral model. Pub.Met., No.92, A.M.R.C., McGill Univ., Montreal, Quebec,122pp.

Saltzman,B.,1957: Equations governing the energetics of the larger scales of atmospheric turbulence in the domain of wave number. J.Meteor.,14,513-523.

Scherhag,R.,1952: Die explosionsartigen stratosphärenerwärmungen des Spätwinters 1951/52. Ber.Deutsch.Wetterd.,6,51-63.

Teweles,S.,1963: A spectral study of the warming epoch of January-February 1958. Mon.Wea.Rev.,91,505-519.

Appendices

A. List of symbols

Symbol	Meaning
a	Radius of the earth
f	Coriolis parameter
f_λ , f_φ	Eastward and northward component of the frictional force ,respectively
g	Acceleration of gravity
h	Non-adiabatic heating rate
i	Imaginary number ($=\sqrt{-1}$)
m , n	Longitudinal wavenumber
p	Pressure
p_1 , p_2	Upper and lower boundary pressures (p_1 = 10 mb, p_2 = 100 mb)
Δp	$= p_2 - p_1$
t	Time
u , v	Eastward and northward component of horizontal velocity $\mathbb{V}$
$\mathbb{V}$	Horizontal velocity vector
z , Z	Geopotential height of an isobaric surface and its Fourier transform
λ	Longitude
φ	Latitude .
β	$= \partial f / a \partial \varphi$; derivative with respect to φ of the Coriolis parameter

φ_1 , φ_2	Southern and northern boundary latitudes ($\varphi_1 = 30^\circ N$, $\varphi_2 = 85^\circ N$)
δ	$= \sin \varphi_2 - \sin \varphi_1$
ζ	Vertical component of relative vorticity
κ	$= R/C_p$; ratio of the gas constant of dry air to specific heat of dry air at constant pressure
ω	$= dp/dt$; vertical p-velocity
ω_{ad}	"Adiabatic omega"; computed under adiabatic assumption
$\Omega(n)$, $\Omega^{ad}(n)$	Fourier-transform function of ω and ω_{ad}
∇	Differential operator on constant pressure surface
θ , $\Theta(n)$	Potential temperature and its Fourier-transform function
AE	Eddy available potential energy
AZ	Zonal available potential energy
A(n)	Eddy available potential energy contributed by the eddy with wavenumber n
AT(n)	Available potential energy contributed by the travelling eddy with wavenumber n
AS(n)	Available potential energy contributed by the quasi-stationary eddy with wavenumber n
KE	Eddy kinetic energy

KZ	Zonal kinetic energy
K(n)	Kinetic energy contributed by the eddy of wavenumber n
KT(n)	Kinetic energy contributed by the travelling eddy of wavenumber n
KS(n)	Kinetic energy contributed by the quasi-stationary eddy of wavenumber n
BAZ	Boundary flux affecting the contribution of the zonal ring to AZ
BA(n)	Same as BAZ except to A(n)
BAT(n)	Same as BAZ except to AT(n)
BAS(n)	Same as BAZ except to AS(n)
BGZ	Boundary flux of zonal mean geopotential or work done by pressure forces at the boundaries
BGE	Same as BGZ except for the eddy $[=\sum_{n=1}^{4} BG(n)]$
BG(n)	Same as BGZ except for the eddy of wavenumber n
BGT(n)	Same as BG(n) except for the travelling eddy of wavenumber n
BGS(n)	Same as BGT(n) except for the quasi-stationary eddy
BKZ	Flux of the zonal kinetic energy through the vertical and horizontal boundaries
BKE	Same as BKZ except for the eddy $[=\sum_{n=1}^{4} BK(n)]$
BK(n)	Same as BKZ except for the eddy of wavenumber n

BKT(n)	Same as BK(n) except for the travelling eddy
BKS(n)	Same as BKT(n) except for the quasi-stationary eddy
CA	Transfer term from AZ to AE [$=\sum_{n=1}^{4} CA(n)$]
CA(n)	Transfer term from AZ to A(n)
CAT(n)	Transfer term from AZ to AT(n)
CAS(n)	Transfer term from AZ to AS(n)
CAKZ	Conversion term from AZ to KZ
CAKE	Conversion term from AE to KE [$=\sum_{n=1}^{4} CAK(n)$]
CAK(n)	Conversion term from A(n) to K(n)
CAKT(n)	Conversion term from AT(n) to KT(n)
CAKS(n)	Conversion term from AS(n) to KS(n)
CATS(n,m)	Transfer term from AS(m) to AT(n)
CK	Transfer term from AZ to KE [$=\sum_{n=1}^{4} CK(n)$]
CK(n)	Transfer term from KZ to K(n)
CKT(n)	Transfer term from KZ to KT(n)
CKS(n)	Transfer term from KZ to KS(n)
CKTS(n,m)	Transfer term from KS(m) to KT(n)
DZ	Viscous dissipation term of the zonal kinetic energy KZ
DE	Viscous dissipation term of KE
DT(n)	Viscous dissipation term of KT(n)
DS(n)	Viscous dissipation term of KS(n)
GZ	Generation term of AZ
GE	Generation term of AE
GT(n)	Generation term of AT(n)

GS(n)	Generation term of AS(n)
LA(n)	Non-linear transfer term of eddy available potential energy of wavenumber n
LAT(n)	Same as LA(n) except for AT(n)
LAS(n)	Same as LAT(n) except for AS(n)
LK(n)	Non-linear transfer term of eddy kinetic energy of wavenumber n
LKT(n)	Same as LK(n) except for KT(n)
LKS(n)	Same as LK(n) except for KS(n)
subscript S	Quantity concerningwith the quasi-stationary eddy
S	Static stability
subscript T	Quantity concerning with the travelling eddy
T	Temperature
C_p	Specific heat of dry air at constant pressure
R	Gas constant of dry air

Fourier Transform Pair

Variable	u	v	z	ω (ω_{nd})	f_λ	f_φ	θ
Spectral function	U	V	Z	Ω (Ω^*)	F_λ	F_φ	Θ

Appendix B. Formal description of the energy equations and their transfer or conversion terms

The governing equations in wavenumber domain are easily derived after Saltzman(1957) from the following three equations:

the equation of motion:

$$\frac{\partial}{\partial t}V(n) + \sum_{m=-\infty}^{\infty}\left\{ V(m)\cdot\nabla V(n-m) + \Omega(m)\frac{\partial}{\partial p}V(n-m)\right\}$$

$$= -g\nabla Z(n) + f\,\mathbb{k}\times V(n) + \frac{\tan\varphi}{a}\sum_{m=-\infty}^{\infty} U(m)\,\mathbb{k}\times V(n-m) \qquad \text{B-1}$$

the equation of continuity:

$$\frac{1}{a\cos\varphi}\left[in\,U(n) + \frac{\partial}{\partial\varphi}\{V(n)\cos\varphi\}\right] = -\frac{\partial}{\partial p}\Omega(n) \qquad \text{B-2}$$

the thermodynamic energy equation:

$$\frac{\partial}{\partial t}\Theta(n) + \sum_{m=-\infty}^{\infty}\left\{ V(m)\cdot\nabla\Theta(n-m) + \Omega(m)\frac{\partial}{\partial p}\Theta(n-m)\right\} = \frac{H(n)}{c_p\left(\frac{p_s}{p}\right)^{\kappa}} \qquad \text{B-3}$$

where the notations of all the above symbols are given in the Appendix A.

The total kinetic energy K can be separated into the wavenumber domain as follows:

$$K = KZ + \sum_{n=1}^{\infty} K(n) \qquad \text{B-4}$$

where $KZ = \frac{1}{2}|V(0)|^2$ and $K(n) = |V(n)|^2$ B-5.

Any quantity X(n) in wavenumber domain may be separated into the travelling and quasi-stationary parts by the time-filter method:

$$X(n) = X_S(n) + X_T(n) \qquad \text{B-6}$$

where the subscripts S and T express the stationary and travelling parts, respectively. If we use the angle bracket $\langle\ \rangle$ for an operator of separating the wave into the travelling and quasi-stationary parts,

$$\langle X(n) \rangle = X_S(n) \qquad \text{B-7.}$$

Here, the separation is performed mainly by applying the time-filter (i.e. weighted running mean). Thereafter, the bracket denotes the weighted running mean.

The kinetic energy of the quasi-stationary part KS(n) and that of the travelling one KT(n) are defined by the following form:

$$KS(n) = |W_S(n)|^2 \quad \text{and} \quad KT(n) = |W_T(n)|^2 \qquad \text{B-8.}$$

From the equations B-1 and B-2, the governing kinetic energy equations for the quasi-stationary and travelling waves can be derived as follows:

the equation of motion for the quasi-stationary part:

$$\frac{\partial}{\partial t}\mathbb{V}_S(n) + \sum_{m=-\infty}^{\infty}\{\mathbb{V}_S(m)\cdot\nabla\mathbb{V}_S(n-m) + \Omega_S(m)\frac{\partial}{\partial p}\mathbb{V}_S(n-m)$$

$$- <\mathbb{V}_T(m)\cdot\nabla\mathbb{V}(n-m) + \Omega_T(m)\frac{\partial}{\partial p}\mathbb{V}_T(n-m)>\}$$

$$= -g\nabla Z_S(n) + f\,\mathbb{k}\times\mathbb{V}_S(n) + \frac{\tan\varphi}{a}\,\mathbb{k}\times\sum_{m=-\infty}^{\infty}\{U_S(m)\cdot\mathbb{V}_S(n-m) \qquad \text{B-9}$$

$$+ <U_T(m)\cdot\mathbb{V}_T(n-m)>\} + \mathbb{F}_S(n)$$

the equation of motion for the travelling part:

$$\frac{\partial}{\partial t}\mathbb{V}_T(n) + \sum_{m=-\infty}^{\infty}\{\mathbb{V}(m)\cdot\nabla\mathbb{V}_T(n-m) + \mathbb{V}_T(m)\cdot\nabla\mathbb{V}_S(n-m)$$

$$- <\mathbb{V}_T(m)\cdot\nabla\mathbb{V}_T(n-m) + \Omega(m)\frac{\partial}{\partial p}\mathbb{V}_T(n-m) + \Omega_T(m)\frac{\partial}{\partial p}\mathbb{V}_S(n-m)$$

$$- <\Omega_T(m)\frac{\partial}{\partial p}\mathbb{V}_T(n-m)>\} = -g\nabla Z_T(n) + f\,\mathbb{k}\times\mathbb{V}_T(n) \qquad \text{B-10}$$

$$+ \frac{\tan\varphi}{a}\,\mathbb{k}\times\sum_{m=-\infty}^{\infty}\{U(m)\mathbb{V}_T(n-m) + U_T(m)\mathbb{V}_S(n-m)$$

$$- <U_T(m)\cdot\mathbb{V}_T(n-m)>\} + \mathbb{F}_T(n)$$

the equation of continuity for the quasi-stationary part:

$$\frac{1}{a\cos\varphi}\left[in\,U_S(n) + \frac{\partial}{\partial\varphi}\{V_S(n)\cos\varphi\}\right] = -\frac{\partial}{\partial p}\Omega_S(n) \qquad \text{B-11}$$

the equation of continuity for the travelling part:

$$\frac{1}{a\cos\varphi}\left[in\,U_T(n) + \frac{\partial}{\partial\varphi}\{V_T(n)\cos\varphi\}\right] = -\frac{\partial}{\partial p}\Omega_T(n) \qquad \text{B-12}$$

From B-9 and B-11, taking into consideration

$$\frac{\partial}{\partial t} KS(n) = \frac{\partial}{\partial t} |V_S(n)|^2 = \frac{\partial}{\partial t} \{ V_S(n) \cdot V_S(-n) \}$$

$$= V_S(-n) \frac{\partial}{\partial t} V_S(n) + V_S(n) \cdot \frac{\partial}{\partial t} V_S(-n) \qquad \text{B-13}$$

the equation for KS(n) is obtained:

$$\frac{\partial}{\partial t} KS(n) = \{\{ - \sum_{\substack{m=-\infty \\ \neq 0}}^{\infty} \Big[\frac{1}{a \cos\varphi} \frac{\partial}{\partial \lambda} \{ V_S(-n) U_S(n-m) V_S(m) \}$$

$$+ \frac{1}{a \cos\varphi} \{ V_S(-n) V(n-m) V(m) \cos\varphi \} + \frac{\partial}{\partial p} \{ V_S(-n) \Omega_S(n-m)$$

$$\cdot V_S(m) \} - V_S(m) \{ \frac{U_S(n-m)}{a \cos\varphi} \frac{\partial}{\partial \lambda} V_S(-n) + \frac{V_S(n-m)}{a} \frac{\partial}{\partial \varphi} V_S(n)$$

$$+ \Omega_S(n-m) \frac{\partial}{\partial p} V_S(-n) \} + V_S(-n) \{ \frac{U_T(n-m)}{a \cos\varphi} \frac{\partial}{\partial \lambda} V_T(m) \qquad \text{B-14}$$

$$+ \frac{V_T(n-m)}{a} \frac{\partial}{\partial \varphi} V_T(m) + \Omega_T(n-m) \frac{\partial}{\partial p} V_T(m) - \frac{\tan\varphi}{a} U_T(n-m) \cdot$$

$$\cdot V_T(m) \times K \} \Big] + j V_S(-n) \cdot V_S(n) \times 1K - V_S(-n) \{ \frac{V_S(n)}{a} \frac{\partial}{\partial \varphi} V(0)$$

$$+ \Omega_S(n) \frac{\partial}{\partial p} V(0) - \frac{\tan\varphi}{a} U_S(n) V_S(0) \times 1K \} \}\}$$

where the bracket $\{\{ \}\}$ means the following expression

$$\{\{ F(n) \}\} = \langle F(n) + F(-n) \rangle \qquad \text{B-15}$$

In the same manner, from B-10 and B-12, the equation for KT(n) is provided:

$$\frac{\partial}{\partial t} KT(n) = \{\{ - \sum_{\substack{m=-\infty \\ \neq 0}}^{\infty} \Big[\frac{1}{a \cos\varphi} \frac{\partial}{\partial \lambda} \{ V_T(-n) U(n-m) V_T(m)$$

$$+ V_T(-n) U_T(n-m) V_S(m) \} + \frac{1}{a \cos\varphi} \frac{\partial}{\partial \varphi} \{ V_T(-n) \cdot$$

$$V(n-m)\,V_T(m)\cos\varphi + V_T(-n)\,V_T(n-m)\,V_S(m)\cos\varphi\Big\}$$

$$+\frac{\partial}{\partial p}\Big\{V_T(-n)\,\Omega(n-m)\,V_T(m) + V_T(-n)\,\Omega_T(n-m)\,V_S(m)\Big\}$$

$$-V_T(m)\Big\{\frac{-i\,n\,U(n-m)}{a\cos\varphi}\cdot V_T(-n) + \frac{V(n-m)}{a}\frac{\partial}{\partial\varphi}V_T(-n)$$

$$+\Omega(n-m)\frac{\partial}{\partial p}V_T(-n) - \frac{\tan\varphi}{a}U(n-m)\,V_T(-n)\times k\Big\}\Big] \qquad \text{B-16}$$

$$+ f\,V_T(-n)\,V_T(n)\times k - g\Big[\frac{1}{a\cos\varphi}\frac{\partial}{\partial\lambda}\{U_T(-n)Z_T(n)\}$$

$$+\frac{1}{a\cos\varphi}\frac{\partial}{\partial\varphi}\{V_T(-n)Z_T(n)\cos\varphi\} + \frac{\partial}{\partial p}\{Z_T(n)\Omega_T(-n)\}$$

$$-\Omega_T(-n)\frac{\partial}{\partial p}Z_T(n)\Big] - V_T(-n)\Big\{V_T(n)\frac{\partial}{a\partial\varphi}V(0) +$$

$$\Omega_T(n)\frac{\partial}{\partial p}V(0) - \frac{\tan\varphi}{a}U_T(n)\,V(0)\times k\Big\}\Big\}$$

The equation for KZ is

$$\frac{\partial}{\partial t}KZ = <-\frac{1}{2}\Big[\frac{1}{a\cos\varphi}\frac{\partial}{\partial\varphi}\{V(0)\,V(0)\,V(0)\cos\varphi\}$$

$$+\frac{\partial}{\partial p}\{V(0)\,\Omega(0)\,V(0)\}\Big] - \sum_{\substack{m=-\infty\\ \neq 0}}^{\infty}\Big[\frac{1}{a\cos\varphi}\frac{\partial}{\partial\lambda}\{V(0)U_S(-m)V_S(m)\}$$

$$+\frac{1}{a\cos\varphi}\frac{\partial}{\partial\varphi}\{V(0)\,V_S(-m)\,V_S(m)\cos\varphi\} + \frac{\partial}{\partial p}\{V(0)\,\Omega_S(-m)\,V_S(m)\}$$

$$-\frac{V_S(m)}{a\cos\varphi}V_S(-m)\frac{\partial}{\partial\varphi}V(0) - V_S(m)\,\Omega_S(-m)\frac{\partial}{\partial p}V(0)$$

$$-\frac{\tan\varphi}{a}V(0)\,U_S(m)\,V_S(-m)\times k + \frac{1}{a\cos\varphi}\frac{\partial}{\partial\lambda}\{V(0)\,U_T(-m)V_T(m)\} \qquad \text{B-17}$$

$$+\frac{1}{a\cos\varphi}\frac{\partial}{\partial\varphi}\{V(0)\,V_T(-m)V_T(m)\cos\varphi\} + \frac{\partial}{\partial p}\{V(0)\,\Omega_T(-m)\,V_T(m)\}$$

$$-\frac{V_T(m)\,V_T(-m)}{a}\frac{\partial}{\partial\varphi}V(0) - V_T(m)\,\Omega_T(-m)\frac{\partial}{\partial p}V(0) - \frac{\tan\varphi}{a}V(0)\cdot$$

$$U_T(m)\cdot V_T(-m)\times k\Big] - g\Big[\frac{1}{a\cos\varphi}\frac{\partial}{\partial\varphi}\{V(0)\,Z(0)\cos\varphi\}$$

$$+ \frac{\partial}{\partial p}\{\Omega(o)Z(o)\} - \Omega(o)\frac{\partial}{\partial p}Z(o)] - V(o)\cdot F(o)\rangle$$

The governing equations concerning the available potential energy are derived from the eq. B-3. And the total available potential energy A is

$$A = AZ + \sum_{n=1}^{\infty}\{AT(n) + AS(n)\} \qquad \text{B-18}$$

where

$$AZ = \frac{1}{2}\beta\langle\bar{\theta}^{*2}\rangle$$

$$AT(n) = \beta\langle\theta_T(n)^2\rangle \qquad \text{B-19}$$

$$AS(n) = \beta\langle\theta_S(n)^2\rangle$$

The respective governing equation for the available potential energies AT(n), AS(n) and AZ can be obtained as follows:

for AT(n),

$$\frac{\partial}{\partial t}AT(n) = \{[-\sum_{\substack{m=-\infty \\ \neq 0}}^{\infty}\Big[\frac{1}{a\cos\varphi}\frac{\partial}{\partial\lambda}\{U_T(n-m)\Theta_T(-n)\Theta_T(m)\}$$

$$+ \frac{1}{a\cos\varphi}\frac{\partial}{\partial\varphi}\{V_T(n-m)\Theta_T(-n)\Theta_T(m)\cos\varphi\} + \frac{\partial}{\partial p}\{\Omega_T(n-m)\cdot$$

$$\Theta_T(-n)\Theta_T(m)\} + \frac{1}{a\cos\varphi}\frac{\partial}{\partial\lambda}\{U_T(n-m)\Theta_T(-n)\Theta_S(m)\}$$

$$+ \frac{1}{a\cos\varphi}\frac{\partial}{\partial\varphi}\{V_T(n-m)\Theta_T(-n)\Theta_S(m)\cos\varphi\} + \frac{\partial}{\partial p}\{\Omega_T(n-m)\Theta_T(-n)\Theta_S(m)\}$$

$$+\Theta_T(-n)\left\{\frac{im\,U_S(n-m)}{a\cos\varphi}\Theta_T(m)+\frac{V_S(n-m)}{a}\cdot\frac{\partial}{\partial\varphi}\Theta_T(m)+\Omega_S(n-m)\frac{\partial}{\partial p}\Theta_T(m)\right\}$$

$$-\Theta_T(m)\left\{\frac{-in\,U_T(n-m)}{a\cos\varphi}\Theta_T(-n)+\frac{V_T(n-m)}{a}\cdot\frac{\partial}{\partial\varphi}\Theta_T(-n)+\Omega_T(n-m)\frac{\partial}{\partial p}\Theta_T(-n)\right\} \qquad \text{B-20}$$

$$-\Theta_S(m)\left\{\frac{-in\,U_T(n-m)}{a\cos\varphi}\Theta_T(-n)+\frac{V_T(n-m)}{a}\cdot\frac{\partial}{\partial\varphi}\Theta_T(-n)+\Omega_T(n-m)\frac{\partial}{\partial p}\Theta_T(-n)\right\}\Big]$$

$$-\Theta_T(-n)\left\{\frac{V_T(n)}{a}\frac{\partial}{\partial\varphi}\bar{\Theta}+\Omega_T(n)\frac{\partial}{\partial p}\bar{\Theta}\right\}+\frac{1}{C_p}\left(\frac{P_0}{P}\right)^{\kappa}H(n)\,\Theta_T(-n)\Big\}\Big\}$$

for AS(n),

$$\frac{\partial}{\partial t}AS(n)=\Big\{\Big\{-\sum_{\substack{m=-\infty\\ \neq 0}}^{\infty}\Big[\frac{1}{a\cos\varphi}\frac{\partial}{\partial\lambda}\left\{\Theta_S(-n)U_S(n-m)\Theta_S(m)\right\}$$

$$+\frac{1}{a\cos\varphi}\frac{\partial}{\partial\varphi}\left\{\Theta_S(-n)V_S(n-m)\Theta_S(m)\cos\varphi\right\}+\frac{\partial}{\partial p}\left\{\Theta_S(-n)\Omega_S(n-m)\Theta_S(m)\right\}$$

$$-\Theta_S(m)\left\{\frac{-in\,U_S(n-m)}{a\cos\varphi}\Theta_S(-n)+\frac{V_S(n-m)}{a}\frac{\partial}{\partial\varphi}\Theta_S(-n)+\Omega_S(n-m)\frac{\partial}{\partial p}\Theta_S(-n)\right\} \qquad \text{B-21}$$

$$+\Theta_S(-n)\left\{\frac{im\,U_T(n-m)}{a\cos\varphi}\Theta_T(m)+\frac{V_T(n-m)}{a}\frac{\partial}{\partial\varphi}\Theta_T(m)+\Omega_T(n-m)\frac{\partial}{\partial p}\Theta_T(m)\right\}\Big]$$

$$-\Theta_S(-n)\left\{\frac{V_S(n)}{a}\frac{\partial}{\partial\varphi}\bar{\Theta}+\Omega_S(n)\frac{\partial}{\partial p}\bar{\Theta}\right\}+\frac{1}{C_p}\left(\frac{P_0}{P}\right)^{\kappa}H_S(n)\Theta_S(-n)\Big\}\Big\}$$

for AZ,

$$\frac{\partial}{\partial t}AZ=\Big\langle-\frac{1}{a\cos\varphi}\frac{\partial}{\partial\varphi}\left\{\bar{\Theta}^{*}V(0)\cdot\bar{\Theta}\right\}-\frac{\partial}{\partial p}\left\{\bar{\Theta}^{*}\Omega(0)\cdot\bar{\Theta}\right\}$$

$$+\bar{\Theta}\left\{\frac{V(0)}{a}\frac{\partial}{\partial\varphi}\bar{\Theta}^{*}+\Omega^{*}(0)\frac{\partial}{\partial p}\bar{\Theta}^{*}\right\}-\sum_{\substack{m=-\infty\\ \neq 0}}^{\infty}\Big[\frac{1}{a\cos\varphi}\frac{\partial}{\partial\lambda}\Big\{$$

$$\bar{\Theta}^{*}U(-m)\Theta(m)\Big\}+\frac{1}{a\cos\varphi}\cdot\frac{\partial}{\partial\varphi}\left\{\bar{\Theta}^{*}V(-m)\Theta(m)\cos\varphi\right\} \qquad \text{B-22}$$

$$+\frac{\partial}{\partial p}\left\{\bar{\Theta}^{*}\Omega(-m)\Theta(m)\right\}-\Theta_S(m)\left\{\frac{V_S(-m)}{a}\frac{\partial}{\partial\varphi}\bar{\Theta}^{*}+\Omega_S(-m)\frac{\partial}{\partial p}\bar{\Theta}^{*}\right\}$$

$$-\Theta_T(m)\left\{\frac{V_T(-m)}{a}\frac{\partial}{\partial\varphi}\bar{\Theta}^{*}+\Omega_T(-m)\frac{\partial}{\partial p}\bar{\Theta}^{*}\right\}\Big]+\frac{1}{C_p}\left(\frac{P_0}{P}\right)^{\kappa}H(0)\bar{\Theta}^{*}\Big\rangle$$

The above energy equations will be further integrated for a region bounded by two isobaric surfaces 10 mb and 100 mb, and two constant latitudes 30°N and 85°N. After Muench(1965a,b), Perry(1966,67), etc., the various energy conversion or transfer terms in the righthand side of the energy equations may be written in the symbolical form presented in the section II [eqs. (1), (3), (4), (5), (7) and (8)]. Their energy exchange terms are given as follows:

$$BKZ = -\frac{1}{g\Delta p}\left\langle \left[\frac{1}{2}U(0)^2\Omega(0) + \sum_{\substack{m=-\infty \\ \neq 0}}^{\infty} U(0)\Omega_T(m)U_T(-m)\right]_{p_1}^{p_2}\right\rangle$$
$$-\frac{1}{\Delta p}\int_{p_1}^{p_2}\left\langle \left[\frac{\cos\varphi}{a\delta}\sum_{\substack{m=-\infty \\ \neq 0}}^{\infty} U(0)V_T(-m)U_T(m)\right]_{\varphi_1}^{\varphi_2}\right\rangle \frac{dp}{g} \qquad \text{B-23}$$

$$BKT(n) = -\left\{\left\{\frac{1}{g\Delta p}\left[\sum_{\substack{m=-\infty \\ \neq 0}}^{\infty}\left\{U_T(-n)\Omega(n-m)U_T(m) + V_T(-n)\Omega(n-m)V_T(m)\right\}\right]_{p_1}^{p_2}\right.\right. \qquad \text{B-24}$$
$$\left.\left. + \frac{1}{\Delta p}\int_{p_1}^{p_2}\left[\frac{\cos\varphi}{a\delta}\sum_{\substack{m=-\infty \\ \neq 0}}^{\infty}\left\{U_T(-n)V(n-m)U_T(m) + V_T(-n)V(n-m)V_T(m)\right\}\right]_{\varphi_1}^{\varphi_2}\frac{dp}{g}\right\}\right\}$$

$$BKS(n) = -\left\{\left\{\frac{1}{g\Delta p}\left[\sum_{m=-\infty}^{\infty}\left\{U_S(-n)\Omega_S(n-m)U_S(m) + V_S(-n)\Omega_S(n-m)V_S(m)\right\}\right]_{p_1}^{p_2}\right.\right. \qquad \text{B-25}$$
$$\left.\left. + \frac{1}{\Delta p}\int_{p_1}^{p_2}\left[\frac{\cos\varphi}{a\delta}\sum_{\substack{m=-\infty \\ \neq 0}}^{\infty}\left\{U_S(-n)V_S(n-m)U_S(m) + V_S(-n)V_S(n-m)V_S(m)\right\}\right]_{\varphi_1}^{\varphi_2}\frac{dp}{g}\right\}\right\}$$

$$BGZ = -\left\langle \frac{1}{\Delta p}\left[Z(0)^*\Omega(0)^*\right]_{p_1}^{p_2} + \frac{1}{\Delta p}\int_{p_1}^{p_2}\left[\frac{\cos\varphi}{a\delta}V(0)Z(0)\right]_{\varphi_1}^{\varphi_2}dp\right\rangle \qquad \text{B-26}$$

$$BGT(n) = -\left\{\left\{\frac{1}{\Delta p}\left[Z_T(n)\Omega_T(-n)\right]_{p_1}^{p_2} + \frac{1}{\Delta p}\int_{p_1}^{p_2}\left[\frac{\cos\varphi}{a\delta}V_T(-n)Z_T(n)\right]_{\varphi_1}^{\varphi_2}dp\right\}\right\} \qquad \text{B-27}$$

$$BGS(n) = -\left\{\left\{\frac{1}{\Delta p}\left[Z_S(n)\Omega_S(-n)\right]_{p_1}^{p_2} + \frac{1}{\Delta p}\int_{p_1}^{p_2}\left[\frac{\cos\varphi}{a\delta}V_S(-n)Z_S(n)\right]_{\varphi_1}^{\varphi_2}dp\right.\right. \qquad \text{B-28}$$

$$CKT(n) = -\{\{ \bar{U}_T(-n)\left[\frac{V_T(n)}{a}\frac{\partial}{\partial\varphi}U(0) + \Omega_T(n)\frac{\partial}{\partial p}U(0)\right.$$
$$\left. - \frac{\tan\varphi}{a}U_T(n)V(0)\right] + \bar{V}_T(-n)\left[\frac{V_T(n)}{a}\frac{\partial}{\partial\varphi}V(0)\right. \qquad \text{B-29}$$
$$\left. + \Omega_T(n)\frac{\partial}{\partial p}V(0) + \frac{\tan\varphi}{a}U(0)U_T(n)\right]\}\}$$

$$CKS(n) = -\{\{ \bar{U}_S(-n)\left[\frac{V_S(n)}{a}\frac{\partial}{\partial\varphi}U(0) + \Omega_S(n)\frac{\partial}{\partial p}U(0)\right.$$
$$\left. - \frac{\tan\varphi}{a}U_S(n)V(0)\right] + \bar{V}_S(-n)\left[\frac{V_S(n)}{a}\frac{\partial}{\partial\varphi}V(0)\right. \qquad \text{B-30}$$
$$\left. + \Omega_S(n)\frac{\partial}{\partial p}V(0) + \frac{\tan\varphi}{a}U(0)U_S(n)\right]\}\}$$

$$DZ = \left\langle \frac{1}{\Delta p}\int_{p_1}^{p_2}\{U(0)F_\lambda(0) + V(0)F_\varphi(0)\}\frac{dp}{g}\right\rangle \qquad \text{B-31}$$

$$DT(n) = \{\{\frac{1}{\Delta p}\int_{p_1}^{p_2}\left[\bar{U}_T(-n)F_T^\lambda(n) + \bar{V}_T(-n)F_T^\varphi(n)\right]\frac{dp}{g}\}\} \qquad \text{B-32}$$

$$DS(n) = \{\{\frac{1}{\Delta p}\int_{p_1}^{p_2}\left[\bar{U}_S(-n)F_S^\lambda(n) + \bar{V}_S(-n)F_S^\varphi(n)\right]\frac{dp}{g}\}\} \qquad \text{B-33}$$

$$CAKZ = \left\langle \frac{1}{\Delta p}\int_{p_1}^{p_2}\left[S\frac{\partial[\bar{\Theta}]}{\partial p}\Omega(0)^*\bar{\Theta}^*\right]\frac{dp}{g}\right\rangle \qquad \text{B-34}$$

$$CAKT(n) = \{\{\frac{1}{\Delta p}\int_{p_1}^{p_2}\left[S\frac{\partial}{\partial p}[\bar{\Theta}]\Omega_T(-n)\Theta_T(n)\right]\frac{dp}{g}\}\} \qquad \text{B-35}$$

$$CAKS(n) = \{\{\frac{1}{\Delta p}\int_{p_1}^{p_2}\left[S\frac{\partial}{\partial p}[\bar{\Theta}]\Omega_S(-n)\Theta_S(n)\right]\frac{dp}{g}\}\} \qquad \text{B-36}$$

$$BAZ = -\left\langle \frac{1}{g\Delta\varphi}\left[\frac{1}{2}S\bar{\Theta}^{*2}\Omega(0) + S\sum_{\substack{m=-\infty\\ \neq 0}}^{\infty}\bar{\Theta}^*\Omega(-m)\Theta(m)\right]_{p_1}^{p_2}\right. \qquad \text{B-37}$$
$$\left. + \frac{1}{\Delta p}\int_{p_1}^{p_2}\left[\frac{\cos\varphi}{a\partial}S\{\bar{\Theta}^*V(0)\bar{\Theta} + \sum_{\substack{m=-\infty\\ \neq 0}}^{\infty}\bar{\Theta}^*V(-m)\Theta(m)\}\right]_{p_1}^{p_2}\frac{dp}{g}\right\rangle$$

$$BAT(n) = -\{\{\frac{1}{g\Delta\varphi}\left[S\sum_{\substack{m=-\infty\\ \neq 0}}^{\infty}\Theta_T(-n)\Omega_T(n-m)\Theta(m)\right]_{p_1}^{p_2}$$
$$+ \frac{1}{\Delta p}\int_{p_1}^{p_2}\left[\frac{\cos\varphi}{a\partial}S\,V_T(n-m)\Theta_T(-n)\Theta(m)\right]_{p_1}^{p_2}\frac{dp}{g}\}\} \qquad \text{B-38}$$

$$BAS(n) = -\{\{ \frac{1}{g\Delta p}\Big[S \sum_{\substack{m=-\infty \\ \neq 0}}^{\infty} \Theta_S(-n)\Omega_S(n-m)\,\Theta_S(m)\Big]_{p_1}^{p_2}$$

$$+ \frac{1}{\Delta p}\int_{p_1}^{p_2}\Big[\frac{\cos\varphi}{a}S\;\Theta_S(-n)\,V_S(n-m)\,\Theta_S(m)\Big]_{sq}^{p_2}\frac{dp}{g}\}\}$$ B-39

$$CAT(n) = -\{\{\frac{1}{\Delta p}\int_{p_1}^{p_2} S\Big[\Theta_T(-n)\Big\{\frac{\bar{V}_T(n)}{a}\frac{\partial}{\partial\varphi}\bar{\Theta}^* + \Omega_T(n)\frac{\partial}{\partial p}\bar{\Theta}^*\Big\}\Big]\frac{dp}{g}\}\}$$ B-40

$$CAS(n) = -\{\{\frac{1}{\Delta p}\int_{p_1}^{p_2} S\Big[\Theta_S(-n)\Big\{\frac{\bar{V}_S(n)}{a}\frac{\partial}{\partial\varphi}\bar{\Theta}^* + \Omega_S(n)\frac{\partial}{\partial p}\bar{\Theta}^*\Big\}\Big]\frac{dp}{g}\}\}$$ B-41

$$GZ = \Big\langle \frac{1}{\Delta p}\int_{p_1}^{p_2}\frac{S}{c_p}\Big(\frac{p_0}{p}\Big)^{\kappa}\bar{\Theta}^* H^*(0)\frac{dp}{g}\Big\rangle$$ B-42

$$GT(n) = \{\{\frac{1}{\Delta p}\int_{p_1}^{p_2}\frac{S}{c_p}\Big(\frac{p_0}{p}\Big)^{\kappa}\Theta_T(-n)\,H_T(n)\frac{dp}{g}\}\}$$ B-43

$$GS(n) = \{\{\frac{1}{\Delta p}\int_{p_1}^{p_2}\frac{S}{c_p}\Big(\frac{p_0}{p}\Big)^{\kappa}\Theta_S(-n)\,H_S(n)\frac{dp}{g}\}\}$$ B-44

$$LKT(n) = \{\{\frac{1}{\Delta p}\int_{p_1}^{p_2}\sum_{\substack{m=-\infty \\ \neq 0}}^{\infty}\Big[U_T(m)\Big\{\frac{-in\bar{U}(n-m)}{a\cos\varphi}U_T(-n) + \frac{\bar{V}(n-m)}{a}\frac{\partial}{\partial\varphi}U_T(-n)$$

$$+ \Omega(n-m)\frac{\partial}{\partial p}U_T(-n) - \frac{\tan\varphi}{a}\bar{U}(n-m)V_T(-n)\Big\} + \bar{V}_T(m)\Big\{$$ B-45

$$- \frac{in\bar{U}(n-m)}{a\cos\varphi}V_T(-n) + \frac{\bar{V}(n-m)}{a}\frac{\partial}{\partial\varphi}V_T(-n) + \Omega(n-m)\frac{\partial}{\partial p}V_T(-n)$$

$$+ \frac{\tan\varphi}{a}\bar{U}(n-m)U_T(-n)\Big\}\Big]\frac{dp}{g}\}\}$$

$$LKS(n) = \{\{\frac{1}{\Delta p}\int_{p_1}^{p_2}\sum_{\substack{m=-\infty \\ \neq 0}}^{\infty}\Big[U_S(m)\Big\{\frac{-in\bar{U}_S(n-m)}{a\cos\varphi}U_S(-n) + \frac{\bar{V}_S(n-m)}{a}\frac{\partial}{\partial\varphi}V_S(-n)$$

$$+ \Omega_S(n-m)\frac{\partial}{\partial p}V_S(-n) - \frac{\tan\varphi}{a}U_S(n-m)V_S(-n)\Big\}$$ B-46

$$+ \bar{V}_S(m)\Big\{\frac{-in\bar{U}_S(n-m)}{a\cos\varphi}V_S(-n) + \frac{\bar{V}_S(n-m)}{a}\frac{\partial}{\partial\varphi}V_S(-n)$$

$$+ \Omega_S(n-m)\frac{\partial}{\partial p}V_S(-n) + \frac{\tan\varphi}{a}U_S(n-m)U_S(-n)\Big\}\Big]\frac{dp}{g}\}\}$$

$$LAT(n) = -\left\{\left\{\frac{1}{\Delta p}\int_{p_1}^{p_2} S \sum_{\substack{m=-\infty \\ \neq 0}}^{\infty}\left[\Theta_T(-n)\left\{\frac{U_S(n-m)}{a\cos\varphi} im\,\Theta_T(m) + \frac{V_S(n-m)}{a}\frac{\partial}{\partial\varphi}\Theta_T(m)\right.\right.\right.$$
$$\left. + \Omega_S(n-m)\frac{\partial}{\partial p}\Theta_T(m)\right\} - \Theta_T(m)\left\{-\frac{in\,U_T(n-m)}{a\cos\varphi}\Theta_T(-n) + \right. \qquad \text{B-47}$$
$$\left.\left.\left. + \frac{V_T(n-m)}{a}\frac{\partial}{\partial\varphi}\Theta_T(-n) + \Omega_T(n-m)\frac{\partial}{\partial p}\Theta_T(-n)\right\}\right]\frac{dp}{g}\right\}\right\}$$

$$LAS(n) = \left\{\left\{\frac{1}{\Delta p}\int_{p_1}^{p_2} S \sum_{\substack{m=-\infty \\ \neq 0}}^{\infty}\left[\Theta_S(m)\left\{\frac{-in\,U_S(n-m)}{a\cos\varphi}\Theta_S(-n)\right.\right.\right. \qquad \text{B-48}$$
$$\left.\left.\left. + \frac{V_S(n-m)}{a}\frac{\partial}{\partial\varphi}\Theta_S(-n) + \Omega_S(n-m)\frac{\partial}{\partial p}\Theta_S(-n)\right\}\right]\frac{dp}{g}\right\}\right\}.$$

$$CKTS(n,m) = \left\{\left\{\frac{1}{\Delta p}\int_{p_1}^{p_2}\left[U_S(m)\left\{\frac{-in\,U_T(n-m)}{a\cos\varphi}U_T(-n)\right.\right.\right.\right.$$
$$\left. + \frac{V_T(n-m)}{a}\frac{\partial}{\partial\varphi}U_T(-n) + \Omega_T(n-m)\frac{\partial}{\partial p}U_T(-n) - \frac{\tan\varphi}{a}U_T(n-m)V_T(n)\right\}$$
$$+ V_S(m)\left\{\frac{-in\,U_T(n-m)}{a\cos\varphi}V_T(n) + \frac{V_T(n-m)}{a}\frac{\partial}{\partial\varphi}V_T(-n) + \Omega_T(n-m)\frac{\partial}{\partial p}V_T(n)\right.$$
$$\left.\left.\left.\left. + \frac{\tan\varphi}{a}U_T(n-m)U_T(-n)\right\}\right]\frac{dp}{g}\right\}\right\} \qquad \text{B-49}$$

$$CATS(n,m) = \left\{\left\{\frac{1}{\Delta p}\int_{p_1}^{p_2} S\left[\Theta_S(m)\left\{\frac{-in\,U_T(n-m)}{a\cos\varphi}\Theta_T(-n)\right.\right.\right. \qquad \text{B-50}$$
$$\left.\left.\left. + \frac{V_T(n-m)}{a}\frac{\partial}{\partial\varphi}\Theta_T(-n) + \Omega_T(n-m)\frac{\partial}{\partial p}\Theta_T(n)\right]\frac{dp}{g}\right\}\right\}$$

Here, the energy exchange terms between the quasi-stationary wave and the travelling wave CKTS(n,m) and CATS(n,m) express the energy-flow from a quasi-stationary part of wavenumber m to the travelling part of wavenumber n, when the terms are positive.

For the computation of the above terms, a few semi-empirical approximations are adopted here as follows:

i) Zonal and meridional component of the wind U(n) and V(n) are computed from the geopotential height Z(n) under the quasi-geostrophic assumption.

ii) Static stability factor S is a function of time and height, and calculated every day. However, the effect of $\frac{\partial}{\partial t} S$ is neglected in this work, because the magnitude of time-change is considerably small.

iii) Although the operator $\langle\ \rangle$ defined in B-7 should be of the same as that used for separating the waves into the quasi-stationary and travelling parts, 3-day running mean is used for estimation of the energy-exchange terms because of small number of data.

「大気中における超長波の解析的研究(II)」
第2部 成層圏突然昇温前後の超長波エネルギー過程

岩嶋樹也
京都大学理学部地球物理学教室

第1部 [Iwashima(1973)] においては，我々の提案した時間フィルター法により，大気中の超長波を移動部分と準停滞部分に分離し，とくに後者の振幅変動が大きいことを示した。

本論文では，移動・準停滞両波動擾乱に対するエネルギー方程式を導出し，前報と同じ1967／68年成層圏突然昇温前後のエネルギー過程について解析を行なった。

まず，帯状流と擾乱に分離した場合と，さらに擾乱を波数空間で分けた場合のエネルギー変化について調べ，Reed et al.(1963)，Julian & Labitzke(1965) らの示したと同様な結果を得た。

波数1，2の超長波の準停滞・移動両部分のエネルギー過程については以下の結果を得た。

i)突然昇温時には，波数2の準停滞・移動両部分それぞれの運動エネルギー[KS(2)とKT(2)]に増大が見られ，とくに前者のそれが顕著である。

ii)KS(2)の増大あるいは減少は，主にいわゆる気圧力(pressure-interaction)項[BGS(2)]による対流圏からのエネルギー輸送の増減に依存している。

iii)KS(2)の昇温時の増大には，また種々の波数の移動性波動からの運動エネルギー輸送項も寄与している。

iv)波数1の移動・準停滞両部分の有効位置エネルギーにも昇温時における増大が見られるが，これはほとんど帯状流の有効位置エネルギーからの転換によるものである。

Legends

Fig. 1 Computational procedure for kinetic and available potential energies and their conversion or transfer terms.

Fig. 2a Mean meridional circulation for the period from Dec. 23 to 31, 1967. Vertical exaggeration is 100 : 1.

Fig. 2b Same as Fig. 2a except from Jan. 1 to 8, 1968.

Fig. 3 Deviation of the zonal-mean potential temperature ($\bar{\theta}^*$) from the zonal-meridional mean one ($[\bar{\theta}]$) at 10 mb and 100 mb.

Fig. 4 Time-change of the zonal kinetic (KZ), eddy kinetic (KE), zonal available potential (AZ) and eddy available potential (AE) energies. Unit is $10^3 J/m^2/sec$.

Fig. 5 Time-change of the energy conversion and transfer terms in units of $10^{-2} J/m^2/mb/sec$.

Fig. 6a Energy flow diagram during the period from Dec. 23 to 31. Unit is $10^{-3} J/m^2/mb/sec$. Arrows indicate the direction of energy transfer or conversion.

Fig. 6b Same as Fig. 6a except from Jan. 1 to 8.

Fig. 7 Time-change of spectral kinetic energies for wavenumbers one to three. Unit is $10^3 J/m^2/mb$.

Fig. 8 Time-change of spectral available potential energies for wavenumbers one to three. Unit is $10^{3}J/m^{2}/mb$.

Fig. 9 Energy process for wavenumber one. Circles indicate the rate of time-change of energy. Unit is $10^{-2}J/m^{2}mb/sec$.

Fig. 10 Same as Fig. 9 except for wavenumber two.

Fig. 11 Same as Fig. 9 except for wavenumber three.

Fig. 12 Time-change of the kinetic energies of the travelling and quasi-stationary ultra-long waves for wavenumber one and two and of the zonal kinetic energy. Unit is $10^{+3}J/m^{2}/mb$.

Fig. 13 Same as Fig. 12 except the available potential energy.

Fig. 14 Vertical distribution of the kinetic energies for the travelling and quasi-stationary parts of wavenumber two. Unit is $10^{+2}J/m^{2}/mb$.

Fig. 15 Same as Fig. 14 except the available potential energy of wavenumber one.

Fig. 16 Energy processes for kinetic energies of the travelling and quasi-stationary ultra-long waves of wavenumber one. Unit is $10^{-3}J/m^{2}/mb/sec$.

Fig. 17 Same as Fig. 16 except for wavenumber two.

Fig. 18 Energy processes for the available potential energies of the travelling and quasi-stationary ultra-long waves of wavenumber one.

Fig. 19 Same as Fig. 18 except for wavenumber two.

Fig. 20a Energy flow diagram for the zonal flow, travelling and quasi-stationary ultra-long waves during the period from Dec. 23 to 31, 1967. The thickest lines indicate the energy-flow with magnitude greater than 5.0×10^{-3} J/m^2/mb/sec, the second thick lines for the energy-flow from 2.0×10^{-3} to 5.0×10^{-3} J/m^2/mb/sec and the thinnest ones for that less than 2.0×10^{-3} J/m^2/mb/sec.

Fig. 20b Same as Fig. 20 a except from Jan. 1 to 8, 1968.

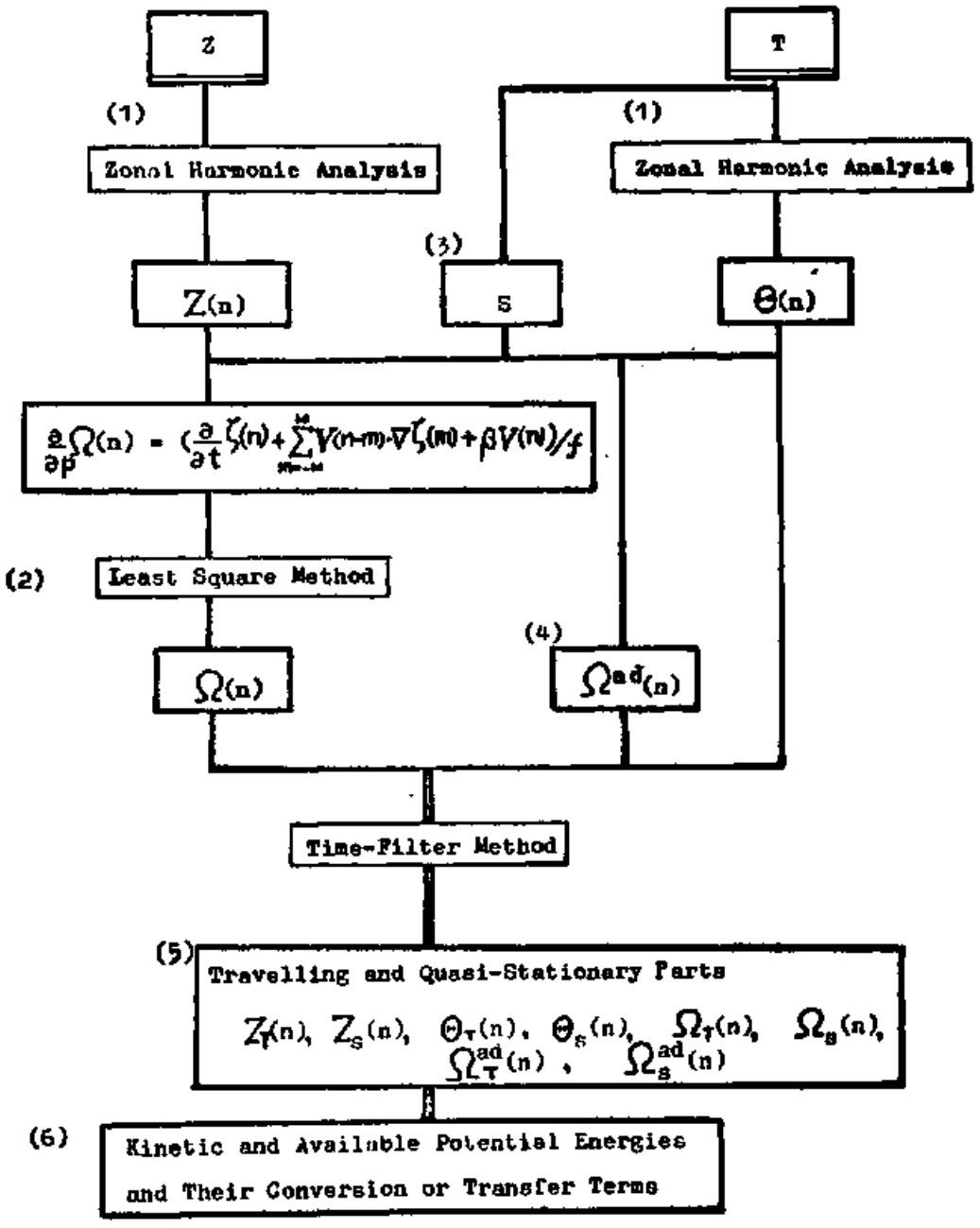
Z
T
(1)
(1)
Zonal Harmonic Analysis
Zonal Harmonic Analysis
(3)
Z(n)
S
Θ(n)
(2)
Least Square Method
(4)
Ω(n)
Time-Filter Method
(5)
Travelling and Quasi-Stationary Parts
(6)
Kinetic and Available Potential Energies
and Their Conversion or Transfer Terms

Fig. 1

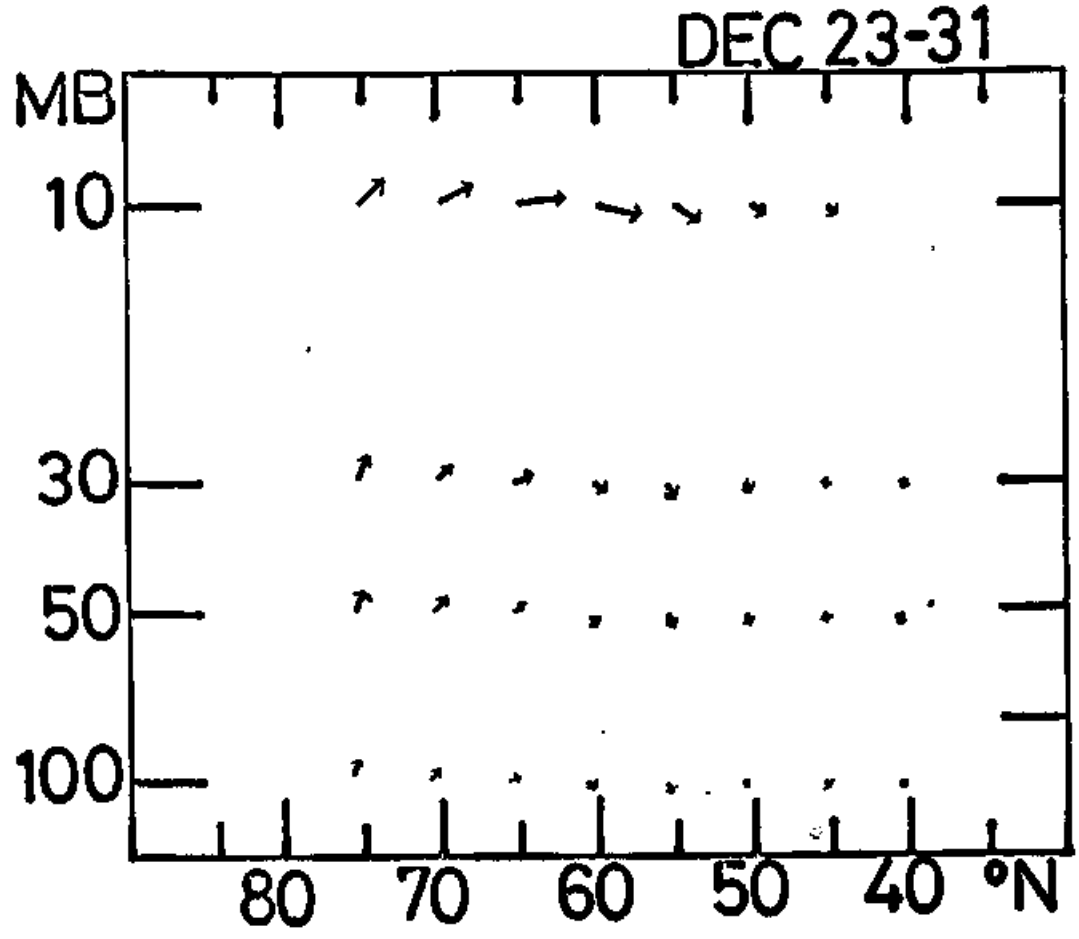

Fig. 2a ⟷ = 1 m/sec [v] = 1 cm/sec [w]

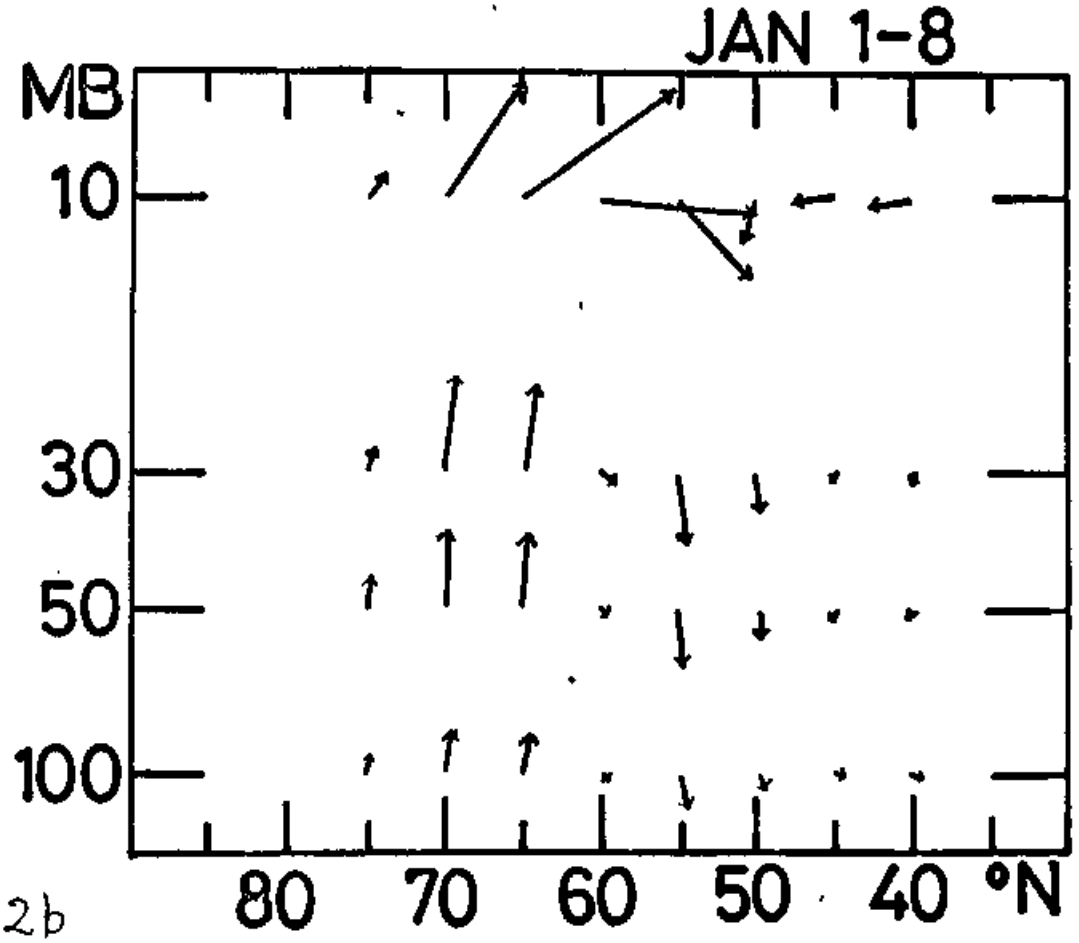

Fig. 2b

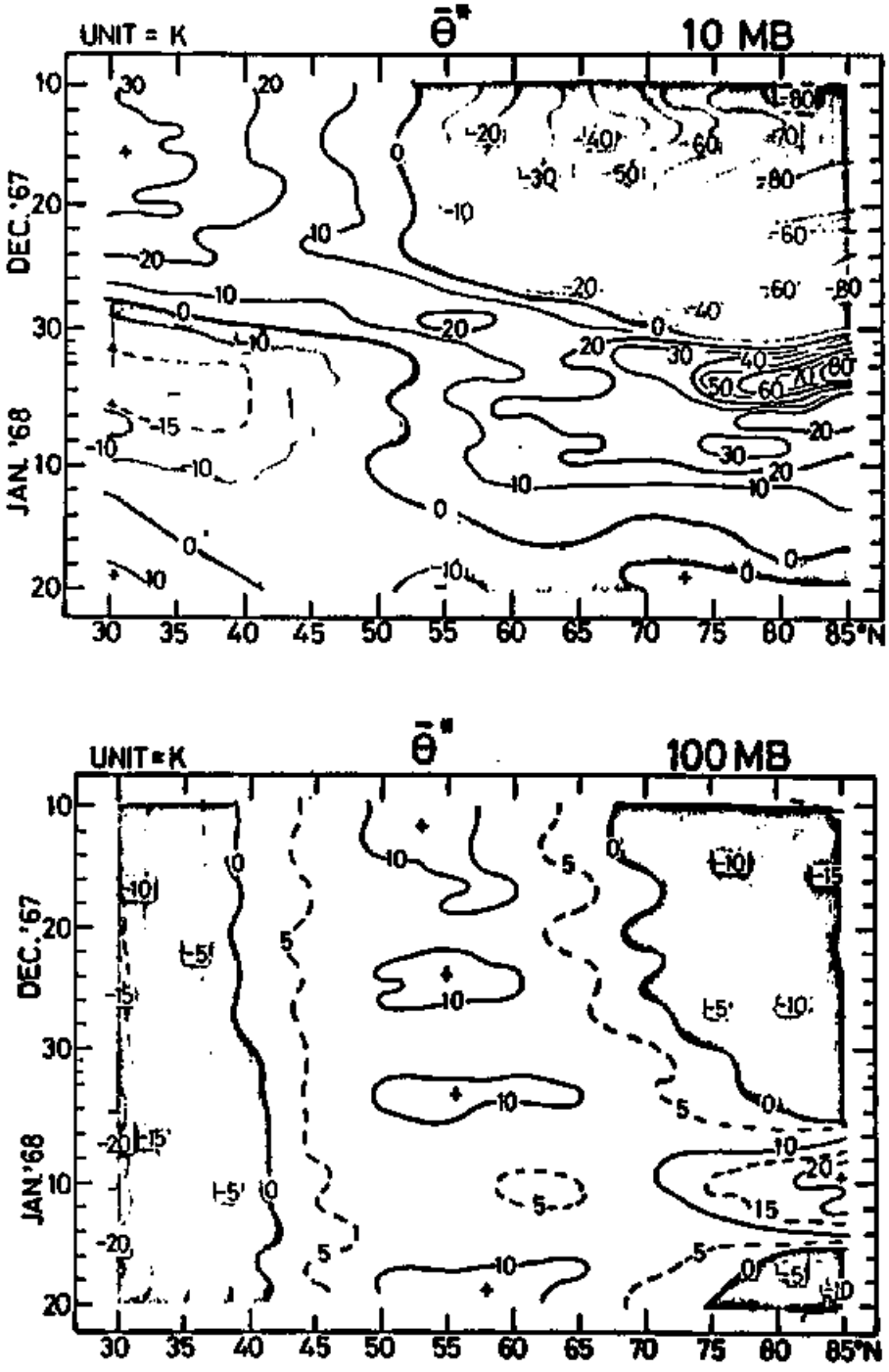
UNIT = K
$\bar{\theta}^*$
10 MB
DEC.'67
JAN.'68
30 35 40 45 50 55 60 65 70 75 80 85°N
UNIT = K
$\bar{\theta}^*$
100 MB
DEC.'67
JAN.'68
30 35 40 45 50 55 60 65 70 75 80 85°N

Fig. 3

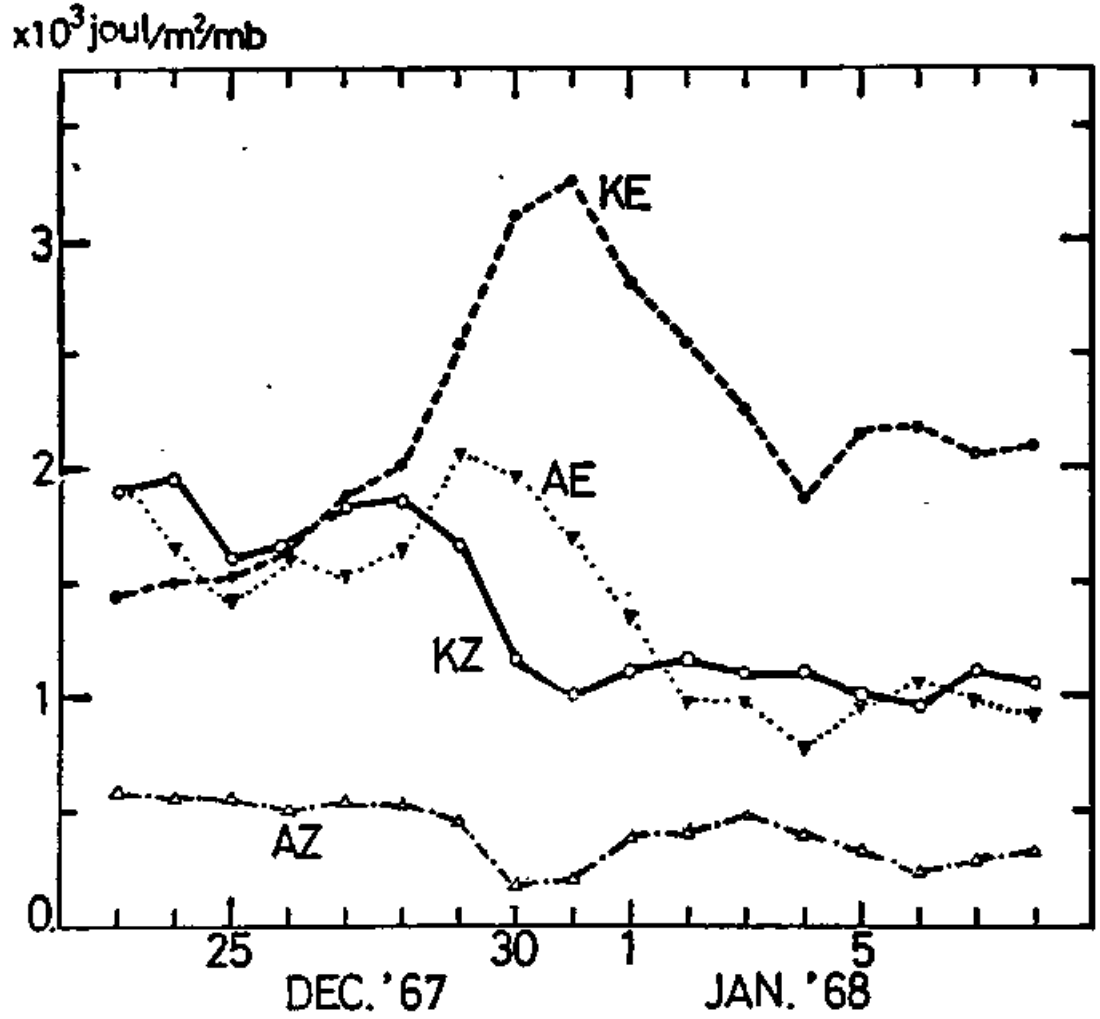

Fig. 4

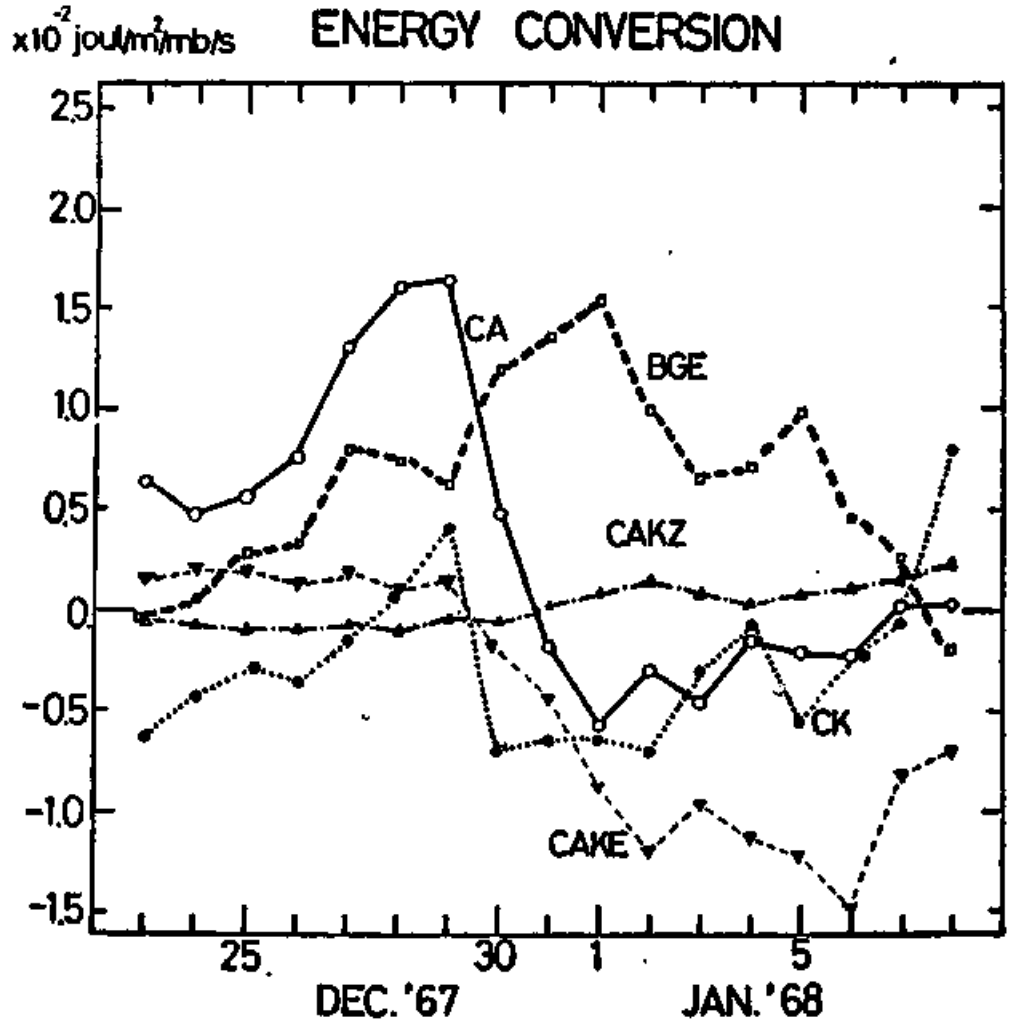
x10^-2 joul/m^2/mb/s
ENERGY CONVERSION
2.5
2.0
1.5
1.0
0.5
0
-0.5
-1.0
-1.5
CA
BGE
CAKZ
CK
CAKE
25
30
1
5
DEC. '67
JAN. '68

Fig. 5

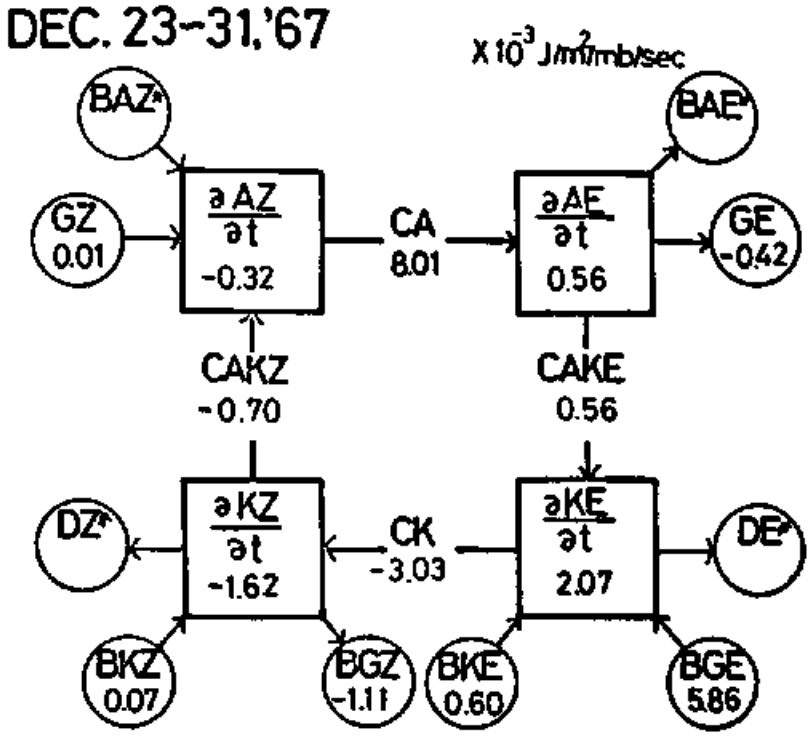
DEC. 23-31,'67
X 10⁻³ J/m²/mb/sec
BAZ
BAE
GZ
0.01
∂AZ/∂t
-0.32
CA
8.01
∂AE/∂t
0.56
GE
-0.42
CAKZ
-0.70
CAKE
0.56
DZ
∂KZ/∂t
-1.62
CK
-3.03
∂KE/∂t
2.07
DE
BKZ
0.07
BGZ
-1.11
BKE
0.60
BGE
5.86

Fig 6a

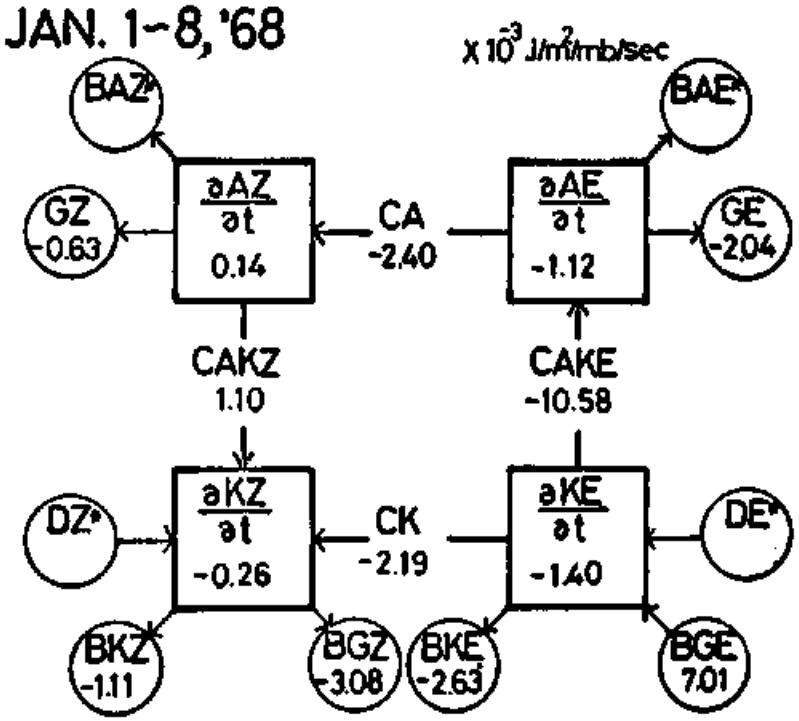
JAN. 1-8,'68
X 10⁻³ J/m²/mb/sec
BAZ
BAE
GZ
-0.63
∂AZ/∂t
0.14
CA
-2.40
∂AE/∂t
-1.12
GE
-2.04
CAKZ
1.10
CAKE
-10.58
DZ
∂KZ/∂t
-0.26
CK
-2.19
∂KE/∂t
-1.40
DE
BKZ
-1.11
BGZ
-3.08
BKE
-2.63
BGE
7.01

Fig. 6b

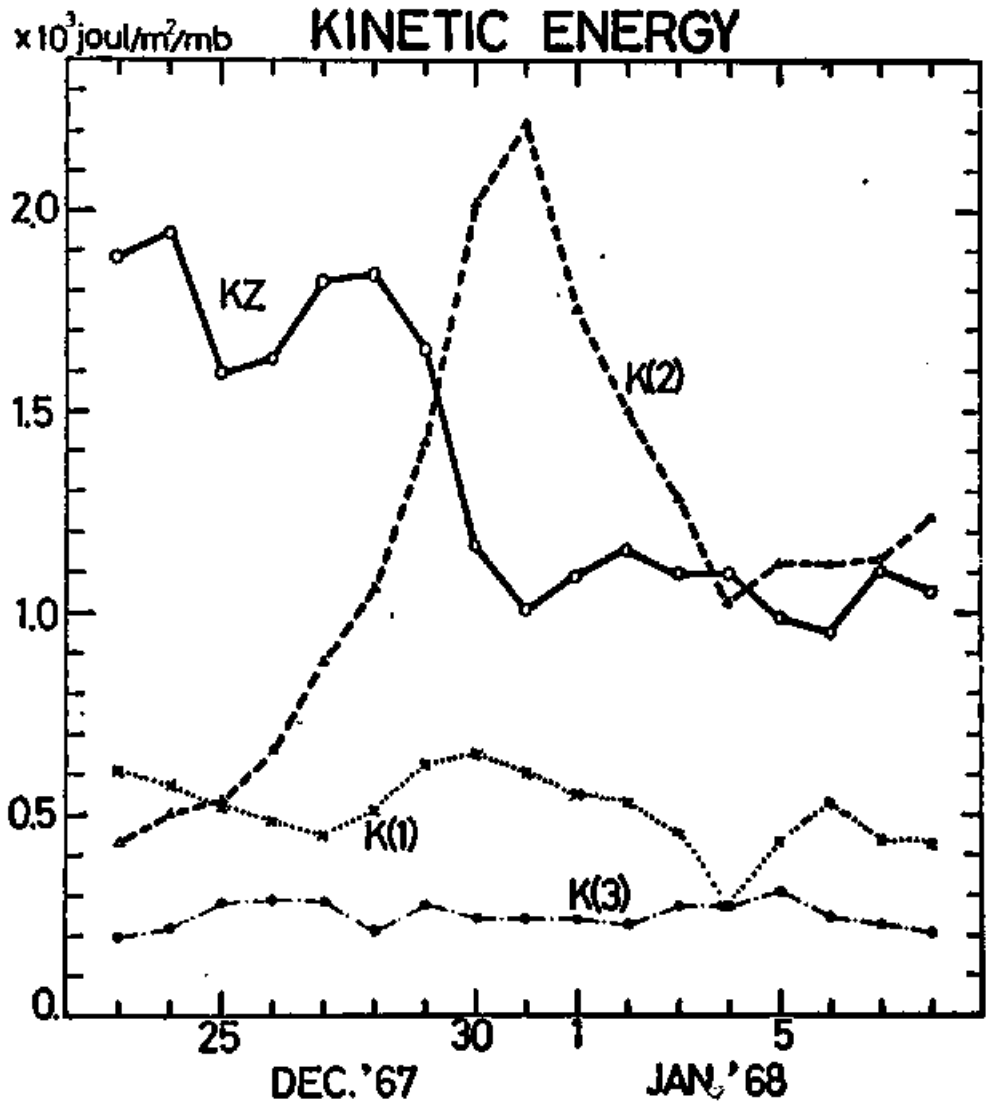
KINETIC ENERGY
x10³joul/m²/mb
2.0
1.5
1.0
0.5
0.
KZ
K(2)
K(1)
K(3)
25
30
1
5
DEC.'67
JAN.'68

Fig. 7

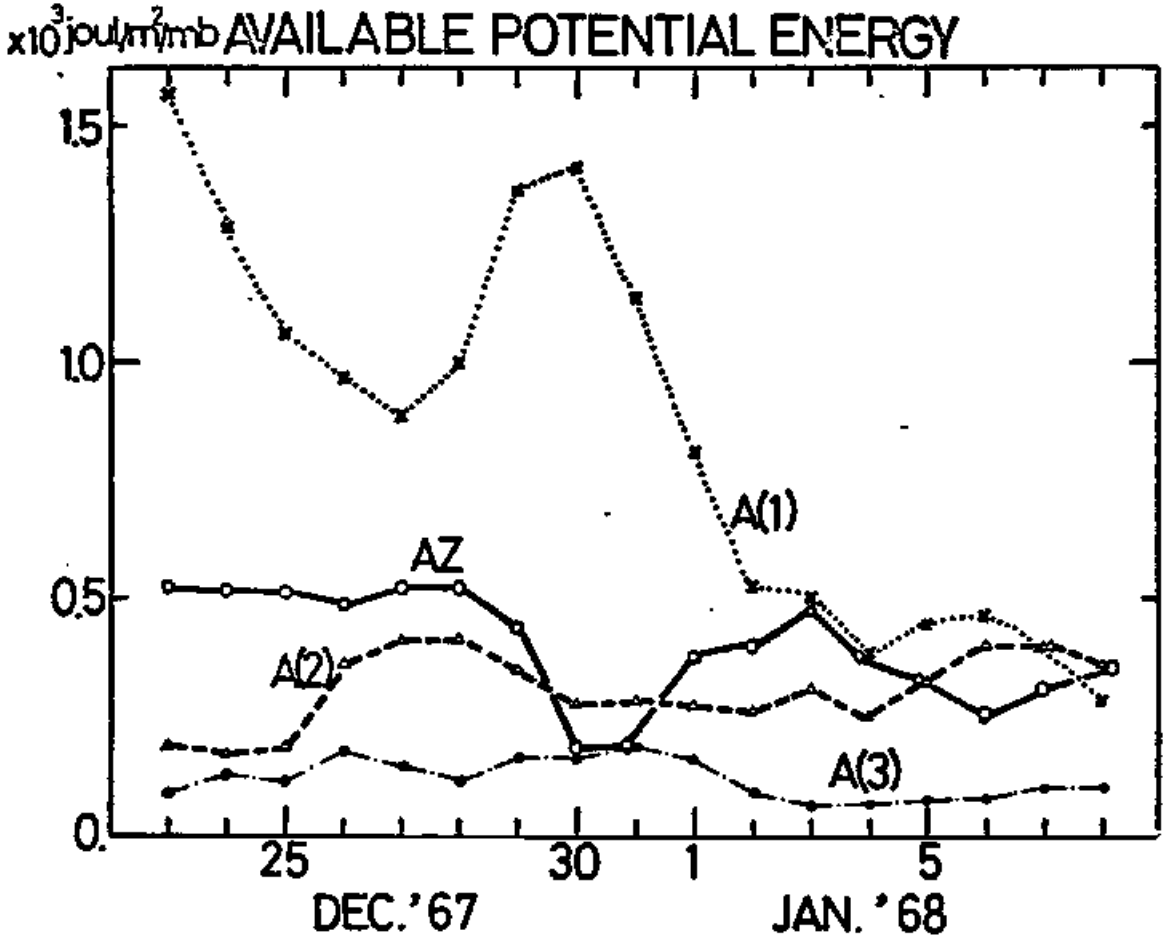
x10³ joul/m²/mb AVAILABLE POTENTIAL ENERGY
1.5
1.0
0.5
0.
A(1)
AZ
A(2)
A(3)
25
30
1
5
DEC.'67
JAN.'68

Fig. 8

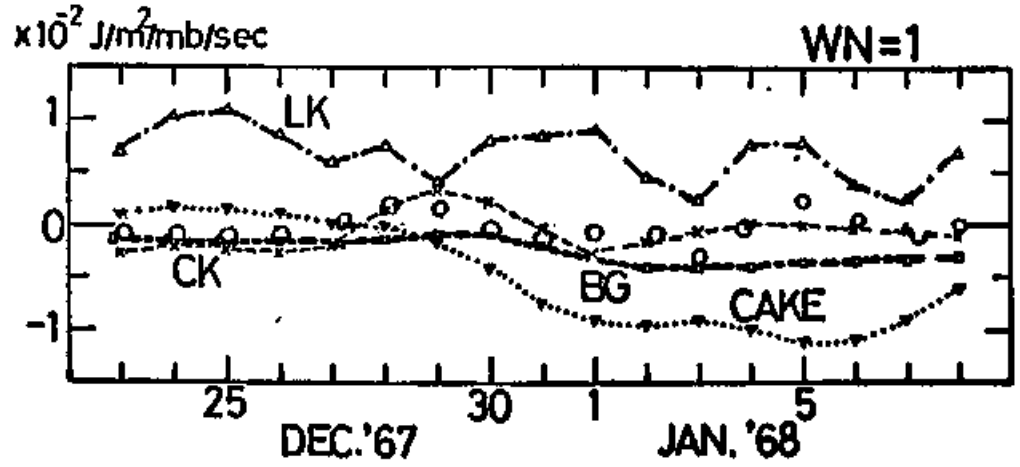

Fig. 9

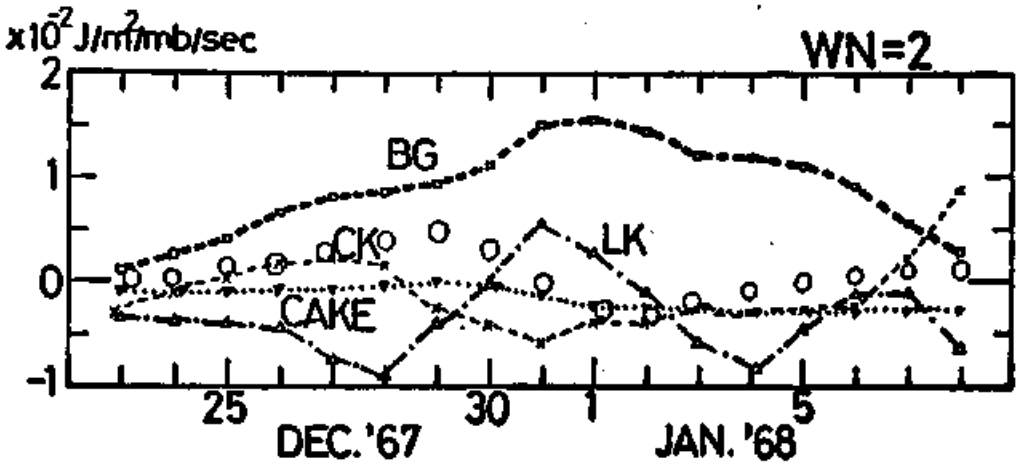

Fig. 10

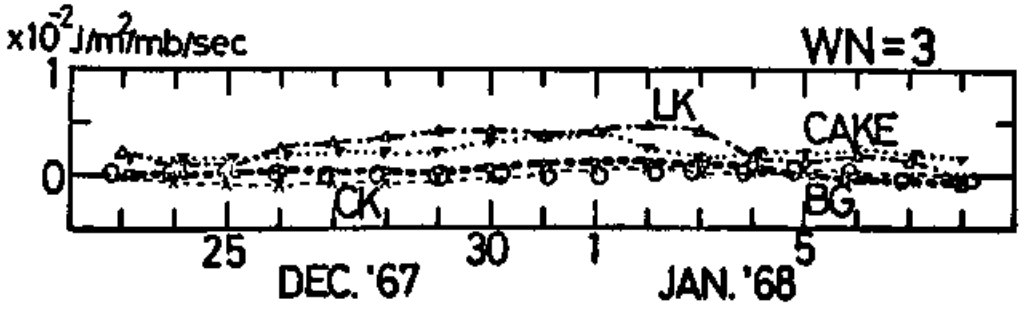

Fig. 11

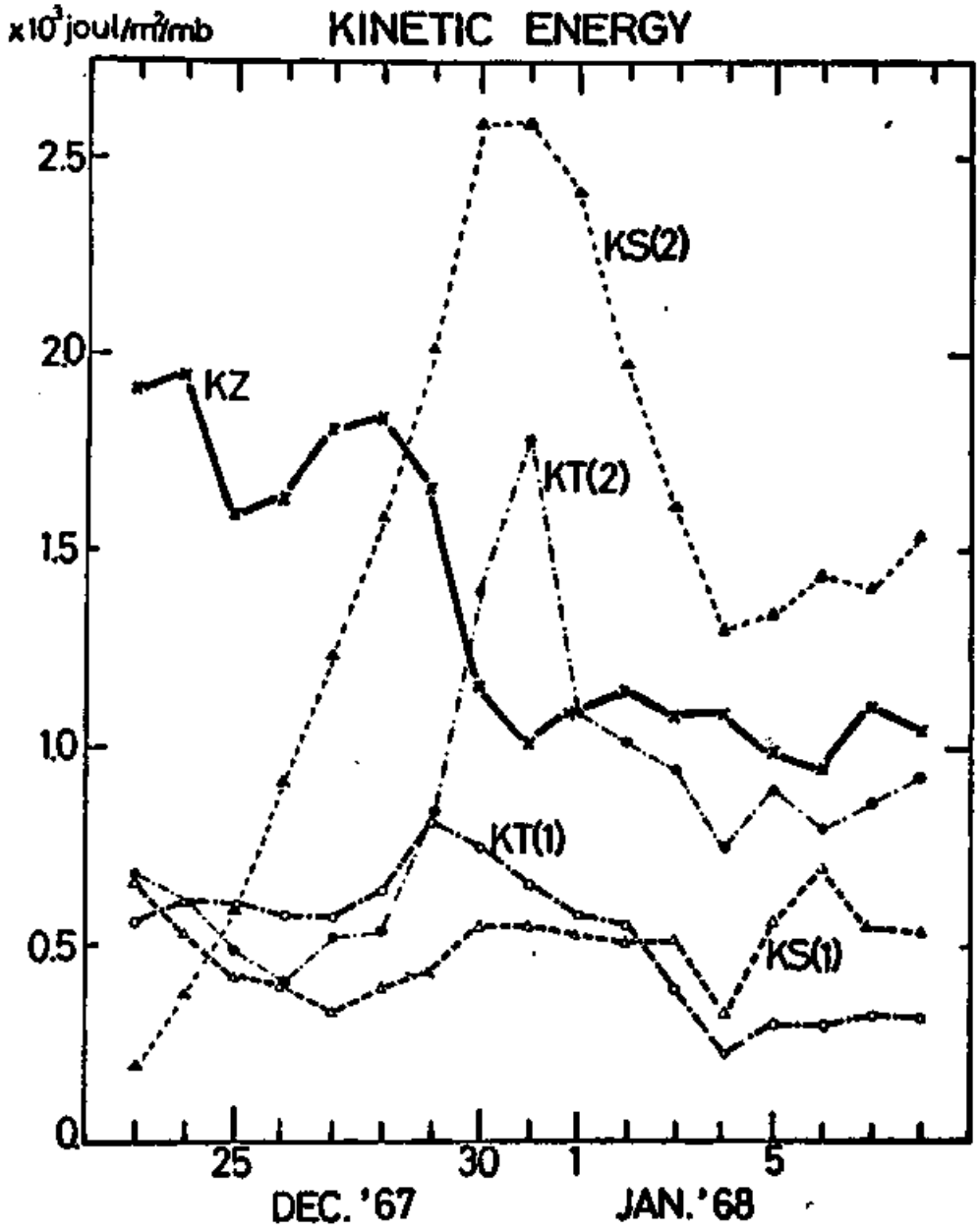
x10³ joul/m²/mb
KINETIC ENERGY
2.5
2.0
1.5
1.0
0.5
0
KS(2)
KZ
KT(2)
KT(1)
KS(1)
25
30
1
5
DEC. '67
JAN. '68

Fig. 12

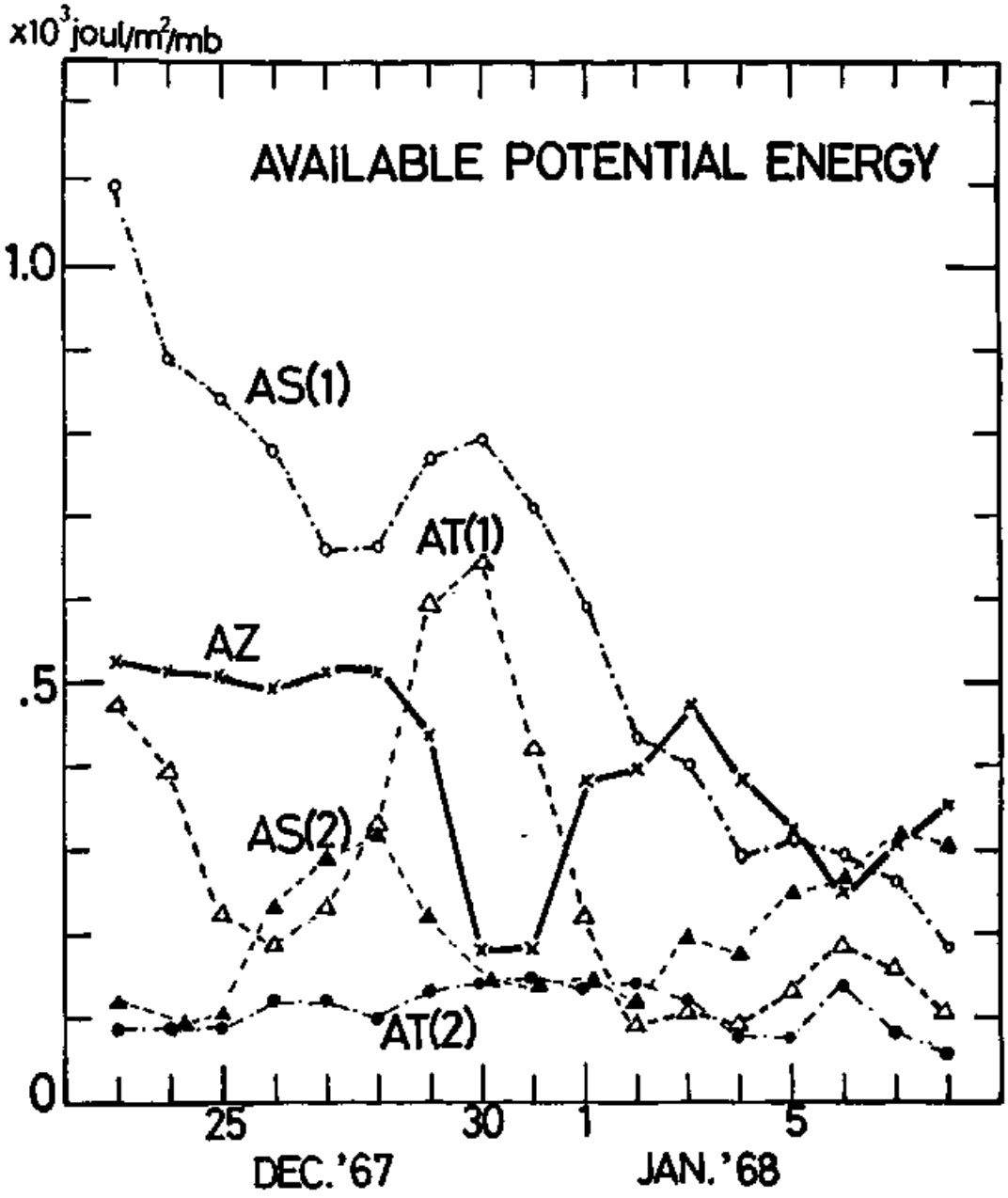
x10³ joul/m²/mb
AVAILABLE POTENTIAL ENERGY
1.0
.5
0
AS(1)
AT(1)
AZ
AS(2)
AT(2)
25
30
1
5
DEC.'67
JAN.'68

Fig. 13

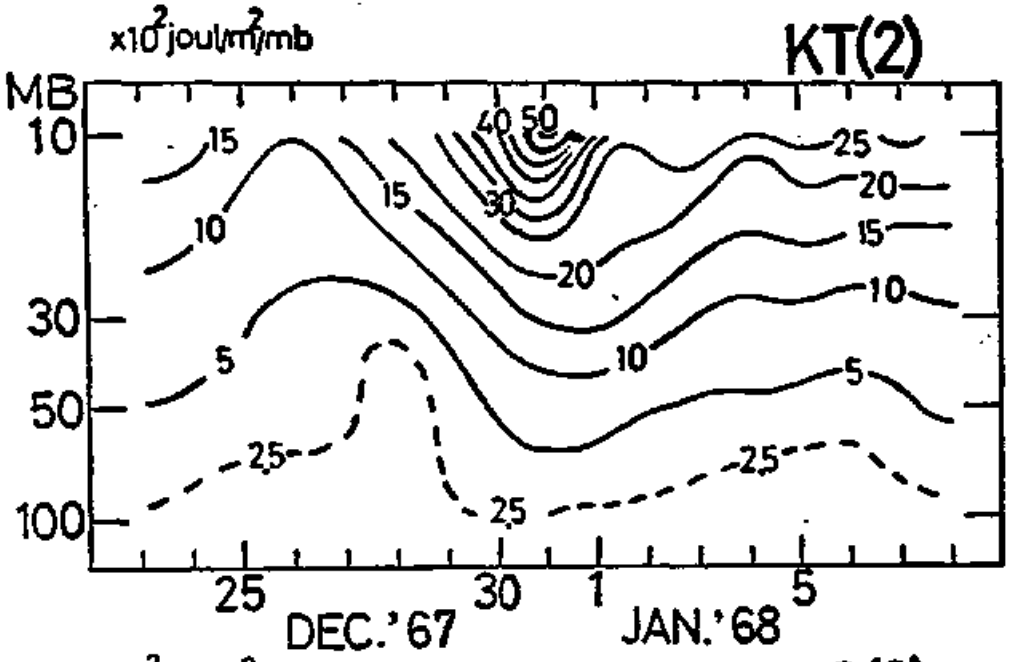
x10² joul/m²/mb
KT(2)
MB
10
30
50
100
25
DEC.'67
30
1
JAN.'68
5

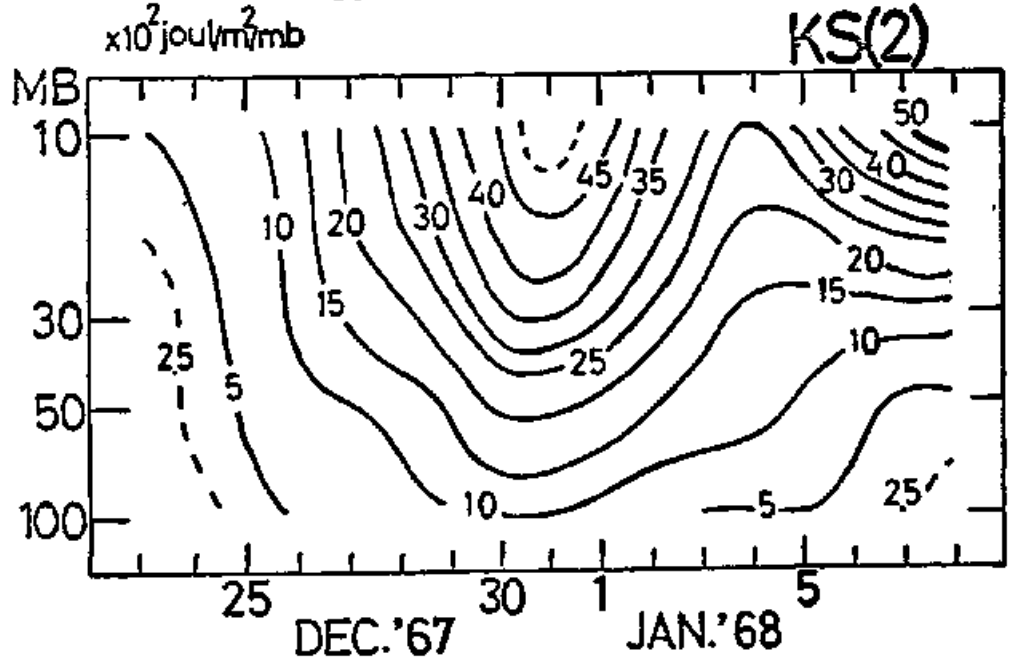
x10² joul/m²/mb
KS(2)
MB
10
30
50
100
25
DEC.'67
30
1
JAN.'68
5

Fig. 14

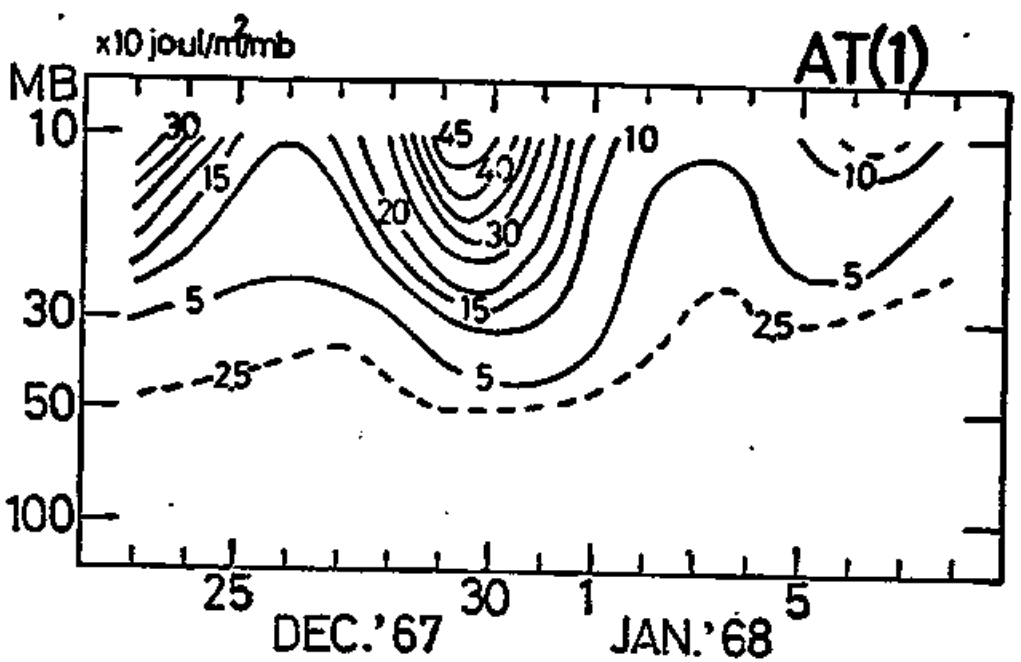
x10 joul/m²/mb
AT(1)
MB
10
30
50
100
25
DEC.'67
30
1
JAN.'68
5

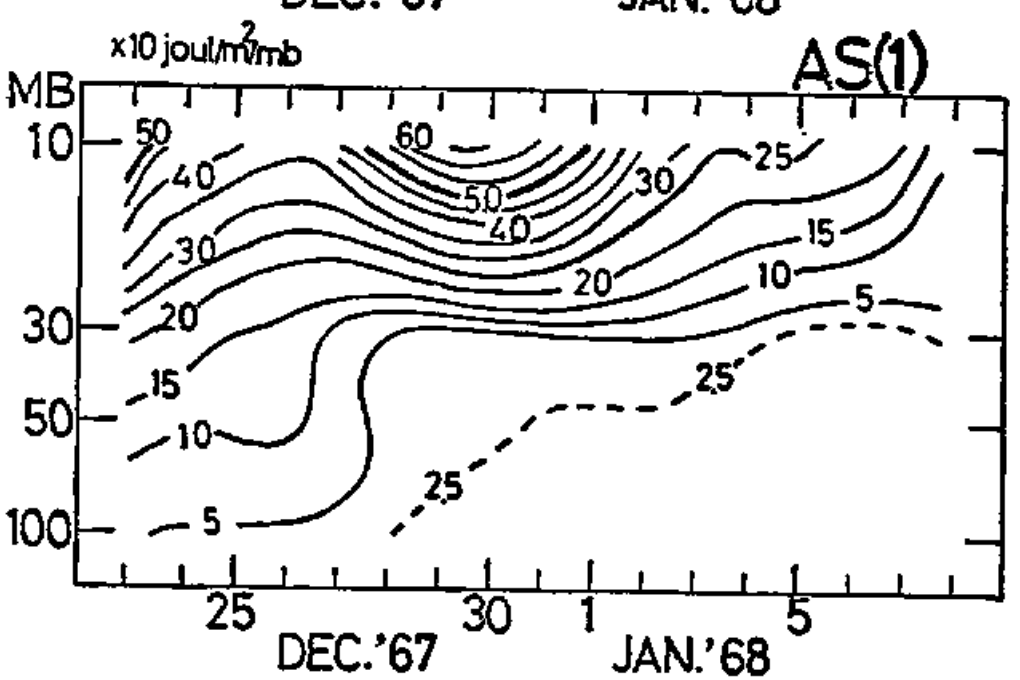
x10 joul/m²/mb
AS(1)
MB
10
30
50
100
25
DEC.'67
30
1
JAN.'68
5

Fig 15

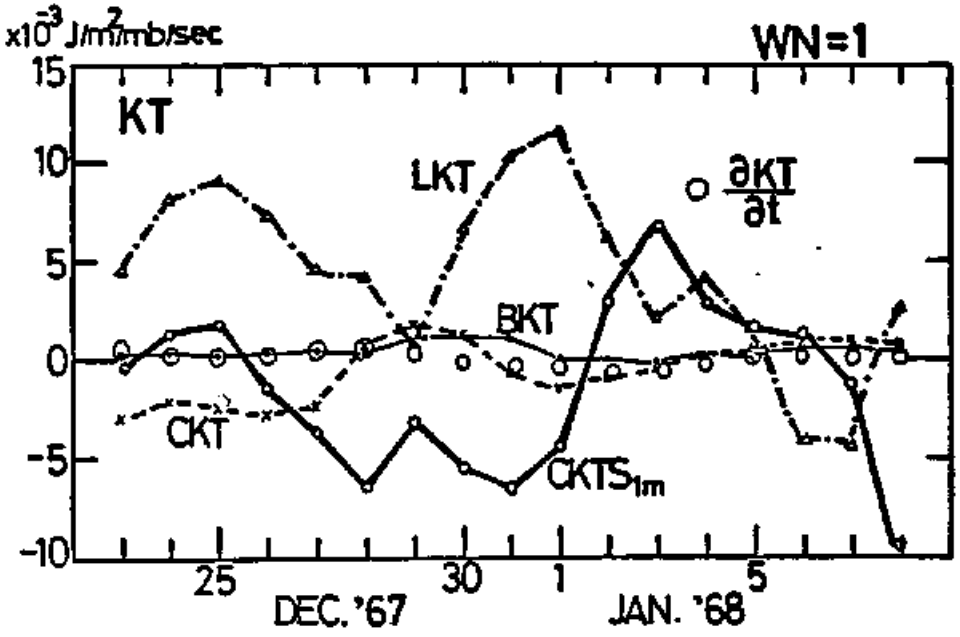
x10⁻³ J/m²/mb/sec
WN=1
KT
LKT
∂KT/∂t
BKT
CKT
CKTS1m
15
10
5
0
-5
-10
25
30
1
5
DEC. '67
JAN. '68

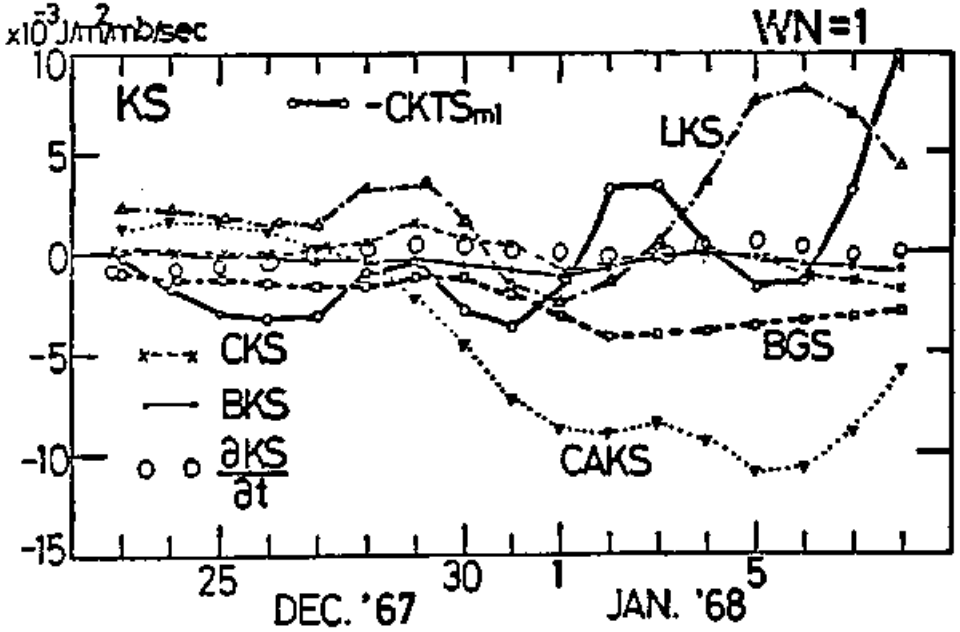
x10⁻³ J/m²/mb/sec
WN=1
KS
-CKTSm1
LKS
BGS
CKS
BKS
∂KS/∂t
CAKS
10
5
0
-5
-10
-15
25
30
1
5
DEC. '67
JAN. '68

Fig. 16

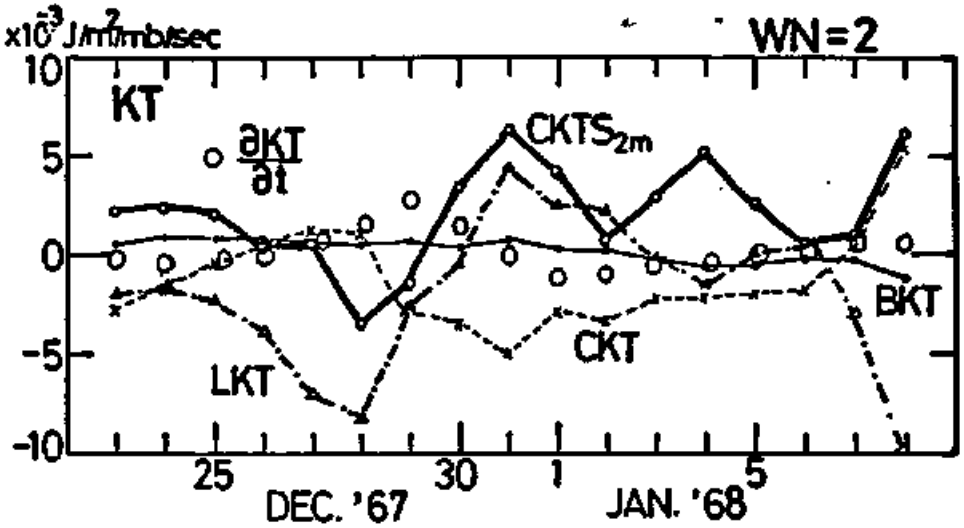
x10⁻³ J/m²/mb/sec
WN=2
KT
∂KT/∂t
CKTS2m
BKT
CKT
LKT
10
5
0
-5
-10
25
30
1
5
DEC. '67
JAN. '68

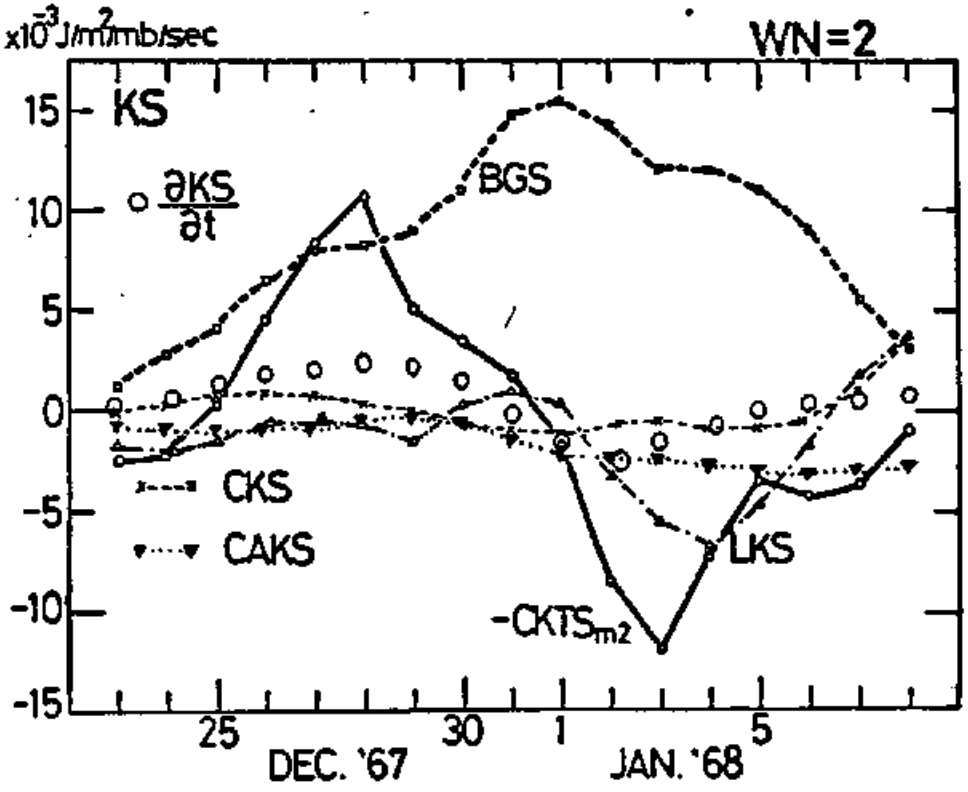
x10⁻³ J/m²/mb/sec
WN=2
KS
∂KS/∂t
BGS
CKS
CAKS
LKS
-CKTSm2
15
10
5
0
-5
-10
-15
25
30
1
5
DEC. '67
JAN. '68

Fig. 17

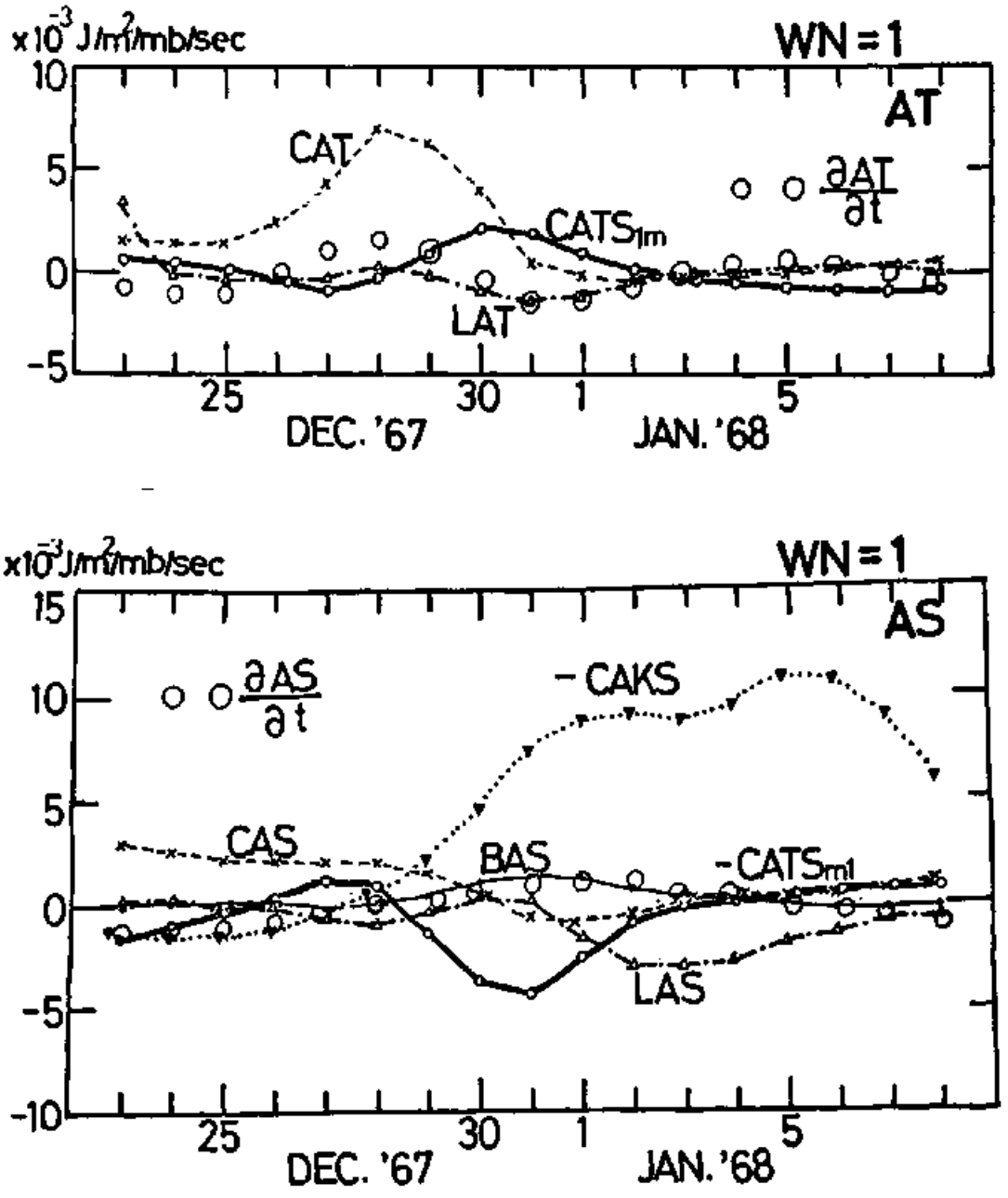
x10⁻³ J/m²/mb/sec
WN=1
AT
CAT
∂AT/∂t
CATS_lm
LAT
10
5
0
-5
25
30
1
5
DEC. '67
JAN. '68
x10⁻³ J/m²/mb/sec
WN=1
AS
∂AS/∂t
-CAKS
CAS
BAS
-CATS_ml
LAS
15
10
5
0
-5
-10
25
30
1
5
DEC. '67
JAN. '68

Fig. 18

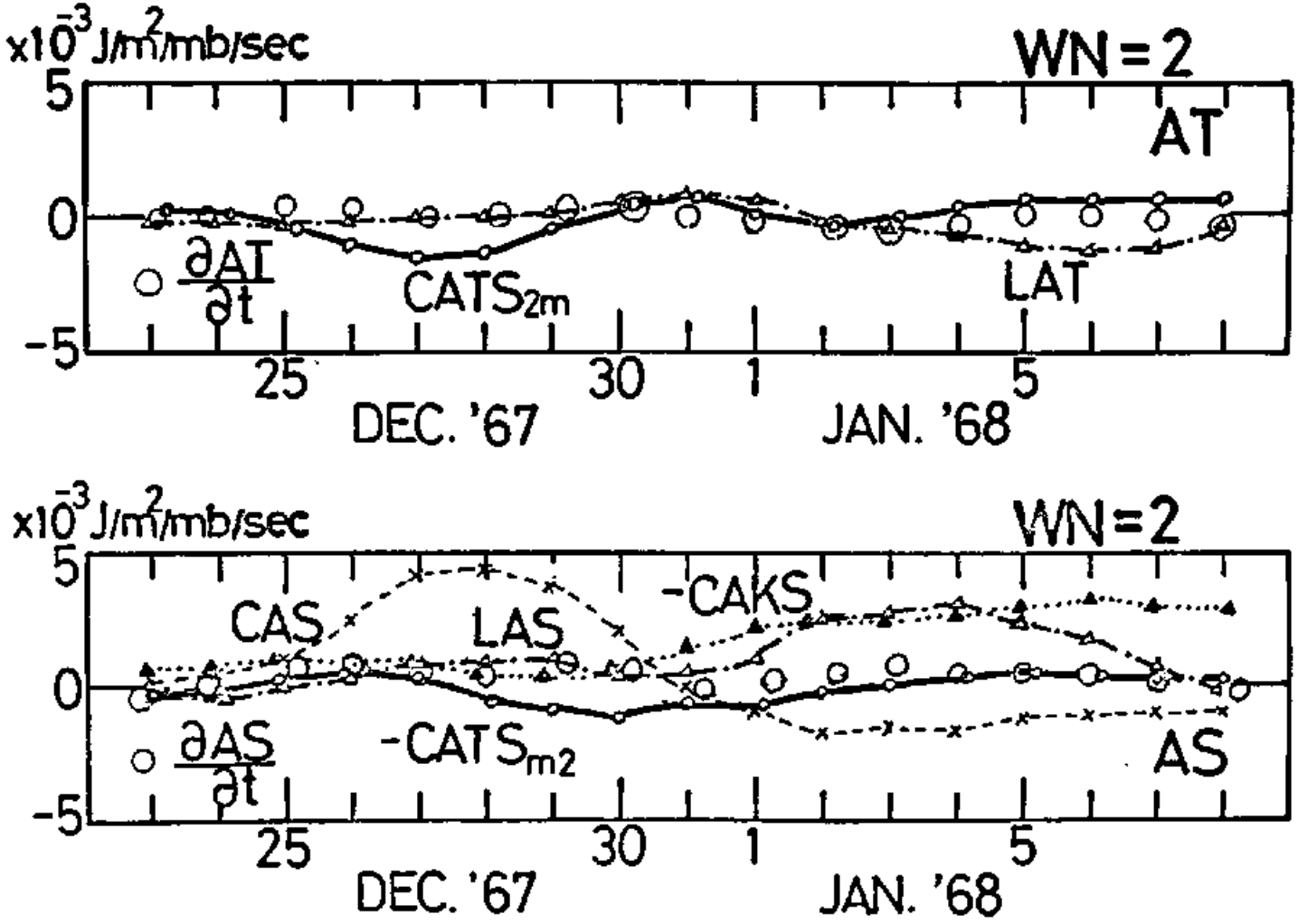
x10⁻³ J/m²/mb/sec
WN=2
5
0
-5
AT
∂AT/∂t
CATS2m
LAT
25
30
1
5
DEC. '67
JAN. '68
x10⁻³ J/m²/mb/sec
WN=2
5
0
-5
CAS
LAS
-CAKS
∂AS/∂t
-CATSm2
AS
25
30
1
5
DEC. '67
JAN. '68

Fig: 19

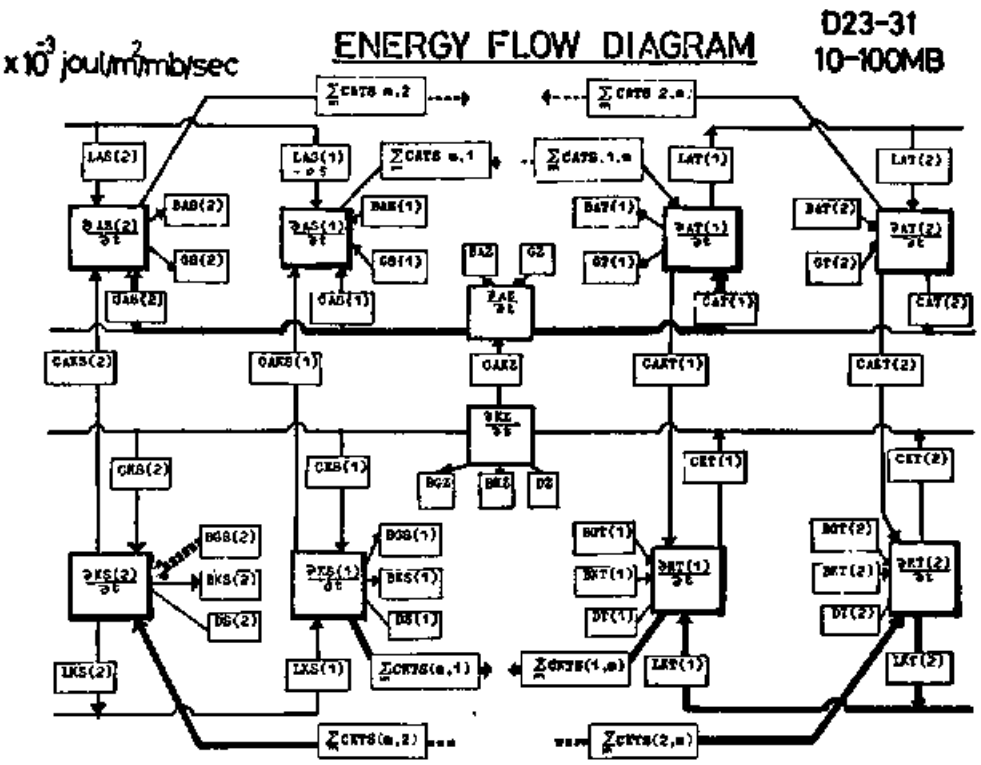

Fig 20a

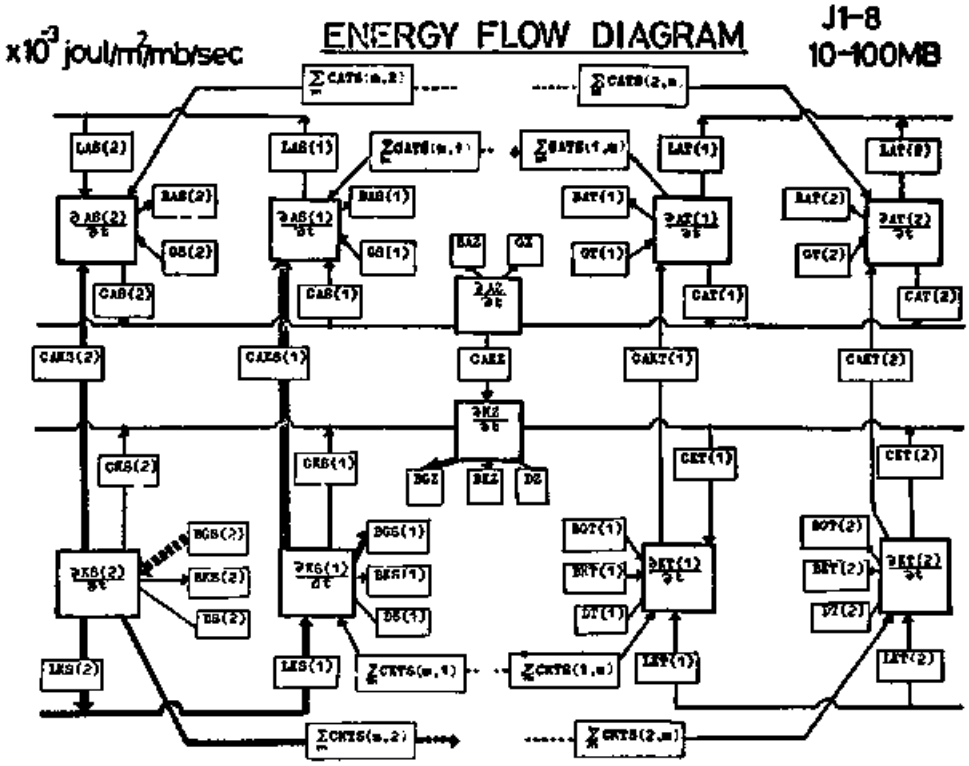

Fig. 20b